RES | THE SCHOOL *for* RENEWABLE ENERGY SCIENCE

Retrograde Alteration of Basaltic Rocks in the Þeistareykir High-Temperature Geothermal Field, North-Iceland

Krisztina Marosvölgyi

UNIVERSITY OF ICELAND

University of Akureyri

RETROGRADE ALTERATION OF BASALTIC ROCKS IN THE ÞEISTAREYKIR HIGH-TEMPERATURE GEOTHERMAL FIELD, NORTH-ICELAND

Krisztina Marosvölgyi

A 30 credit units Master's thesis

Supervisors:
Dr. Hrefna Kristmannsdóttir
Dr. Axel Björnsson

A Master's thesis done at
RES │ the School for Renewable Energy Science
in affiliation with
University of Iceland &
the University of Akureyri

Akureyri, February 2009

Retrograde Alteration of Basaltic Rocks in the Þeistareykir High-Temperature Geothermal Field, North-Iceland

A 30 credit units Master's thesis

RES │ the School for Renewable Energy Science
Solborg at Nordurslod
IS600 Akureyri, Iceland
telephone: + 354 464 0100
www.res.is

Printed in 14/05/2009
at Stell Printing in Akureyri, Iceland

ABSTRACT

Hydrothermal alteration of basaltic rocks in a drill core from well ÞR-7 in the geothermal area on Þeistareykir was studied by microscope and X-ray powder diffraction (XRD) methods. Emphasis was laid on the study of clay minerals (sheet silicates) and zeolites formed by hydrothermal alteration. The reservoir rocks in the area are medium to highly hydrothermally altered. The rock forming minerals have been transformed to clay minerals or sheet silicates and several secondary minerals have been precipitated in vugs and factures. Several different clay mineral types were identified in the altered rocks: smectite, chlorite, mixed-layer minerals of of chlorite/smectite, mostly irregular types and irregular chloritic mixed-layer sheet silicates. Smectie/illite mixed-layer minerals were also encountered. The XRD diffraction patterns of the clay mineral samples from well ÞR-7, are quite complex and not easy to interpret, as the minerals are often poorly crystalline and not pure components of any single type of minerals. A regular clay zonation from smectite through mixed layer smectite-chlorite to chlorite, as is common in high-temperature geothermal fields in Iceland, is not observed in the ÞR-7 core. The zeolite types identified in the core are laumontite, yugawaralite, mordenite and wairakite. The zeolite yugawairalite is quite rare and previously only encountered in three localities in Iceland. The higher temperature zeolite wairakite is found in the middle of a zone dominated by the lower temperature zeolite laumontite. Therefore dispersion of the secondary minerals does not show a very clear zonation of the alteration minerals, and correlation to rock temperature is not easily obtained. Some of the clay minerals/sheet silicates encountered suggest a retrograde alteration of previously formed clay minerals at lower temperatures than the original hydrothermal alteration. The occurrence of zeolites in the core implies a similarity to the higher temperature zeolite wairakite that occurs in a laumontite dominant zone. The rock temperature in well ÞR-7 appears to have been higher at earlier times than at present, showing an overprint of lower temperature secondary minerals.

TABLE OF CONTENTS

LIST OF FIGURES

LIST OF TABLES

1 INTRODUCTION

The aim of this project was to study the alteration of the core from well ÞR-7 at Þeistareykir NE Iceland. The results were used to interpret the present temperature conditions and development of the field and possible changes during the course of hydrothermal alteration.

The main emphasis is laid on the study of secondary minerals in amygdules and the clay minerals (sheet-silicates) formed by dissolution of the primary minerals in the basaltic rocks.

Well ÞR-7 is located 5 km from the most active area with fumaroles and boiling mud pots. This is an exploratory well, which is on the border of the area with surface alteration and high heat transfer. The aim of Landsvirkjun for drilling this well was to explore the extension and borders of the area. The drilling was stopped at 458.1 m depth and did not reach the initial planned depth of 600m. The reason was persistent technical problems (stuck drill string) and cost issues as compared to the potential scientific gain. Drilling operations were therefore terminated at 458.1 m depth and the drill rig was moved to Gjástykki, where another exploration well was drilled (Lacasse et al., 2007).

It was planned to use both XRD and XRF analytical methods to observe the alteration of the reservoir rocks cut by the drill core. However, due to technical problems with the XRF device this thesis only includes the XRD measurements. The XRF spectrophotometer at the RES laboratory broke down in December 2008 and could not be repaired in time before submission of the thesis, so unfortunately no XRF can be reported. All the samples planned to be analyzed were already prepared and will be analyzed later. The results are included in a paper to be published later.

An abstract with the results of the research project has been submitted to the World Geothermal Congress in Bali 2010 and there the results from the XRF analysis will be included.

2 GEOLOGICAL BACKGROUND

2.1 Regional tectonic and geological settings of Iceland

Iceland is located at the junction between the Mid-Atlantic-Ridge, which characterizes the plate boundaries of the American and the Eurasian plate, and the elevated Greenland–Iceland–Faeroes Ridge where the asthenospheric flow under the NE Atlantic plate boundary interacts and mixes with a deep-seated mantle plume, situated (*Figure 1*). The Reykjanes Ridge southwest of Iceland and the Kolbeinsey Ridge to the north are segments of the Mid-Atlantic-Ridge. The spreading rate is around 1cm/y, indicated by blue arrows on the map. Magnetic anomalies (blue lines) indicate the increasing age, in millions of years (Ma), of the ocean bottom with increasing distance from the rift axes. Also, the volcano-tectonic rift zones crossing Iceland from southwest to northeast are shown in red.

The South Iceland Seismic Zone in the south and the Tjörnes Fracture Zone in the north are transverse zones which connect the volcanic rift zones to the segments of the Mid-Atlantic-Ridge (Trønnes, 2002).

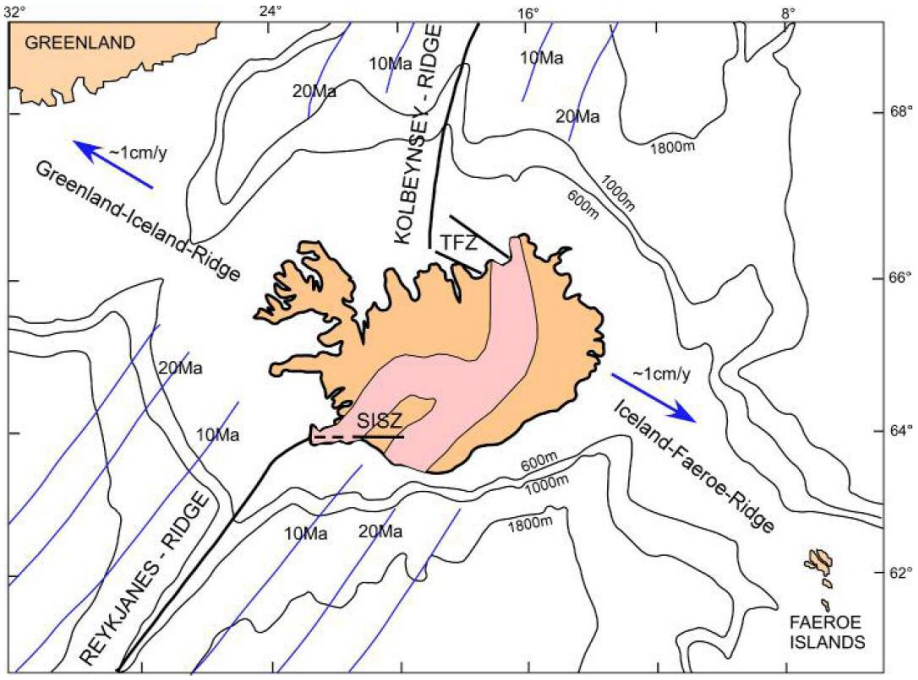

Figure 1: American and the Eurasian plate and the elevated Greenland–Iceland–Faeroes Ridge (Björnsson at al., 2007)

During the last 60 Ma Greenland, Eurasia and the NE Atlantic plate boundary have migrated northwestwards at a rate of 1-3 cm/a relative to the surface expression of the Iceland plume (Lawver and Muller, 1994). Currently, the plume channel reaches the lithosphere under the Vatnajökull glacier, about 200 km southeast of the plate boundary, defined by the Reykjanes and Kolbeinsey Ridges (Wolfe et al., 1997). During the last 20 Ma the Icelandic rift zones have migrated stepwise eastwards to keep their positions near the surface expression of the plume, leading to a complicated and changing pattern of rift zones and transform fault zones (Trønnes, 2002).

2.1.1 The Icelandic volcanic systems, rift zones and off-rift volcanic zones

The currently active volcanic systems in Iceland are shown in *Figure 2* (Sæmundsson, 1979; Einarsson, 1991; Jóhannesson and Sæmundsson, 1998). The 40-50 km wide rift zones (Reykjanes, Western, Eastern and Northern Rift Zones) comprise echelon arrays of volcanic fissure swarms, with 3-4 semi-parallel swarms across the rift zone. The swarms are 5-15 km wide and up to 200 km in length. With time, they develop a volcanic centre with maximum volcanic production somewhere along their length. The volcanic centers will often develop into central volcanoes with high-temperature geothermal systems, sometimes also with caldera structures produced by large ash-flow eruptions of silicic magma. Each fissure swarm, with or without a central volcano, constitutes a volcanic system. In the non-rifting volcanic flank zones (Snæfellsnes, Eastern and Southern Flank Zones) most of the volcanic centers lack well-developed fissure swarms.

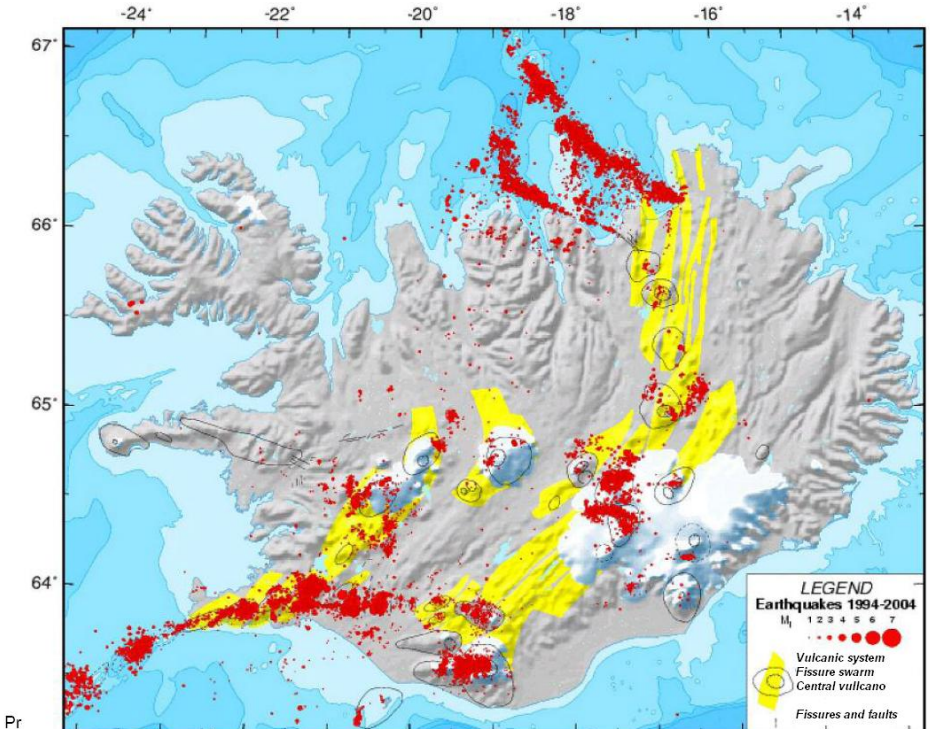

Figure 2: Volcano-tectonic map of Iceland. Spatial distribution of earthquakes in and around Iceland in the years 1994-2004. Red dots of different sizes indicate earthquakes of various magnitudes (Halldórsson, 2005). Central volcanoes, circular areas, mapped by Saemundsson (1978).

The Icelandic rift zone system continues northwards from Vatnajökull as the Northern Volcanic Zone. The Vatnajökull area is currently the locus of the Iceland plume axis (e.g. Wolfe et al., 1997), and the active rifting along the Northern Volcanic Zone propagates southwards from the plume centre as the Eastern Rift Zone.
Whereas the rift zone volcanic systems produce tholeiitic basalts, the major products of the off-rift volcanic zones are mildly alkaline and transitional (tholeiitic to alkaline) basalts (Sæmundsson, 1979). The tholeiitic rift zone volcanism and mildly alkaline flank zone volcanism in Iceland is equivalent to the main shield-building tholeiitic stage and the pre- and post-shield-building alkaline stages of the Hawaiian volcanoes. The current activity along the Snæfellsnes Peninsula represents dying volcanism and unconformable overlying tholeiitic lavas of Tertiary and Pleistocene age, whereas the Southern flank zone has incipient volcanism related to the southward propagation of the Eastern Rift Zone into Tertiary rift zone. The mildly alkaline and transitional tholeiitic volcanism along the Eastern Flank Zone may also represent incipient activity associated with an imminent propagation of a new rift zone east of the Northern Volcanic Zone-Eastern Rift Zone (Trønnes, 2002).

2.2 The hydrothermal systems on Iceland

Geothermal areas in Iceland have been investigated during the last 40-50 years, but intensive research started in about 1950, when deep drilling was initiated, and was performed in most of the areas under investigation.

The geothermal areas in Iceland are divided into two distinct groups. The high-temperature volcanic geothermal systems (*Figure 3*), which are located within the recent volcanic zones have reservoir temperature around 200-400 °C (>200 °C at 1 km depth) (Kristmannsdóttir and Tómasson, 1978). In all the high-temperature areas the dominant rock formations are basaltic hyaloclastic rocks and basalt lavas, but there are also silicic rock formations (e.g. rhyolites). The heat source is a magma chamber or a cooling intrusion. Solfatara and mud pools indicate that the area is a high-temperature zone, which can typically be connected to the phenomena of sulfur precipitation and rock alteration. High concentration of dissolved solids and volcanic gases in the geothermal fluids (Björnsson, 1990) are also typical for the high-temperature fields (Böðvarsson 1961, Kristmannsdóttir and Tómasson, 1978). High temperature areas in Iceland include Krafla and Theistareykir, the latter being the research area of this thesis.

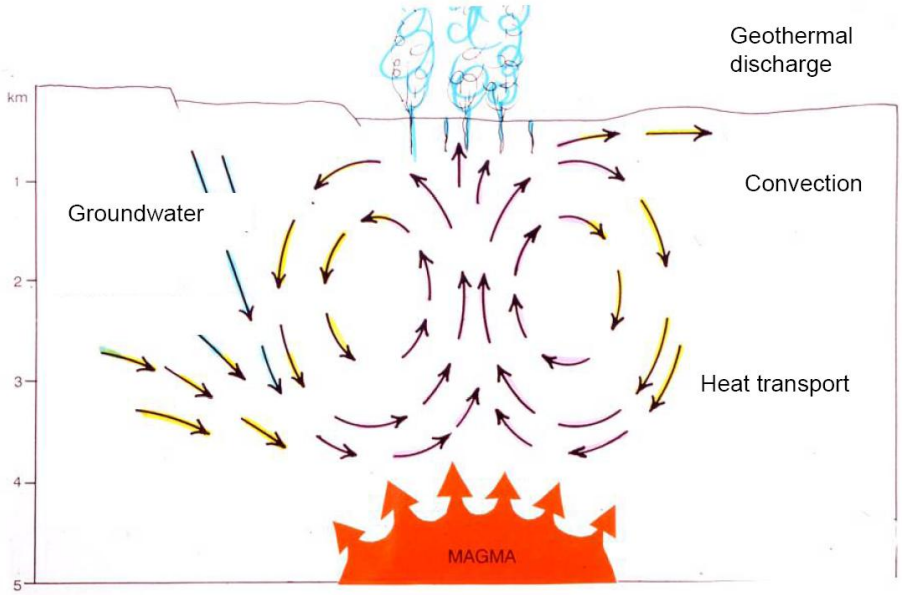

Figure 3: High temperature geothermal system (Björnsson, 1990)

The other type of geothermal fields is the low-temperature one (medium and low-enthalphy geothermal systems) (*Figure 4*) which is found outside the volcanic zone (in Quaternary and Tertiary rock formations younger than 3.1 Ma). In the low temperature areas the temperature is below 150 °C at 1km depth. The heat source is the surrounding rocks and the hot water circulating in the faults and fissures (Björnsson et al., 1990). The geothermal fluid is generally water of meteoric origin with a comparatively low content of dissolved solids and alkaline compounds (Arnórsson, 1974). The meteoric water first percolates down into the underground rocks where it is warmed up. Convection starts due to the difference in density between the hot and cold water, and steam emerges up to the surface.

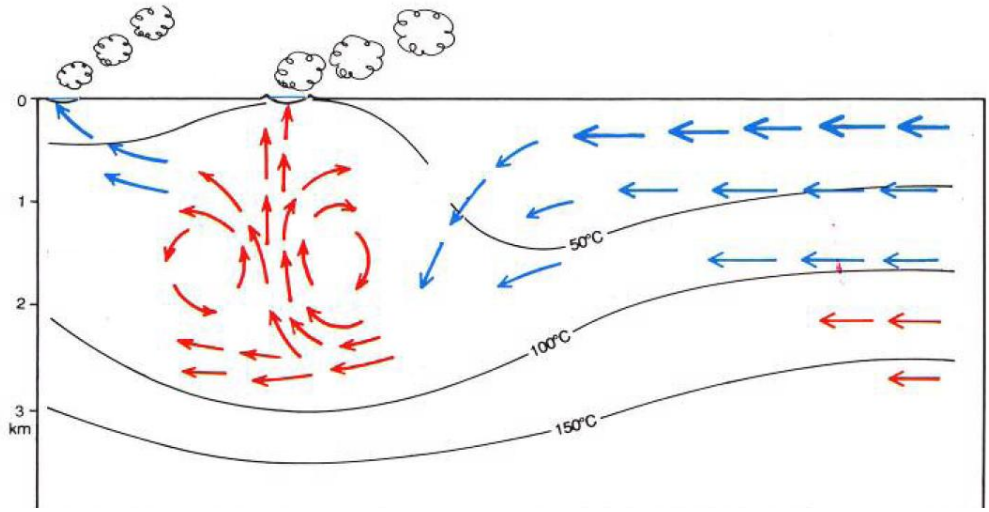

Figure 4: Low temperature geothermal system (Björnsson, 1990).

2.3 Geological background of the research area

The Theistareykir high-temperature geothermal area lies in the Theistareykir fissure swarm in northest Iceland. The location of the area is shown in (*Figure 5*) (Ármannsson et al., 1986)**.**

The active part of the geothermal area lies in the eastern half of the Theistareykir fissure swarm; although there has not been volcanic activity in the region during the last 1000 years. The geothermal activity covers an area of nearly 10.5 km^2, and the most intense activity is on the northwestern and northern slopes of Mount Bæjarfjall and in the pastures extending from there northwards to the western part of Mount Ketilfjall (Theistareykjagrundir) (*Figure 6*). If the old alteration in the western part of the swarm is considered as a part of the thermal area it covers nearly 20 km^2.

The bedrock in the area is divided into hyaloclastite ridges formed by subglacial eruptions during the Ice Age, interglacial lava flows, and recent lava flows (younger than 10 000 yrs); all of them are basaltic. Acidic rocks are found on the western side of the fissure swarm, from subglacial eruptions up to the last glacial period. Rifting is still active in the fissure swarm (*Figure 7*).

Volcanic activity has been relatively infrequent in the area in recent times. Approximately 14 volcanic eruptions have occurred in the last 10 000 yrs, but none in the last 2500 yrs. Large earthquakes (up to M: 6.9) occur mainly north of the area in the Tjörnes Fracture Zone, which is a right–lateral transform fault in the fissure swarm itself during rifting. The Tjörnes Fracture Zone strikes northwest, crosscutting the north-striking fractures as it enters into the fissure swarm some 5 km north of the thermal area. The volcanic activity ceases in the fissure swarm as it crosses the Tjörnes Fracture Zone, although its northern part remains seismically active (Ármannsson et al., 1986).

The most active parts of the area are related to active fractures, increasing permeability and enabling geothermal fluids to circulate and reach the surface.

Surveys indicate that a low resistivity structure (<10 Ωm) is located at the depth of 400-600 m elongated in an east-west direction from Mount Bæjarfjall in the east towards Mount Mælifell in the west. Below this low resistivity structure the resistivity increases sharply. Similar structures were detected by gravity and magnetic field studies. This could

be interpreted as an east-west trending heat source crossing a north-south tectonic structure. Thus, the distribution of the surface manifestations reflects the direction of vertically permeable faults and fissures rather than that of the heat source (Ármannsson et al., 1986).

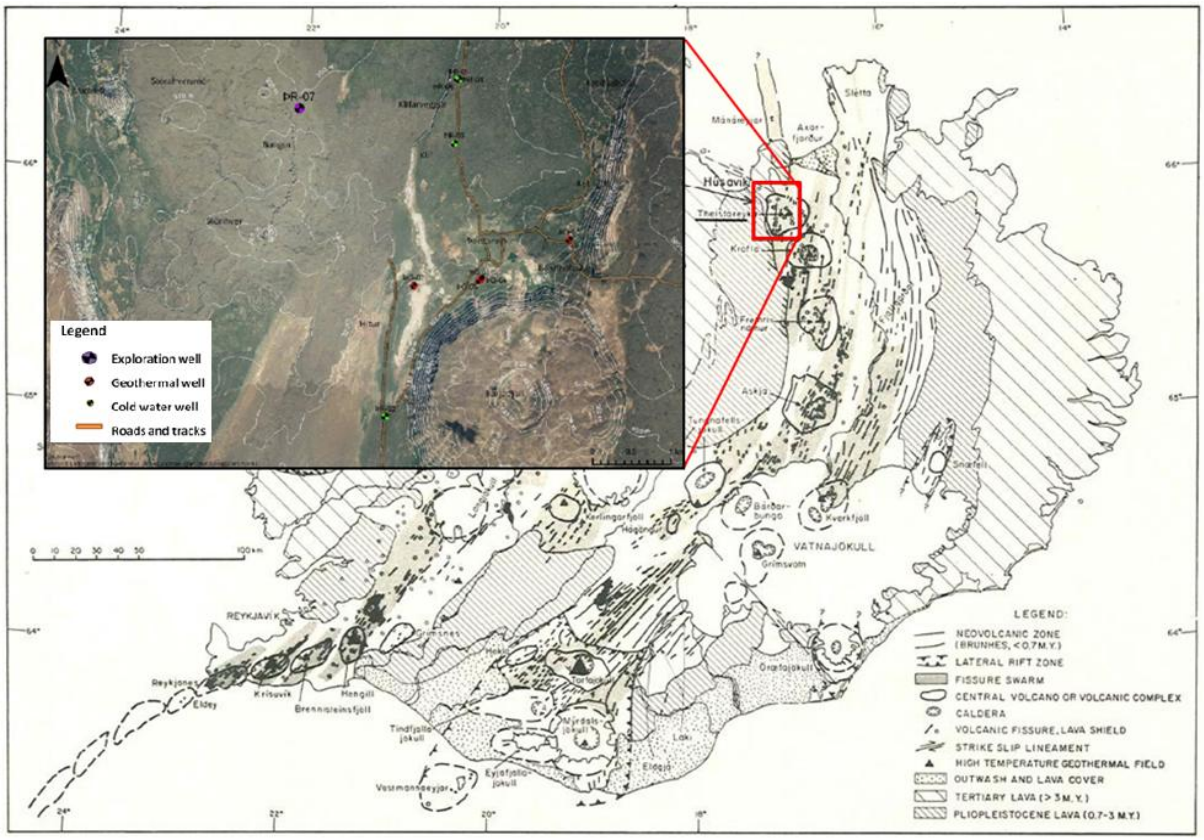

Figure 5: Outline of geology of Iceland showing the study area and the location of Theistareykir (Compiled by Sæmundsson, 1979) and of the drill sight ÞR-07 (Lacasse et al., 2007)

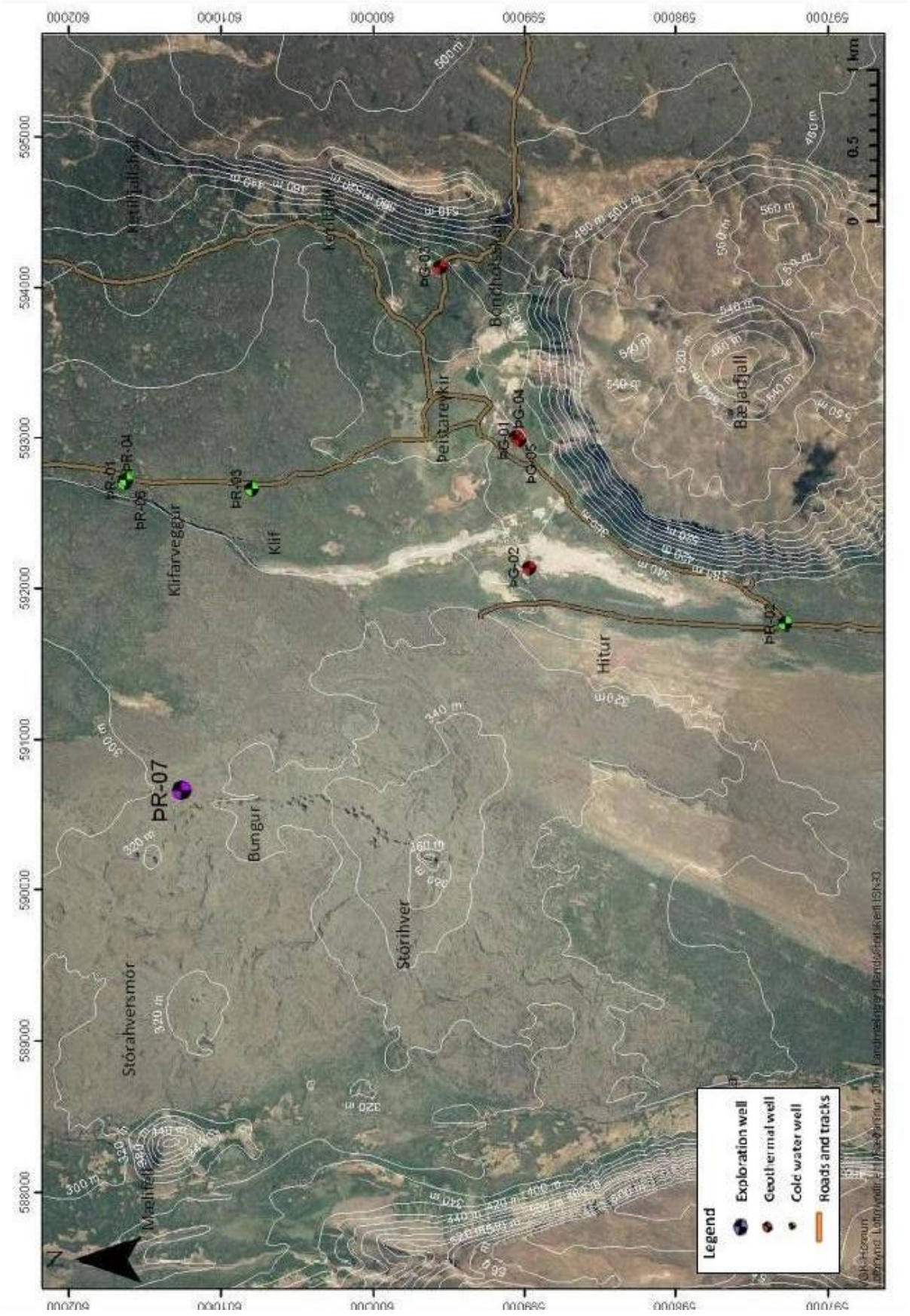

Figure 6: Map of the Theistareykir area (Lacasse et al., 2007)

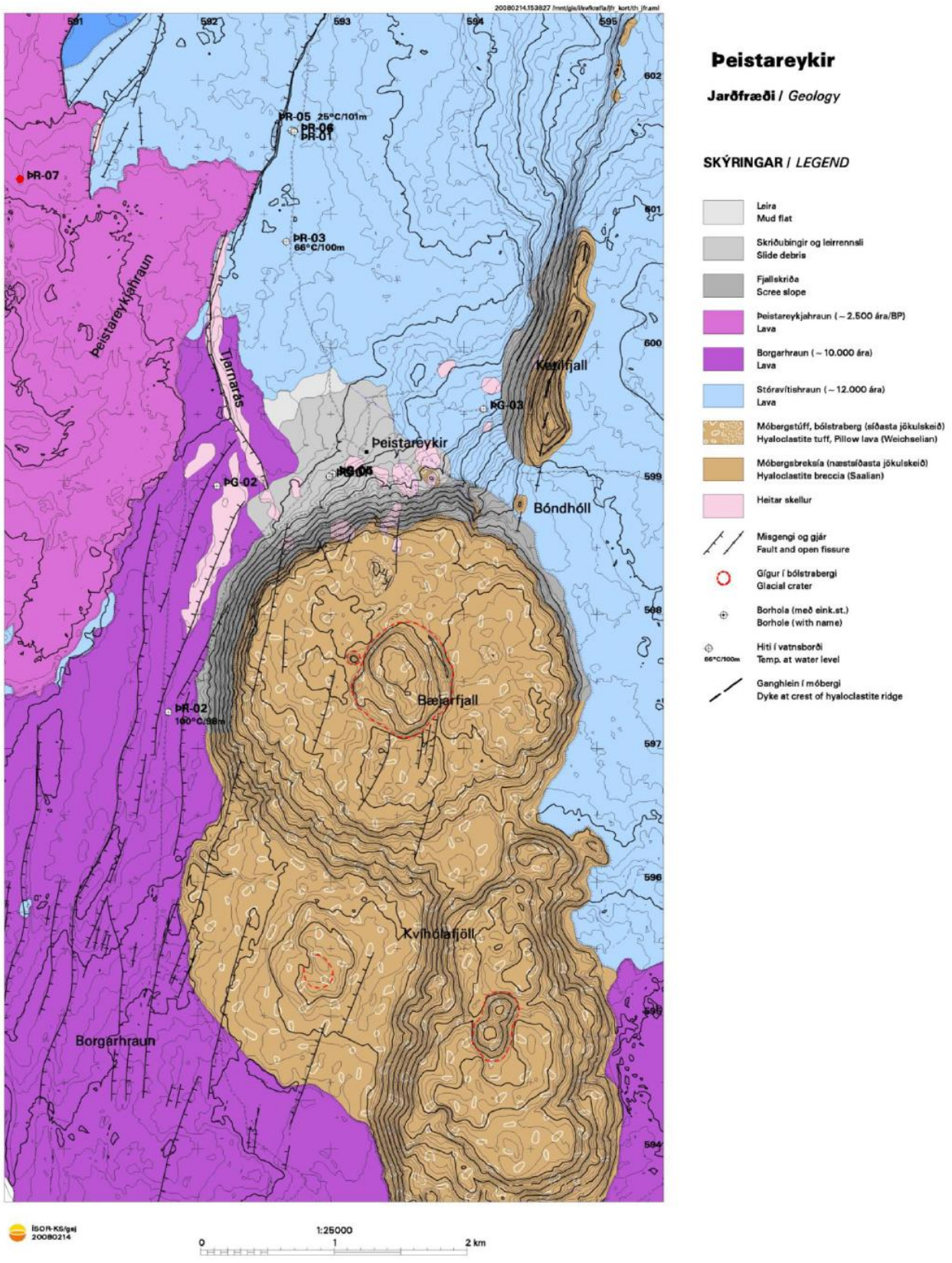

Figure 7: Geological map of the research area (Sæmundsson, 2007)

2.4 Geothermal exploration in the area

Surface exploration in the area started just after 1970 with geological mapping, geophysical exploration and geochemical survey (Gíslason et al., 1984). It was continued with intervals through the next twenty years (Gíslason et al., 1984). Drilling started in 2002. Besides well ÞR-7, which is an exploration well, five geothermal wells have been drilled in the Theistareykir geothermal area. The first was ÞG-1 drilled down to a depth of 1953 m in 2002 reaching a maximum temperature around 332 °C. This was followed by well ÞG-2 of 1723 m depth in 2004 and its temperature is around 242 °C. Then ÞG-3 was drilled to a depth of 757 m in 2006, with a temperature of 380 °C. In 2007 two additional geothermal wells were drilled, ÞG-4 and ÞG-5. ÞG-4 is 839 m deep with a temperature of 320 °C, ÞG-5 is 847 m deep with a temperature of 259 °C. The maximum temperature of the wells decreases with increasing distance from the volcanic caldera (Bæjarfjall).

3 GEOTHERMAL ALTERATION AND HYDROTHERMAL MINERALS

Hydrothermal alteration results from an interaction of the primary rocks and hot water and steam causing dissolution of primary minerals, replacement and precipitation of new minerals and changes in permeability (Henley and Ellis, 1983). The hydrothermal fluids transport dissolved solids, either from the close-by igneous source or from leaching out of some close-by rocks. The primary minerals and secondary minerals change by the changes in the hydrothermal environment. Secondary minerals partly precipitate in open cavities, vesicles and fractures in the rock formations. The primary minerals are also replaced in situ by secondary minerals. An example of this is albitization of more calcic plagioclase by increasing temperature and alteration. The olivines and pyroxenes in basaltic igneous rocks are commonly replaced by clay minerals and chlorite. Generally, the primary minerals formed at the highest temperature have the least stability by hydrothermal alteration (Stefánsson et al. 2001). Basaltic glass is the most unstable phase and the first to be altered. The hydrothermal alteration in geothermal fields shows zoning by increased temperature and depth in terms of special index minerals. The index minerals are different in different reservoir rocks (Kristmannsdóttir, 1985). Lowering of the reservoir temperature may also be demonstrated by retrograde alteration and overprint of mineralization formed by lower temperature alteration over mineralization formed by older high temperature alteration.

The intensity or degree of alteration depends on several factors such as: permeability (related to gas content and hydrology of system), temperature, duration of activity, rock composition, pressure, hydrothermal fluid composition (pH value, gas concentration, vapor- or water dominated, magmatic, meteoric), number of superimposed hydrothermal regimes (overprinting of alteration), and hydrology (Kristmannsdóttir, 1975, Browne, 1978, Reyes, 2000; Franzson, 2006; Franzson, 2008). The special features of the alteration in Icelandic geothermal areas are the result of the bedrock being dominantly basaltic hyaloclastites and lavas. Whereas, some alteration minerals may be the same or almost the same as high temperature geothermal fields elsewhere in the world, others in turn, are completely different. This applies to the clay minerals, which were first described when the high temperature geothermal systems of Reykjanes and Nesjavellir were first investigated by deep drilling (Kristmannsdóttir and Tómasson, 1974, Kristmannsdóttir, 1976). The zeolites formed in Icelandic geothermal areas are dominantly calcium zeolites, in contrast

to more common sodium and potassium zeolites in more acidic volcanic and sedimentary reservoir rocks. Temperature and permeability play the most important role in the stability of most hydrothermal minerals. Temperatures vary from below 100 to 300 ^{o}C. The source of permeability may be faults and fracture zones, lithological contacts, formation permeability (clasts and breccias fragments), and paleosols (Reyes, 2000). The compositions of fluids and gasses are extremely variable. The mineralogical and alteration signatures may vary from one geothermal system to another. The rock temperature and the mineral scale relationships of Icelandic geothermal systems are illustrated in *Figure 8*. The principal components, glass and olivine, are the first to alter at low temperature, followed by plagioclase and pyroxene at much higher degrees, and, finally the ore and high-temperature minerals above 200 ^{o}C (Franzson, 2008).

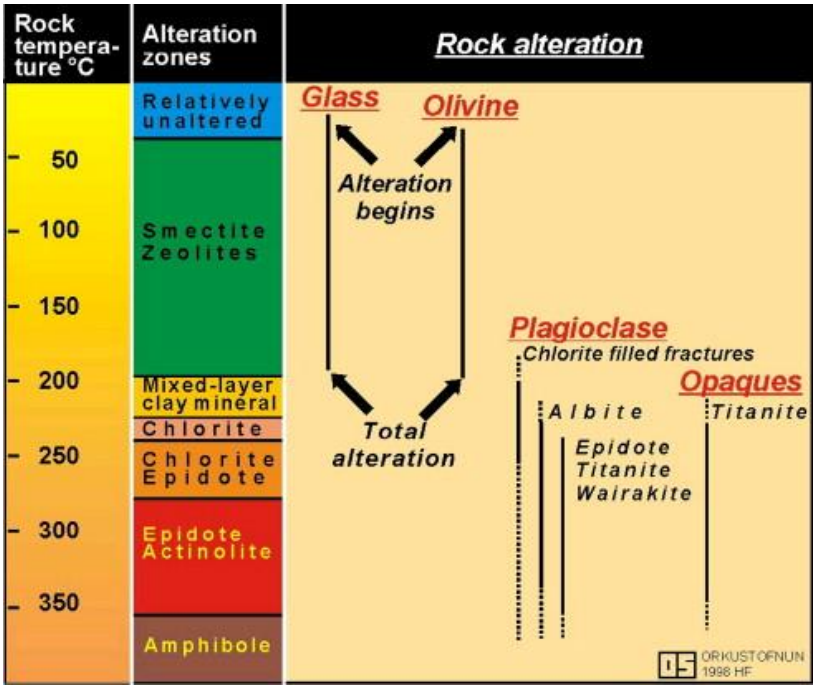

Figure 8: Mineral alteration-temperature diagram (Slightly modified from Franzson, 2008)

Comparing the geothermal alteration between the low-temperature geothermal fields and the high-temperature geothermal fields, the alteration in low-temperature geothermal fields is much less extensive and more localized than in the high-temperature geothermal fields.

In the case of low temperature geothermal fields, alteration may be more complex and it is often difficult to separate geothermal alteration due to present activity of regional alteration from older high temperature alteration.

4 GENERAL BACKGROUND OF MINERALOGY AND METHODOLOGY

In the following chapter a short review of the theoretical knowledge of the alteration minerals is given, which focuses on species found in the Þeistareykir core as well as the methods used to identify them.

4.1 Mineralogical overview

4.1.1 Zeolite group

The zeolites are framework silicates consisting of interlocking tetrahedrons of SiO_4 and AlO_4. In order to be a zeolite the ratio (Si +Al)/O must equal 1/2. The aluminosilicate structure is negatively charged and attracts the positive cations that reside within it. Unlike most other tectosilicates, zeolites have large vacant spaces or cages in their structures which allow space for large cations such as sodium, potassium, barium and calcium and even relatively large molecules and cation groups such as water, ammonia, carbonate ions and nitrate ions. In the more industrial zeolites, the spaces are interconnected and form long wide channels of varying sizes depending on the mineral. These channels allow the easy movement of the resident ions and molecules into and out of the structure. Zeolites are characterized by their ability to lose and absorb water without damage to their crystal structures. The large channels explain the consistent low specific gravity of these minerals (Amethyst Galleries, The Zeolite Group of Minerals, 2009).

Zeolites have a porous structure that can accommodate a wide variety of cations, such as Na^+, K^+, $Ca2^+$, Mg^{2+} and others. These positive ions are rather loosely held and can readily be exchanged for others in a contact solution. Cation exchange capacity in general diminishes with the loss of water; cations are most mobile in zeolites with low cation content (Wikipedia Contributors, Zeolite, 2009).
Natural zeolites form where volcanic rocks and ash layers react with alkaline groundwater. Zeolites are the aluminosilicate members of the family of micro porous solids known as "molecular sieves." The term molecular sieve refers to a particular property of these materials, i.e., the ability to selectively sort molecules based primarily on a size exclusion process. This is due to a very regular pore structure of molecular dimensions. The dimensions of the channels control the maximum size of the molecular or ionic species that can enter the pores of a zeolite. Those are conventionally defined by the ring size of the aperture where, for example, the term "8-ring" refers to a closed loop that is built from 8 tetrahedrally coordinated silicon (or aluminum) atoms and 8 oxygen atoms. These rings are not always perfectly symmetrical due to a variety of effects, including strain induced by the bonding between units that are needed to produce the overall structure or coordination of some of the oxygen atoms of the rings to cations within the structure. Therefore, the pores in many zeolites are not cylindrical.

The calcium zeolites are most common in the Icelandic geothermal fields (Kristmannsdóttir and Tómasson, 1978). In this study the calcium zeolites laumontite, yugawaralite and wairakite were encountered, as well as the sodium zeolite mordenite. The characteristic properties of those zeolites are described below.

Laumontite
$Ca(AlSi_2O_6)_2\ H_2O$??

This mineral is monoclinic (tectosilicates (zeolite group)). The axes of the crystal are: a = 14.8538, b = 13.1695, c=7.5421 Å, and the angles between the axes α=90°, β=110.323°, γ=90° and space group *C2/m* and Z=4 for ideal composition $Ca(AlSi_2O_6)_2{\cdot}4H2O$. Refinement of the structure of Laumontite by least-squares technique yields a discrepancy index R_{wp}=0.115, R_p=0.090, R_F^2=0.046 (Veichow and Huann-Jih, 1971)

Its framework structure is characterized by chains of four-ring and six-ring tetrahedral secondary building units (Baerlocher et al., 2001) alternating along the c axis to form ten-ring channels *(Figure 9)* (Armbruster and Gunter, 2001).

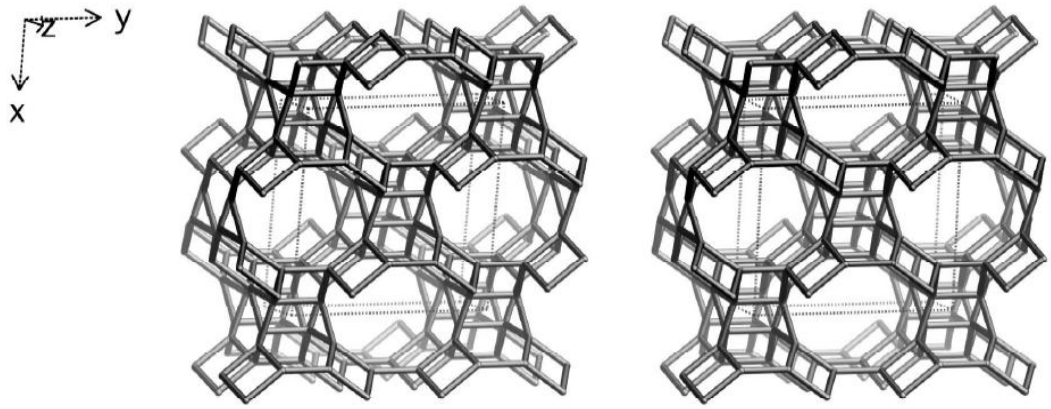

Figure 9: Perspective view of the framework of laumontite (Baerlocher et al., 2001).

Yugawaralite

$CaAl_2Si_6O_{16} \bullet 4H_2O$

Yugawaralite has a monoclinic structure. The axes of the crystal are: a = 6.73, b = 13.96, c = 10.02 Å, β = 111°310´, space group *Pc*, and Z = 2 for ideal composition $CaAl_2Si_6O_{16} \bullet 4H_2O$. Refinement of the structure of Yugawaralite by least-squares technique yields a discrepancy index R of 0.14 and weighted R of 0.13 (Leimer and Slaughter, 1968).
The structure of Yugawaralite is characterized by four-member ring groups approximately perpendicular to the c axis, by five–member ring groups at about 65° to either side of ac plane, and by eight-member ring groups which form channels parallel to the a and c axes. The axes of these channels lie on planes parallel to the ac plane at distance approximately 0.25 and 0.75 on the b axis (*Figure 10*) (Deer et al., 2003).

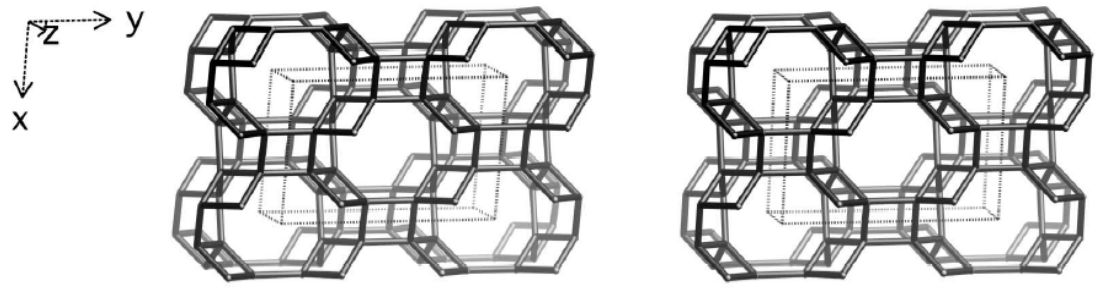

Figure 10: Perspective view of the framework of yugawaralite (Baerlocher et al., 2001)

Mordenite

$(Ca; Na_2; K_2)Al_2Si_{10}O_{24} \bullet 7H_2O$

Mordenite has an orthorhombic structure. Axes of the crystal are: a = 18.11, b =20.53, c = 7.501-7.528 Å, space group *Cmcm, or* $Cmc2_1$ *and* Z=1 for ideal composition $(Ca; Na_2; K_2)Al_2Si_{10}O_{24} \bullet 7H_2O$. X-ray single crystal refinement, R = 0.07 (Baerlocher et al., 2001).

The crystal structure of mordenite characterized by 5-member tetrahedral rings, which are all part of the *tes* (54) polyhedron. These polyhedra are linked by edge-sharing into chains, which are in turn linked together by 4-rings to form a sheet perforated with 8-ring holes (*Figure 11*) (Deer et al., 2003).

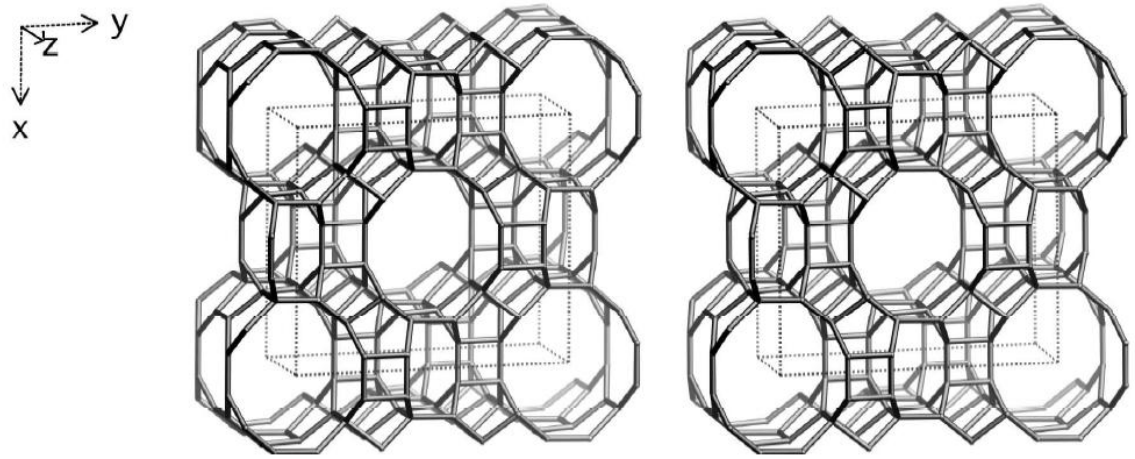

Figure 11: Perspective view of the framework of mordenite (Baerlocher et al., 2001)

Wairakite

$CaAl_2Si_4O_{12} \bullet 2H_2O$

Wairakite has a monoclinic structure. Axes of the crystal are: a= 13.65, b =13.66, c = 13.56 Å, and the angle between the axes β=90°20′, space group *I 2/a* and Z=8 for ideal composition $CaAl_2Si_4O_{12} \bullet 2H_2O$, the calcium analogue of analcime (Liou, 1970).
The analcime framework consists of singly-connected 4-rings, arranged in a chain coiled around tetrad screw axes. Parallel chains alternate 4, screw axes. Every 4-ring is a part of three mutually perpendicular chains, each parallel to a crystallographic axis. Cages, each containing the Na-cations and water molecules, occur near where chains interconnect (*Figure 12*), and each T-site is part of three cages. In the cubic space group every T-site is equivalent to every other T-site, and therefore Si, Al distribution among these sites must be random. Na cations are in the centre of these cages, but there are 24 cages in the unit cell. Therefore, the Na cations must also be randomly distributed. Water molecules fully occupy the 16 sites in the unit cell. Any excess water must be randomly distributed in unoccupied Na sites (Deer et al., 2003).

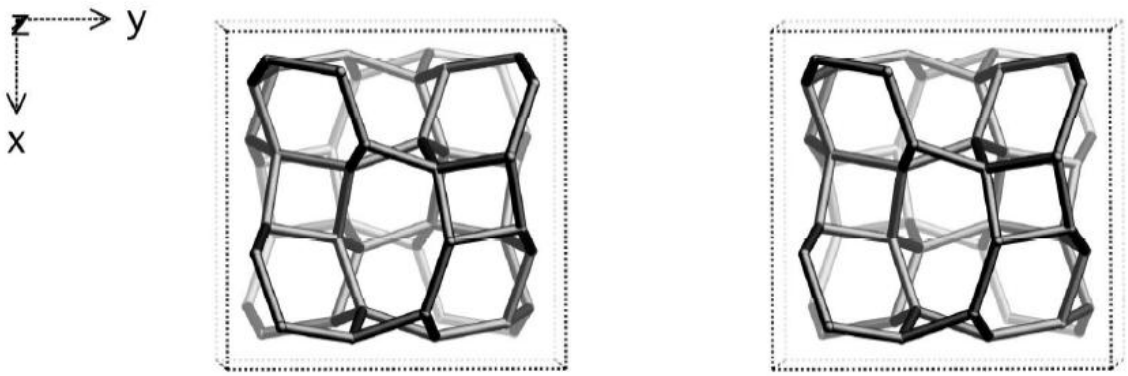

Figure 12: Perspective view of the framework of wairakite (Baerlocher et al., 2001)

4.1.2 Clay minerals

Clay minerals are common and abundant alteration products in the hydrothermal system (*Figure 13*). They are the dominant alteration minerals in both high- and low-temperature fields in Iceland (Kristmannsdóttir and Tómasson, 1976). Primary minerals like olivine, plagioclase and pyroxene are altered to different types of clays, depending on the temperature and permeability.

There are four distinguished main alteration zones in Icelandic geothermal fields. The first three zones are mainly characterized by a gradual transformation of trioctahedric Fe/Mg smectite (Fe-Mg rich saponite) to chlorite through the interlayer smectite to smectite-chlorite mixed-layer stage. These changes have been correlated with an alteration temperature of 200-240 °C. Above this temperature, chlorite is the dominant sheet-silicate and the change to the fourth alteration zone, which is the actinolite zone, occurs at temperatures of 280-290 °C. A correlation temperature of the alteration zones found in Icelandic high-temperature geothermal fields with tholeiite basaltic subsurface rocks and dilute water is shown in *Figure 14* (Kristmannsdóttir, 1985).

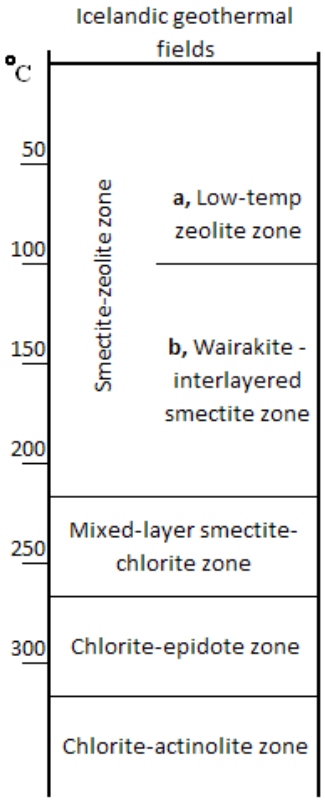

Figure 13: Alteration zones in geothermal field (Kristmannsdóttir, 1985).

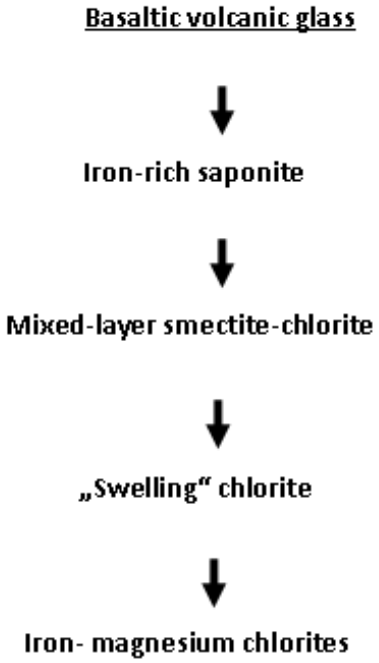

Figure 14: The clay mineral group conversions typical for alteration of basaltic volcanic glass (Kristmannsdóttir, 1976)

The clay minerals are part of a general but important group within the phyllosilicates or sheet silicates that contain large percentages of water trapped between the silicate sheets. The chlorite minerals are sheet silicates structurally related to the clay minerals, but not included in the group of clay minerals. Most clay minerals are chemically and structurally analogous to other phyllosilicates but contain different amounts of water and a slight substitution of their cations (Amethyst Galleries, The Clay Mineral Group, 2009).

Smectite Group

The basic structural unit of smectite is a layer consisting of two inward-pointing tetrahedral sheets with a central alumina octahedral sheet. The layers are continuous in the directions of the a and b crystal axes. The layers are slightly negatively charged and held together by interlayer cations. The bonds between the layers are weak and have excellent cleavage, allowing water and other molecules to enter between the layers causing expansion in the c direction (Grim, 1962).

Smectites commonly result from the weathering of basaltic rocks. Smectite formation is favored by level to gently sloping terrenes that are poorly drained, mildly alkaline (such as in marine environments), and have high Si and Mg potentials (Borchardt, 1977). Other factors that favor the formation of smectites include the availability of Ca and the paucity of K. Poor drainage is necessary because otherwise water can leach away ions (e.g. Mg) freed in the alteration reactions. Smectites are used in the industry as fillers, carriers, absorbents, and a component in drilling fluids (Grim, 1962).

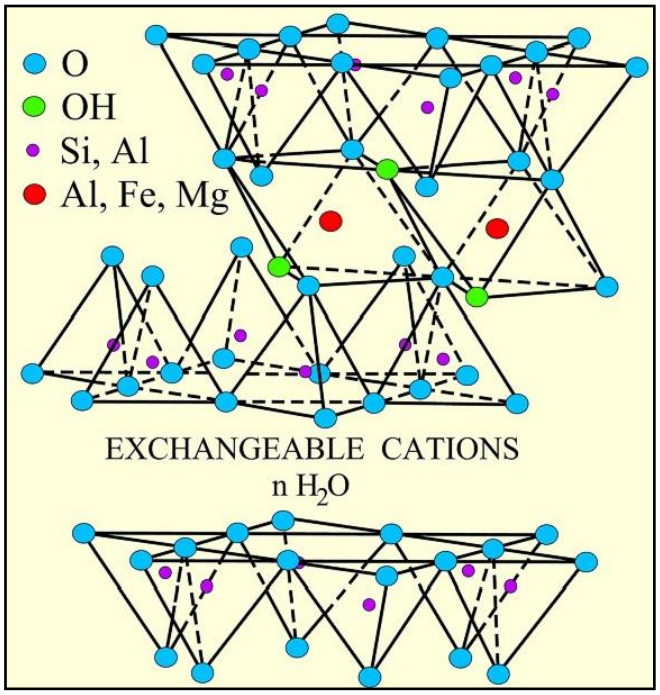

Figure 15: Structure of montmorillonite (modified from Grim (1962) (USGS Open-file report 01-041, Smectite Group, 2009)

Smectites yield X-ray diffraction patterns characterized by basal reflections (001) at 13-15 Å that vary with humidity, exposure to certain organic molecules, heat treatment, and exchangeable cations (Wilson, 1987). When saturated with ethylene glycol, the 001 reflection of most smectites will swell to about 17 Ångstroms (about 17.8 Ångstroms with glycerol); when heated to 400 °C, the 001 reflection will collapse to about 10 Ångstroms (the exact amount of collapse is often related to the exchange cations present and to the smectite itself). Individual smectites can sometimes be differentiated by their higher-order peaks or by cation saturation (Figure 15) (USGS Open-file report 01-041, Smectite Group, 2009).

Illite Group

Illite is essentially a group name for non-expanding, clay-sized, dioctahedral, micaceous minerals. It is structurally similar to muscovite in that its basic unit is a layer composed of two inward-pointing silica tetragonal sheets with a central octahedral sheet. However illite has, on average, slightly more Si, Mg, Fe, and water and slightly less tetrahedral Al and interlayer K than muscovite (Bailey, 1980). The weaker interlayer forces caused by fewer interlayer cations in illite also allows more variability in the manner of stacking (Grim, 1962). Glauconite is the green iron-rich member of this group (*Figure 16*).

Illite, which are the dominant clay minerals in argillaceous rocks, form by the weathering of silicates (primarily feldspar), through the alteration of other clay minerals, and during the degradation of muscovite. Formation of illite is generally favored by alkaline conditions and by high concentrations of Al and K. Glauconite forms authigenically in marine environments and occurs primarily in pelletal form.

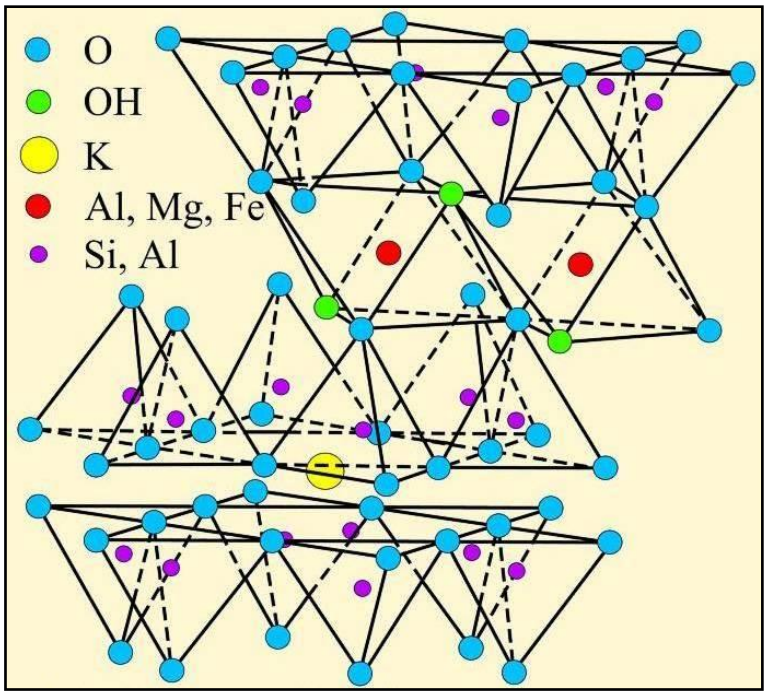

Figure 16: Structure of illit/mica (modified from Grim, 1962) (USGS Open-file report 01-041, Illite group, 2009)

Members of the illite group are characterized by intense 10-Ångstrom 001 reflection and a 3.3-Ångstrom 003 peaks that remain unaltered by ethylene glycol or glycerol solvation, potassium saturation, and heating to 550 °C (Fanning and others, 1989). Glauconite can be differentiated from illite by a 1.5- to 1.52-Ångstrom 060 peak (illite's 060 peak occurs at 1.50 Ångstroms), and by the presence of only a very weak 5-Ångstrom 002 peak.

(USGS Open-file report 01-041, Illite Group, 2009)

Chlorite Group

The basic structure of chlorites consists of negatively charged mica-like (2:1) layers regularly alternating with positively charged brucite-like (octahedral) sheets (Grim, 1962). Members of the chlorite group include: brunsvigite, chamosite, clinochlore, cookite, diabantite, nimite, pennantite, penninite, ripidolite, sheridanite, and thuringite. Ripidolite is the most common chlorite in Icelandic high-temperature geothermal fields (Kristmannsdóttir, 1984). The various members are differentiated by the kind and amount of substitutions within the brucite-like layer and the tetrahedral and octahedral positions of the mica-like layer (*Figure 17*).

The chlorite minerals are common components of low-grade greenschist facies metamorphic rocks, and of igneous rocks as hydrothermal alteration products of ferromanganese minerals. Chlorites are also common constituents of argillaceous sedimentary rocks where these minerals occur in both detrital and authigenic forms.

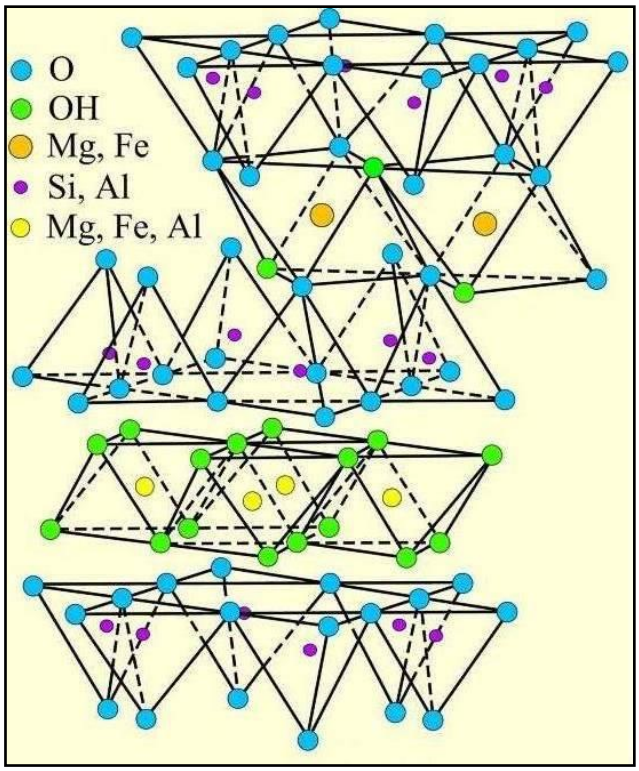

Figure 17: Structure of chlorite (modified from Grim, 1962) (USGS Open-file report 01-041, Chlorite Group, 2009)

Chlorites have their 001 peak at 14 to 14.4 Ångstroms, depending on the individual species. Peak positions are unchanged by ion saturation, solvation with ethylene glycol, or heating. However, heat treatments above 500 °C alter peak intensities (Barnhisel and Bertsch, 1989; Moore and Reynolds, 1997). Typically, the 001 chlorite peak may increase dramatically and higher-order peaks may be conspicuously weakened. In poly-mineralic samples, chlorites can be distinguished from kaolinite by comparisons of the 3.58 Ångstrom kaolinite and 3.54 Ångstrom chlorite peaks, from smectites by the expansion and contraction of the 001 smectite peak after ethylene glycol solvation and heating to 400 °C, and from vermiculite by the progressive collapse of the 001 vermiculite peaks during heat treatments (USGS Open-file report 01-041, Chlorite Group, 2009).

Mixed layer sheet silicates

Clay minerals are composed of only two types of structural units (octahedral and tetrahedral sheets), therefore different types of clay minerals can articulate with each other, giving rise to mixed-layer clays. The most common type of mixed-layer clay is mixed-layer illite/smectite, and chlorite/smectite. In Iceland the most common type is chlorite/smectite, which is composed of an interstratification of various proportions of chlorite and smectite layers. The interstratification may be random or ordered. The ordered mixed-layer clays may be given separate names. A regularly interstratified trioctahedral mixed-layer clay mineral containing approximately equal proportions of chlorite and smectite layers is termed corrensite (Clay minerals, Sci-Tech Encyclopedia, Answers.com, 2009).

4.2 X-Ray diffraction (XRD) overview

Powder diffractometry is mainly used for the identification of compounds by diffraction patterns. An electron in an alternating electromagnetic field will oscillate with the same frequency as the field. When an X-ray beam hits an atom, the electrons around the atom start to oscillate with the same frequency as the incoming beam. In almost all directions we will have destructive interference because, the combining waves are out of phase and there is no resultant energy leaving the solid sample. However the atoms in a crystal are arranged in a regular pattern, and there will be constructive interference in very few directions. Then the waves will be in phase and well defined X-ray beams will leave the sample in various directions. Hence, a diffracted beam may be described as a beam composed of a large number of scattered rays mutually reinforcing one another.

If we use the three dimensional diffraction grating as a mathematical model, the three indices h, k, l become the order of diffraction along the unit cell axes a, b and c respectively (Scintag, Inc., 1999).

Let us consider an X-ray beam incident on a pair of parallel planes P1 and P2 (*Figure 18*), separated by an interplanar spacing d. The two parallel incident rays 1 and 2 make an angle (θ) with these planes. A reflected beam of maximum intensity will result if the waves represented by 1’ and 2’ are in phase. The difference in path length between 1 to 1’ and 2 to 2’ must then be an integral number of wavelengths, (λ). This relationship can be explained mathematically in Bragg’s law (Scintag, Inc., 1999).

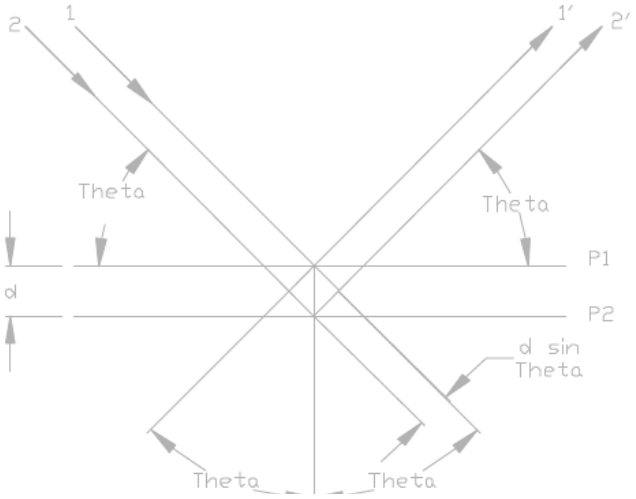

Figure 18: (Scintag, Inc., 1999)

$$n\lambda = 2d\sin\theta$$

$$\lambda = 2d_{hkl}\sin\theta_{hkl}$$

The process of reflection is described here in terms of incident and reflected (or diffracted) rays, each making an angle θ with a fixed crystal plane. Reflections occur from planes set at angle θ with respect to the incident beam and generates a reflected beam at an angle 2θ from the incident beam.

The possible d-spacing defined by the indices h, k, l are determined by the shape of the unit cell.

Therefore the possible 2θ values where there can be reflections are determined by the unit cell dimensions. However, the intensities of the reflections are determined by the distribution of the electrons in the unit cell. The highest electron density is found around atoms. Therefore, the intensities depend on what kind of atoms there are and where they are located in the unit cell (Scintag, Inc., 1999).

Preparation techniques for the analysis of amygdule minerals

For the analysis of amygdule minerals, the samples are first ground in the agate mortar. Care is taken not to grind them too heavily, as the crystal structure may be damaged. The grain size has to be uniform and not too coarse and not too fine. Grinding using a mortar is preferred to the HERZOG grinding mill for this kind of preparation.

For the XRD powder analysis gray plastic sample cups provided by the manufacturer were used. When a very small amount of material was available for analysis, the sample cup used was partly filled up by either cardboard or a coin before the powder was filled in.

The following procedure is followed while preparing the powder sample:

1. Fill up the sample cup with the powder,
2. Use a glass plate to press it into the cup and even it out, getting a smooth surface.

Now the sample is ready for the XRD. More information about running the samples is included in the XRD chapter of this manual.

Preparation techniques of the clays

The extent to which clays must be treated prior to X-ray examination depends on the materials to be studied and the objectives of the work. All preparation techniques may have an impact on modifying the clay minerals. Even such an apparently mild treatment as standing in water can modify smectites significantly. Clays, being layer silicates, are easily damaged by mechanical processes and, being very fine-grained with large surface areas, they may be modified by chemical treatments. Therefore all pre-treatments must be kept to a minimum and must be as mild as possible (Brindley and Brown, 1980).

In relation to particle size, clay is a material with a particle size less than 1 μm (the precise value is a matter of definition, and sometimes 2 μm is taken as the upper limit).
The separation of particles larger than 1 μm by settling in water under gravity often removes the non-clay minerals such as quartz, feldspars, coarse-particle micas, and carbonate minerals (Brindley and Brown, 1980).

The procedure that has been used for the preparation of the clay samples in this study is as follows:

1. First the clay needs to be extracted out of the rock sample that is being examined. The crusher was used to get the sample into small pieces 0,5-2 cm in diameter, that can fit into a glass bottle. Extra caution must be taken not to use the finest material in the crusher tray as it might be crushed rock rather than clay.
2. Add distilled water to the bottle to dissolve the clay.
3. Put the bottle into a *New Brunswick Scientific: Innova 44 - Incubator Shaker Series* and let it run for about 12 hours until the clay has been shaken out.
4. Pour the liquid material with suspended fine grained material into a beaker and let it set. The time depends on the composition of the sample, but about 20-30 minutes is often adequate.
5. Carefully sip up the finest material using a drop counter and put it on a sample glass plate. Let it stand until it is dry. When the material can be safely moved, put it into the desiccators.
6. Put the clay samples on small glass plates that fit into the gray sample cups.

There need to be three runs for each sample on the glass plate in the XRD to get the results:

- first run after equilibration at a fixed hydration in a deccicator with a saturated $CaCl_2$ solution,
- second after being saturated with ethylene glycol in a deccicator,
- third after being heated to about 560 °C for an hour so the smectite structure collapses.

For these runs the clay slit setup and the *clay mains* method defined by Bruker were used for the analysis of clay minerals.

5 PREVIOUS STUDIES

5.1 General exploration

The geothermal research on Þeistareykir high-temperature geothermal area started in 1972. As descibed in chapters 2.3 and 2.4 the geological mapping of the area and general exploration were conducted by intervals over the next 25 years (Gíslason et al., 1984, Ármannsson et al., 1986, Björnsson et al., 2007). The first five boreholes were drilled in 2001.

5.2 Borehole location

Well ÞR-07 is a shallow exploration drill hole with a total depth of 458.1 meters cored from 3 m depth to the bottom. It is located on the 2.500 years BP Þeistareykjahraun lava flow at Lat. N65°53´43.5´´, Long. W17°00´40.0´´ (Garmin GPS) or X=590672, Y=601274 (ÍSNET93 coordinate system), at an elevation of 310 meters above sea level (m.a.s.l.) *Figure 18.* Only 458.1 meters were drilled of the initially planned 600 meters. Core samples from the drill hole were stored and preserved in wooden boxes (each with 7x1.4 m long rows) (Lacasse et al., 2007).

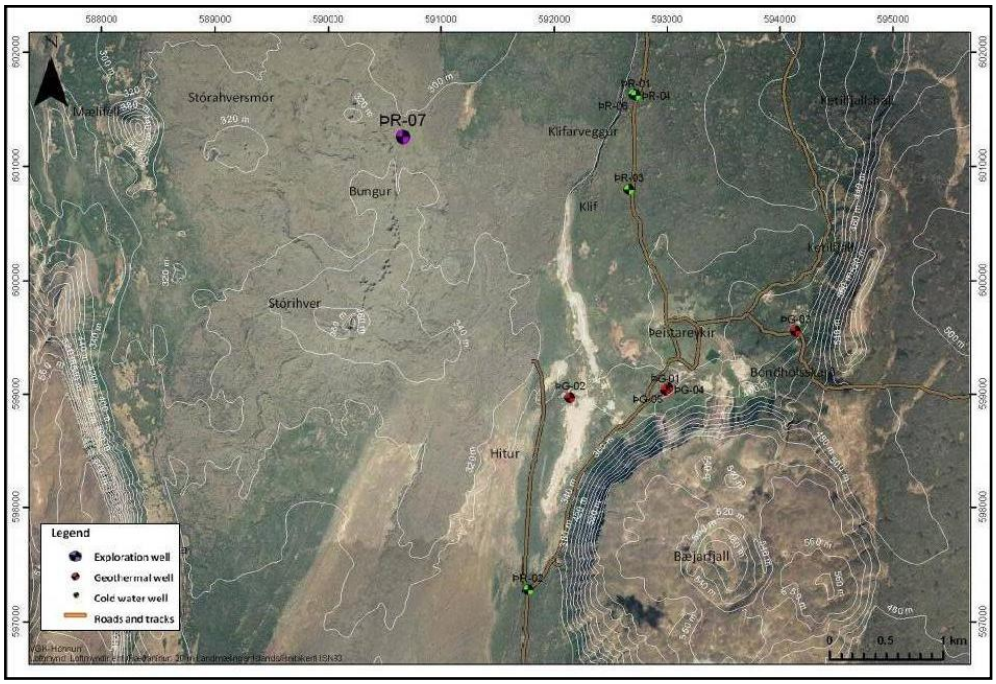

Figure 19: Photo from the area and location map of the drill site ÞR-07(Laccase et al., 2007)

5.3 Temperature logging at ÞR-07

The upper most temperature inversion at 200-210 m depth is confirmed by both Ræktunarsamband Flóa og Skeiða and VGK-Hönnun measurements and appears to be a constant feature with time (1-15 October). It is associated with an altered volcanic sandstone/conglomerate of relatively high porosity. The sequence is characterized by a low core recovery (70%) (*Figure 19*).

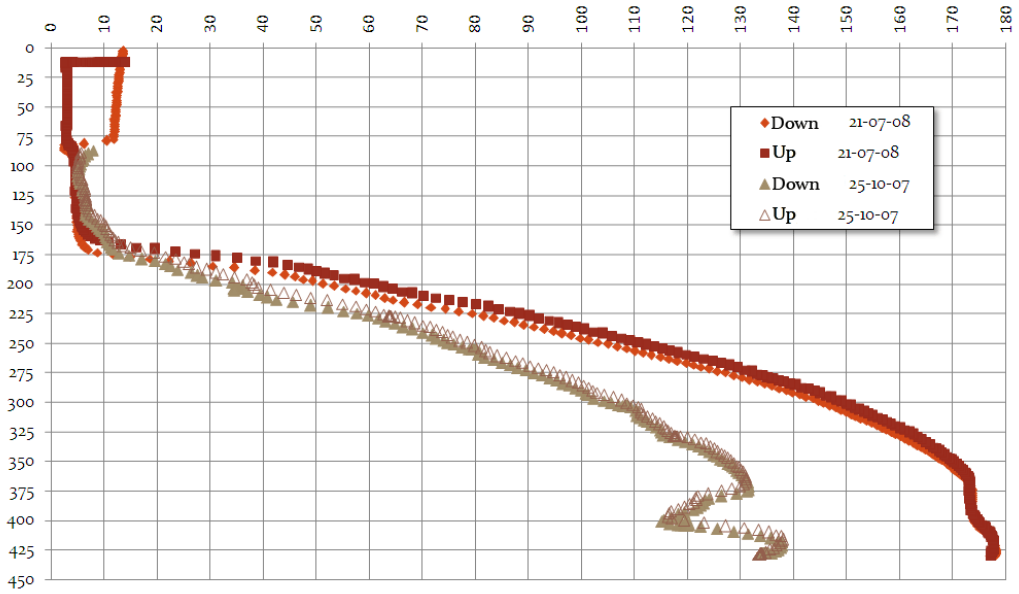

Figure 20: Temperature logging of boreholeÞR-07 (courtesy of Ræktóand VGK-Hönnun, 25.10.07: in Lacasse et al., 2007.

The intermediate temperature inversion at 374-404 m corresponds to a succession of lava flow units characterized by a vesicular and oxidized upper part *(Figure24*).

The lower zone of the temperature inversion is the most significant. It overlaps the same basaltic lava flow succession described above. These basalts are however more vesicular and often bear cm-size void spaces. The resulting higher rock porosity likely enhanced water circulation (Lacasse et al., 2007).

5.4 Geological logging at ÞR-7

The well was drilled down to 458 m total depth by a normal drill bit and cuttings were sampled for examination. The cuttings range from 0.4 to 2.5 cm in size and consist mainly of relatively fresh basalt that is light to dark grey in color.

Several lava flow units were identified as being more vesicular, like their upper part, due to degassing during cooling. The most vesicular cuttings (lapilli, scoria) may have a pyroclastic origin due to a more explosive character of the eruption. Phenocrysts of plagioclase, pyroxene, and rare olivine occur in the rocks. The amount of phenocrysts varies in cuttings and can fill up to 30-40% of the rock volume. Phenocrysts generally occur in the central part of the lava flow units, where cooling was slow and allowed crystals to grow. Fine grained matrix is mainly observed at the top and bottom of the lava flow units where rapid cooling has occurred. The rock texture is therefore aphyric with no phenocryst. Rock alteration is heterogeneous along the 150 m depth interval and is illustrated by variation in the angle of fracture at the ends of the cuttings, by Fe oxidization

and palagonitization of basaltic glass. The reddish surface coating is evidence of a state of oxidization (Lacasse et al., 2007).

Below 153 m depth the rock types observed in cores ÞR-7 can be subdivided into 4 main categories that include volcaniclastic sandstone, "fresh" basalt, altered volcanic breccia, and altered basalt. Volcaniclastic sandstone (*Figure 20*) occurs along the 173-186 m and 200-205 m depth intervals. The dark grey to dark brown sedimentary rock is generally well sorted, stratified, and poorly consolidated (Lacasse et al., 2007).

Figure 21: Representative volcaniclastic sandstone core sample (ÞR-7 K2)

The unconsolidated state of the rock has resulted in poor core recovery as low as 35% (*Figure 21*) with fragments falling down to the bottom of the hole and disturbing core drilling.

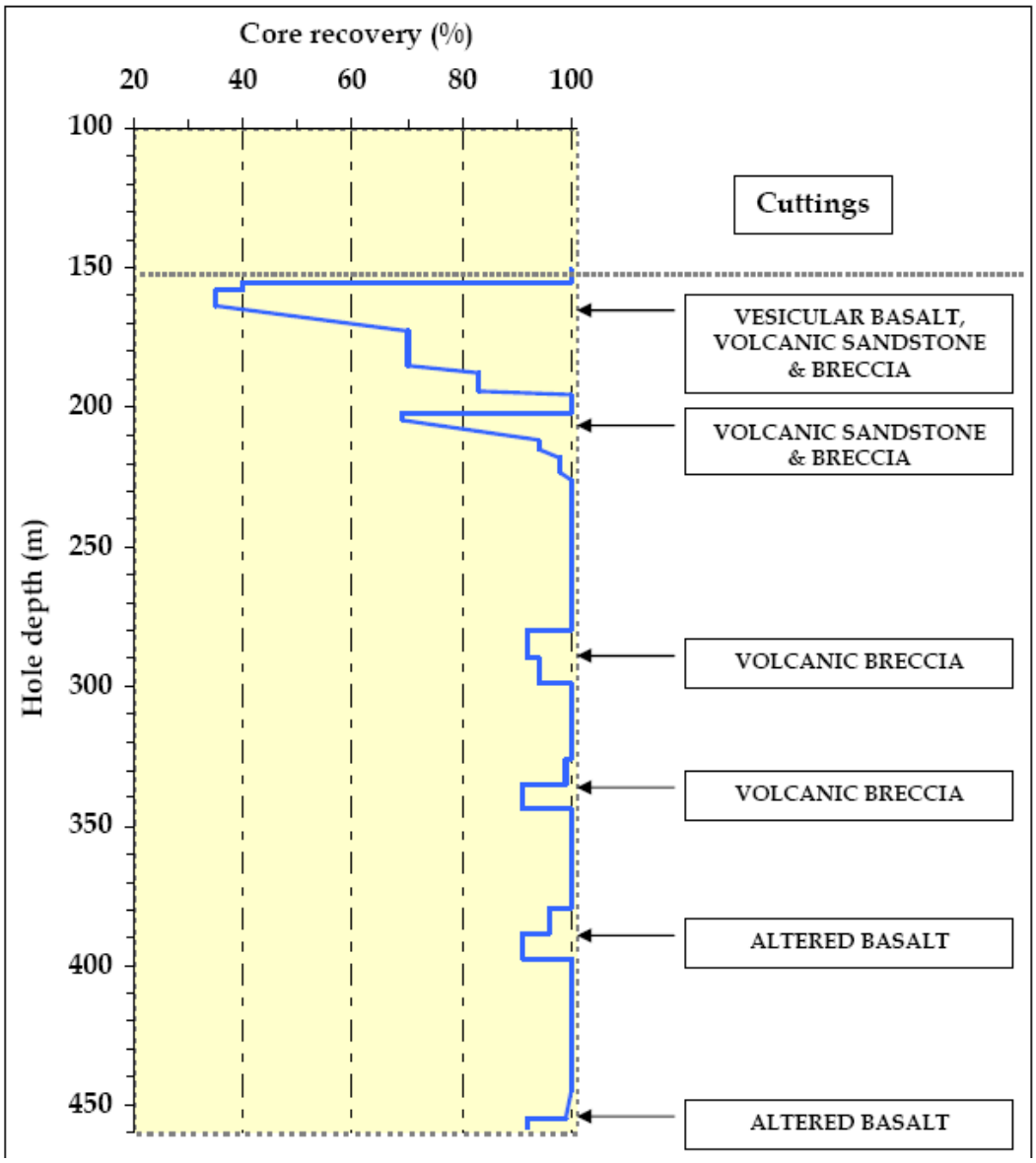

Figure 22: Rate of core recovery at drill site ÞR-7

Relatively less altered basalt occurs along the 151-170 m and 190-200 m depth intervals (*Figure 22*). It is medium to dark grey in color and has few vesicles up to 1.5 cm in diameter. The matrix is fine grained and bears occasional large phenocrysts of plagioclase up to 6 mm in size and rare phenocrysts of pyroxene and olivine (Lacasse et al., 2007).

Figure 23: Representative cores of "fresh" basalt (case ÞR-7-K8)

Volcanic breccia, including tuff horizons, is by far the dominant rock type and represents almost one third of the whole sequence that was drilled at site ÞR-07 (*Figure 23*). The volcanic breccia is mainly originated from subglacial eruptions forming hyaloclastite (móberg) accumulation up to 40-50 m thick, e.g. between 255 and 304 m depth and between 320 and 362 m depth (Lacasse et al., 2007).

Figure 24: Representative cores of altered volcanic breccia (case ÞR-7-K12)

Basaltic rock also occurs as altered individual flow units between 362 m and 425 m depth, with their upper part being vesicular and reddish in color due to oxidization and their lower part being fine grained, non vesicular, and enriched in smectites (*Figure 24*). This rock sequence bears the largest amygdules with macroscopic secondary mineralization (e.g. zeolite) of low to moderate temperatures (Lacasse et al., 2007).

Figure 25: Representative cores of altered basalt (case ÞR-7-K26)

6 APPLIED ANALYTICAL METHODES

The rock samples are washed and cleaned thoroughly with tap water to remove unwanted mud, clay and other contaminants from the drilling activity. After that the representative samples are studied and identified and their relationship interpreted under the binocular microscope. Thin sections for the study by petrographic microscope were also made from a few selected sections of the core. Those were primarily aimed at the study of alteration by replacement of the primary minerals in the rock matrix. A few of the thin sections cut through into vesicles filled by secondary minerals.
As some minerals are not easily identified by examination under the binocular and petrographic microscopes, X-ray diffraction (XRD) was used for the identification of clay minerals and other secondary minerals (mainly zeolites) which can give some information about the hydrothermal alteration (temperature, change in the textural, mineralogical, and chemical composition of the host rocks). A *Bruker* D8 Focus diffractometer was used to analyze the samples with XRD.

Petrographic investigations were conducted on eight representative core samples to determine lithologies and mineral parageneses at Theistareykir. Both bulk samples and mineral habits as well as the optical proportions of minerals were studied in thin sections in transmitted light by the use of an *Euromex polarization microscope ME.2895*. The aim of the study was also to confirm and augment field observations in terms of mineral parageneses and phase relations.

A set of analytical techniques was used to confirm phase identities and compositions. Power *X-Ray Diffractions* (XRD) were conducted on mineral separates using a *Bruker* D8 Focus diffractometer with CuKα operating at 40 kV and 40 mA. Samples for XRD identification were extracted from amygdules and vesicles with dentist tools and pulverized with a mortar. Zeolite mineral compositions were planned to be determined using *Bruker* AXS S4 Pioneer Sequential X-ray spectrometer and an automated *X-Ray fluorescence* (XRF) *spectrometer*, but due to a breakdown of the equipment those measurements were postponed.

7 ANALYTICAL RESULTS

In this chapter are summaries of all the results obtained from the analytical methods.

7.1 Petrography

When choosing the samples, for making thin sections, the goal was to investigate changes in the rock texture with increasing depth and to observe the increasing replacement of primary minerals (*Table 1*). Therefore samples enriched in secondary minerals and with an altered matrix were preferentially selected. The thin sections were made at Nýsköpunarmiðstöð Íslands, to the specification of the author. All of them have a thickness about 30 µm.

Table 1: Thin sections with depth

Num	ID	Depth (m)
01	ÞR-07 / K4	196.4
02	ÞR-07 / K6	224.4
03	ÞR-07 / K6	224.4
04	ÞR-07 / K17	320.7
05	ÞR-07 / K21	356.3
06	ÞR-07 / K21	356.3
07	ÞR-07 / K26	407.8
08	ÞR-07 / K32	458

In all samples the rock type is dominated by clinopyroxene, plagioclase and olivine. Between the samples the differences are shown in the alteration rate and the type of the secondary minerals. In the amygdules and fractures the generation of the minerals were clearly visible. The sheet silicates appear first on the wall, quartz and/or zeolite appear second, and finally calcite appears (*Figures 26, 27*).

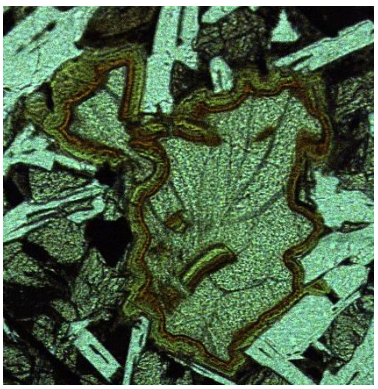

Figure 26: Clay minerals and zeolite in amygdules, 224.4 m (magnification 100X)

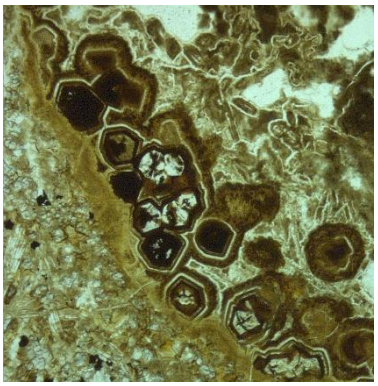

Figure 27: Clay minerals in the amygdule, 458 m (magnification 50X)

<u>01 (ÞR-7/K4)</u>

Sample number 01 from depth 196.4 m is a volcanic breccia which has vesicular clasts ~1cm. It has an average grain size 0.5 – 1 mm, but in the clasts the grain size can be 1.5 mm. The main mineral is the plagioclase; some of the plagioclase twins are altered. Between the plagioclase, clinopyroxene and secondary minerals – like clay – can be found. Amygdules and holes filled with quartz.

The rock fabric is *intersertal*.

<u>02 (ÞR-7/K6)</u>

Sample number 02 from depth 224.4 m is altered basalt with amygdules. The matrix is mainly altered plagioclase and clinopyroxene. The average grain size is 0.5-1 mm. In the vesicles of the altered plagioclase and also around the mineral clay minerals with radial structure can be seen. The amygdale walls are covered with clay minerals with radial structure and overgrowth calcite crystals and sometimes zeolite crystals.

The rock fabric is *porphyritic intersertal*.

<u>03 (ÞR-7/K6)</u>

Sample number 03 from depth 224.4 m is altered basalt with amygdules. The matrix is mainly altered plagioclase and clinopyroxene. The average grain size is 0.5-1 mm, but some of the plagioclase is sometimes more than ~2 mm. In the vesicles of the altered plagioclase and also around the mineral clay minerals with radial structure can be seen. The amygdale walls are covered with clay minerals and overgrowth calcite crystals and zeolite crystals.

The rock fabric is *porphyritic intersertal*.

<u>04 (ÞR-7/K17)</u>

Sample number 04 from depth 320.7 m is volcanic breccia, with basalt clasts and amygdules. The matrix is poorly crystallized. The clasts have a highly crystallized matrix with euhedral plagioclase and pyroxenes, which are partly altered and changed to clay. In the vesicles of the altered plagioclase and also around the pyroxene and the opaque

minerals clay minerals with radial structure are visible. The amygdale walls are covered with clay minerals and overgrowth calcite crystals and zeolites.

The rock fabric is *intersertal*.

05 (ÞR-7/K21)

Sample number 05 is from a depth of 356.3 m (the volcanic tuff zone). It has amygdules and vesicles. The matrix includes plagioclase, clinopyroxene, opaque minerals and quartz. The feldspar and the pyroxene are altered between the grains, where greenish radial clay minerals are shown. In the amygdules and fissures there is radial clay, some with quartz and zeolite.

The rock fabric is *ophitic*.

06 (ÞR-7/K21)

Sample number 06 from a depth of 356.3 m is also from the volcanic tuff layer. The matrix builds up with plagioclase, pyroxene and opaque minerals; some of the pyroxene have a grain size ~2 mm. These minerals are altered, the vesicles of the plagioclase are filled with clay minerals and sometimes the whole pyroxene and plagioclase crystals have changed to clay and just the shape persists (pseudomorph). The amygdules are filled with radial structured clays and some of them with overgrown quartz and zeolites.

The rock fabric is *ophitic*.

07 (ÞR-7/K26)

Sample number 07 is from a depth of 407.8 m, which is the altered basalt layer. The matrix of the samples has an unoriented structure, which is built up from plagioclase and pyroxene and opaque minerals. These minerals are strongly altered. The vesicles of the plagioclase are filled with clay minerals. Some of them have just their own shape, filled with clay (pseudomorph). The walls of the amygdules are covered with radial structural clays and overgrown zeolite (laumontite) which is well crystallized. Some of these amygdules also have quartz.

The rock fabric is *intersertal*.

08 (ÞR-7/K32)

Sample number 08 is from a depth of 458.1 m, also from the altered basalt layer. The matrix builds up with plagioclase and pyroxene. There is some plagioclase which has a grain size ~5 mm. The alteration is visible in the vesicles of the plagioclase, they are filled with clay. These big plagioclases have fluid inclusions. These inclusions are found in the growth face. The amygdules have radial structured clay, some of them with overgrown quartz and zeolites.

The rock fabric is *porphyritic intersertal*.

7.2 Results of XRD analysis of secondary minerals in amygdules and fractures

Table 2: Zeolite samples with depth

Samples	Depth (m)	Secondary minerals
K13	283.9	Calcite
K19	333.9	Mordenite, Quartz
K20	345.4	Laumontite
K21	356.3	Laumontite
K22	369	Laumontite, Yugawaralite, Q, Calcite
K23	380.3	Laumontite
K24	386.9	Laumontite, Calcite
K25	393.3	Laumontite
K26	407.8	Yugawaralite
K27	413.8	Wairakite, Quartz
K28	423.5	Laumontite, Calcite

The following zeolite minerals were identified by XRD analysis of ÞR-7 core: laumontite, yugawaralite, mordenite, and wairakite.
Other minerals identified with XRD were: quartz and calcite, which are found together with the zeolites as shown in *Table 2*.

From the eleven samples measured, six contained Laumontite, which is the most common secondary mineral encountered in amygdules and fractures in the core. In *Figure 28* a typical XRD pattern for laumontite identified in the samples is illustrated. All the XRD patterns (K20, K21, K23, K24, K25 and K28) are completed in Appendix A. The typical patterns for mordenite, wairakite and yugawaralite are displayed in *Figures 29, 30, 31*.

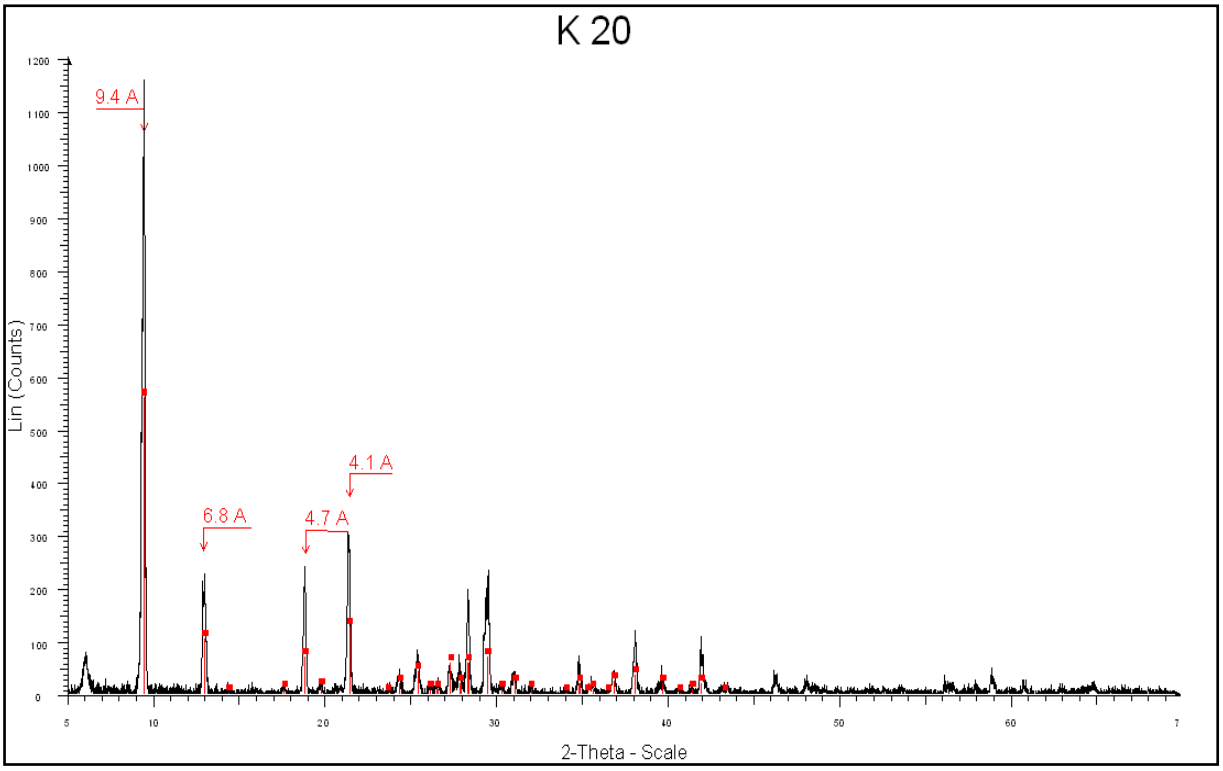

Figure 28: Sample K20 showing the XRD diffraction pattern of laumontite

In some samples, laumontite (*Figure 28*) appears with calcite and in one sample also with yugawaralite and quartz. Yugawaralite (*Figure 31)* is also a quite common zeolite in the amygdules of the core. Mordenite is found in one sample, as well as wairakite.

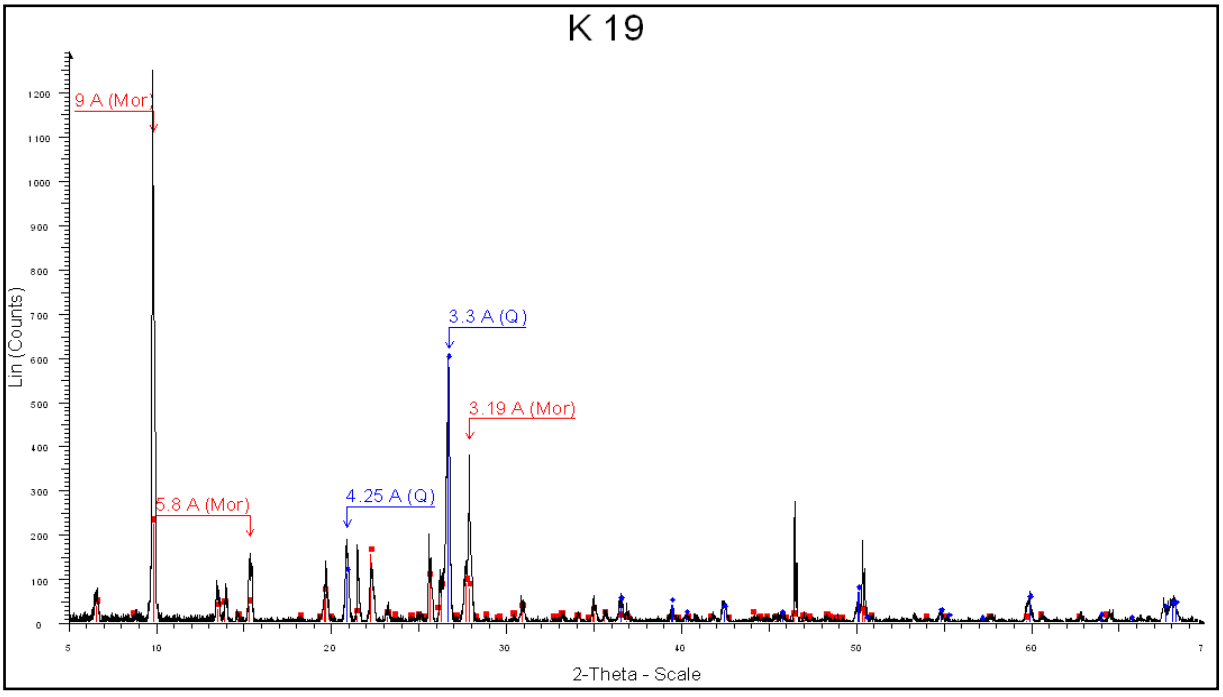

Figure 29: Sample K19 (Mordenite) X-Ray Powder diffraction pattern

These different zeolite minerals were identified in the other samples by the 2°θ and lattice spacing (Å) values. These minerals were yugawaralite, mordenite and wairakite. Two more

minerals were identified: calcite was found to be dispersed in samples from top to bottom and quartz was found in samples taken from a depth of 330 meters, down to the bottom.

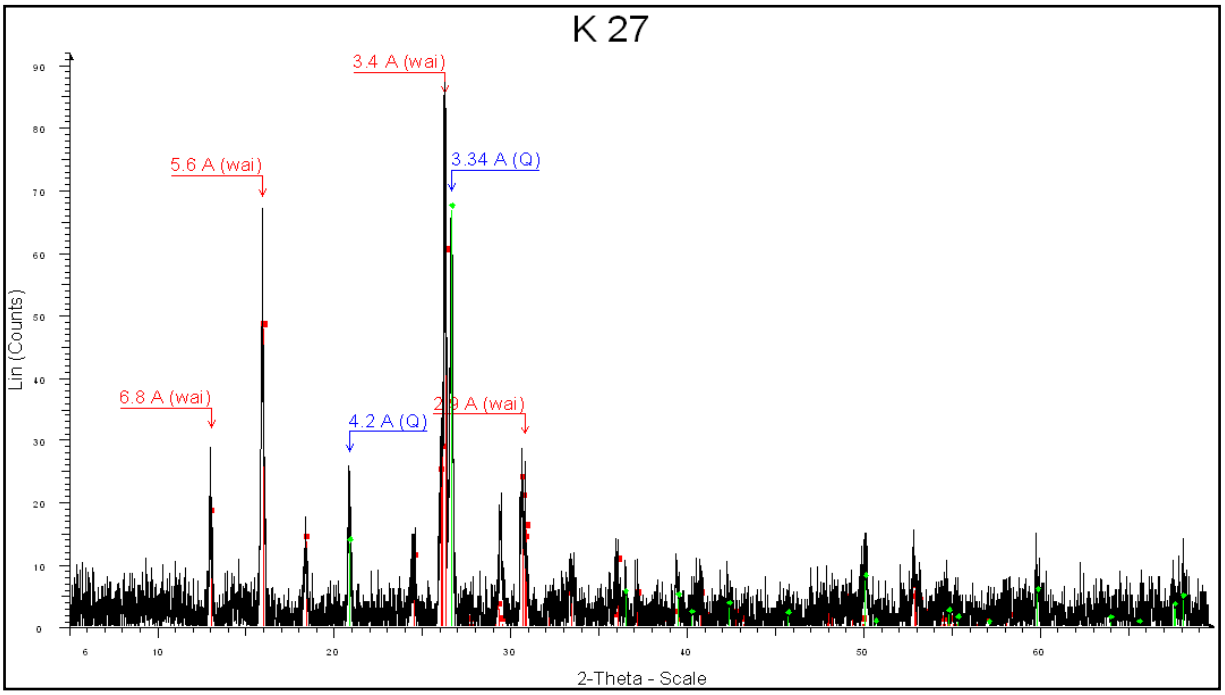

Figure 30: Sample K27 (Wairakite) X-Ray Powder diffraction pattern

Yugawaralite is very rare in Iceland. It has been found in three localities before: in eastern Iceland, in Sthe Snæfellsnes peninsula and in Hvalfjördur in the south west part of Iceland (Barrer et al., 1965; Sigurdsson, 1970; Jakobsson, 1988; Weisenberger and Selbekk, 2008). In the studied well yugawaralite is not the most common mineral, but is by no means rare and appears in well crystalline aggregates.

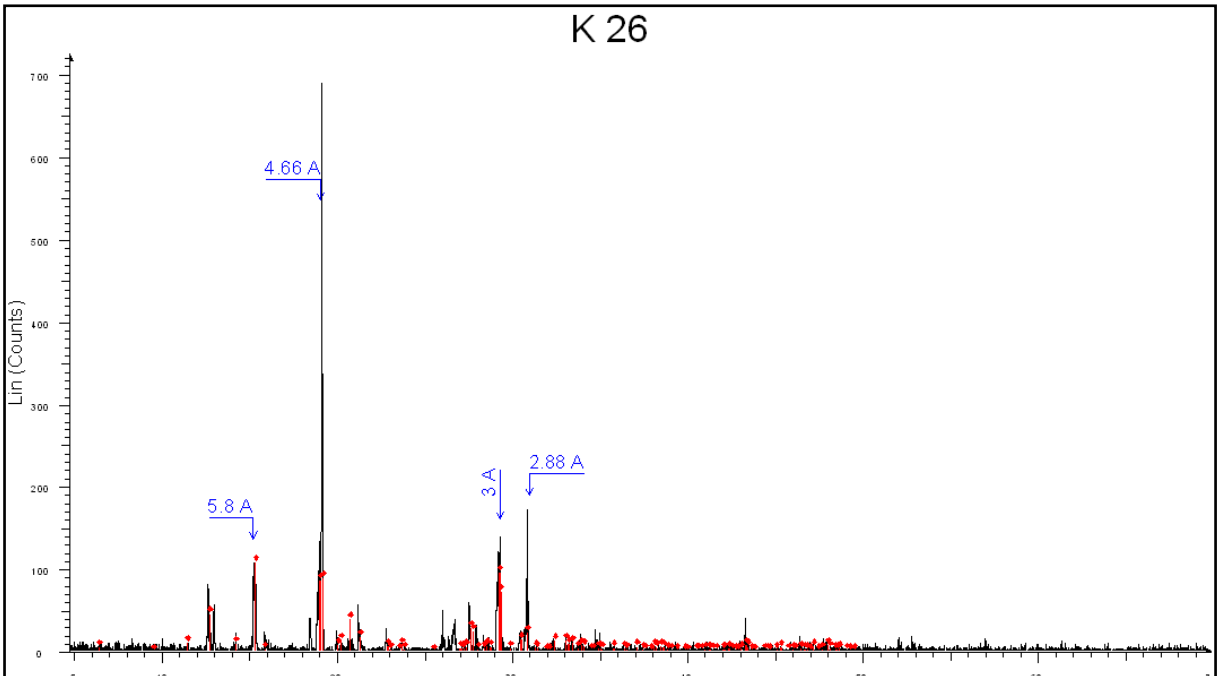

Figure 31: Sample K26 (Yugawaralite) X-Ray Powder diffraction pattern

8.1.2 Clay minerals (sheet silicates)

In the present study seven samples were selected from the core to study the clay mineral-sheet silicate composition. The analytical methods are described in chapter 4.2.1. An additional fourteen samples had been analyzed earlier by Ísor (Jónsson, 2008). The XRD diffraction patterns from that study were reanalyzed in this study because there was disagreement with their conclusions. All the diffraction patterns from both studies are compiled in Appendix A. The results of the interpretation of the XRD patterns are shown in *table* 3. In *Figures 32, 33 and 34* typical diffraction patterns of all the main types of identified sheet silicates are shown. The main motivation in choosing the samples was to select samples with as much clay material as possible, but also to select a representative variation on alteration. Samples were chosen at almost every 100 m depth and the depth of the samples studied by Ísor was also considered in the selection of samples.
The identification of the clay minerals from the diffraction patterns - both the seven from the present study and the fourteen from the Ísor report was based on methods from Brown and Brindley (1980) as well as older clay mineral studies from Icelandic geothermal fields.

As was recounted in *table 3* no clay minerals were encountered in the uppermost 200 m of the core (Jónsson, 2008). Smectite is one of the principal phases present in clay samples K06, K07, K13 and K25 As demonstrated in *figure 32* the d(001) peaks are at about 14 Å in the untreated samples, at 17 Å in glycolated samples and break down to about 10 Å by heating to 560 °C. Well defined chlorite is identified in sample #13 with d(001) at about 14.7 Å in untreated, glycolated and heated samples (*Figure 33*). The d(002) peak is at 7.25 in untreated and glycolated samples, but disappears after heating at 560 °C. In samples #07, 09, 10, 11 and 14 the chlorite is associated with mixed-layer minerals (*Figure 34, 35*) of different kinds and does not withstand heating to 550 °C. Sample K17 is a mixed-layer mineral of smectite and chlorite which breaks down into two different components when heated (*Figure 34*). As seen in *table 3* and from the XRD diffraction patterns some of the

interpretations are complex as the minerals are often poorly crystalline and not pure components of any single type of mineral. Some of the minerals are probably the result of retrograde change of minerals formed previously at higher temperature conditions.

Table 3: XRD samples identification with depth

# ID	Depth m.	d(001) Å UNT.	d(001) Å GLY.	d(001) Å HIT.	Type
#01	-55	n.d	n.d	n.d	No clay
#02	-99	n.d	n.d	n.d	No clay
#03	-117	n.d	n.d	n.d	No clay
#04	-160	n.d	n.d	n.d	No clay
#05	-190	n.d	n.d	n.d	No clay
#06	-220	13.0+higher shoulder	14.2	10	*Smectite/Illite-Chlorite*
K06	-224	13-14 broad	17	10	**Smectite**
K07	-236	13-14 broad	17	10	**Smectite**
#07	-250	14 broad	14	-	*Chlorite-(Smectite/Chlorite)*
#08	-280	Mound: tops at 13.2and 14.6	15.8+lower shoulder	Trace at 10	*Smectite/Illite+Chlorite*
K13	-284	14 broad	17	9.8	**Smectite**
#09	-310	14.6+lower shoulder	14.6	Trace at 10	*Chlorite-Smectite/Illite*
K17	-320	14.5	15.7	14.3 and 12.5	*Mixed-Layer Smectite/Chlorite*
#10	-340	14.5	14.5	14 and 12.6	*Mixed-layer chlorite type/poorly heat resistent*
#11	-370	14.5 +lower shoulder	14.6	12.2+10	*Chlorite- Chlorite /Illite/Smectite*
K25	-393	14+lower shoulder	17	10	**Smectite**
#12	-400	15.1* and lower shoulder	14.5	Trace at 10	**Smectite**
K29	-433	14	14.9	-	*Mixed-Layer Chlorite/Smectite*
#13	-430	14.7	14.7	14.7	**Chlorite**
K30	-442	14.5	15.6	13.8 and 12.3	*Mixed-Layer Chlorite/Smectite*
#14	-458	14.5+lower shoulder	14.5+lower shoulder	14.5+12.8	*Chlorite-Illite/Chlorite*
*** humidity not standardized**					

On the XRD patterns the black line shows the untreated samples, the red line the glycolated samples and the blue line shows the pattern after heating the samples over 560 °C. On the pictures from the Ísor report (*Figure 33, 35*) the blue line shows the stage after the ethylene glycol preparation and the red one the sample after heating (560 °C).

The pictures show the typical results of the clay measurement. *Figure 32* is a typical smectite pattern, the d(001) peaks are at about 14 Å in the untreated samples, at 17 Å in glycolated samples and broken down to about 10 Å by heating to 560 °C.

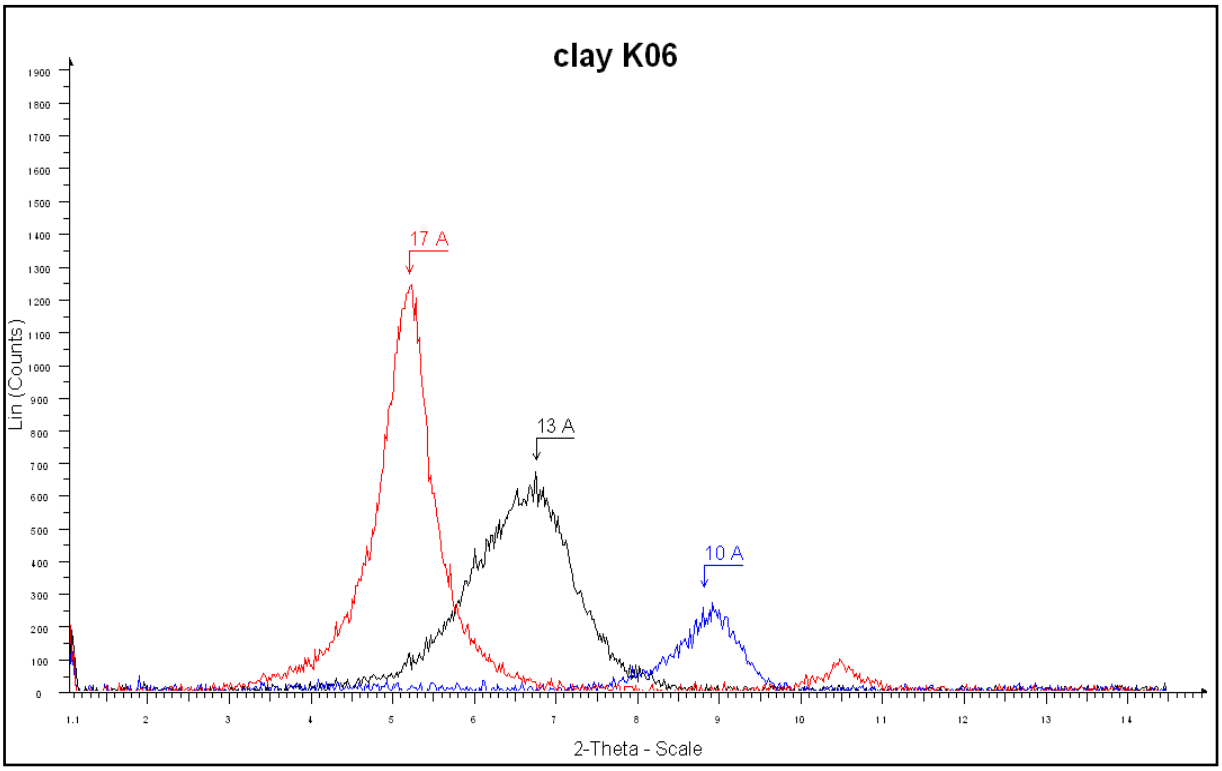

Figure 32: XRD pattern of a typical smectite (sample clay K06)

In sample #13 (Figure 33) the mineral is identified as chlorite with a peak at about 14.7 Å in untreated, glycolated and heated samples. The peak is at 7.25 in untreated and glycolated samples, but disappears after heating at 560 °C. Chlorite does not swell with glycol so in the pattern there is no change in the position of the peaks. Only after heating, the peak does not broke down to 10 Å.

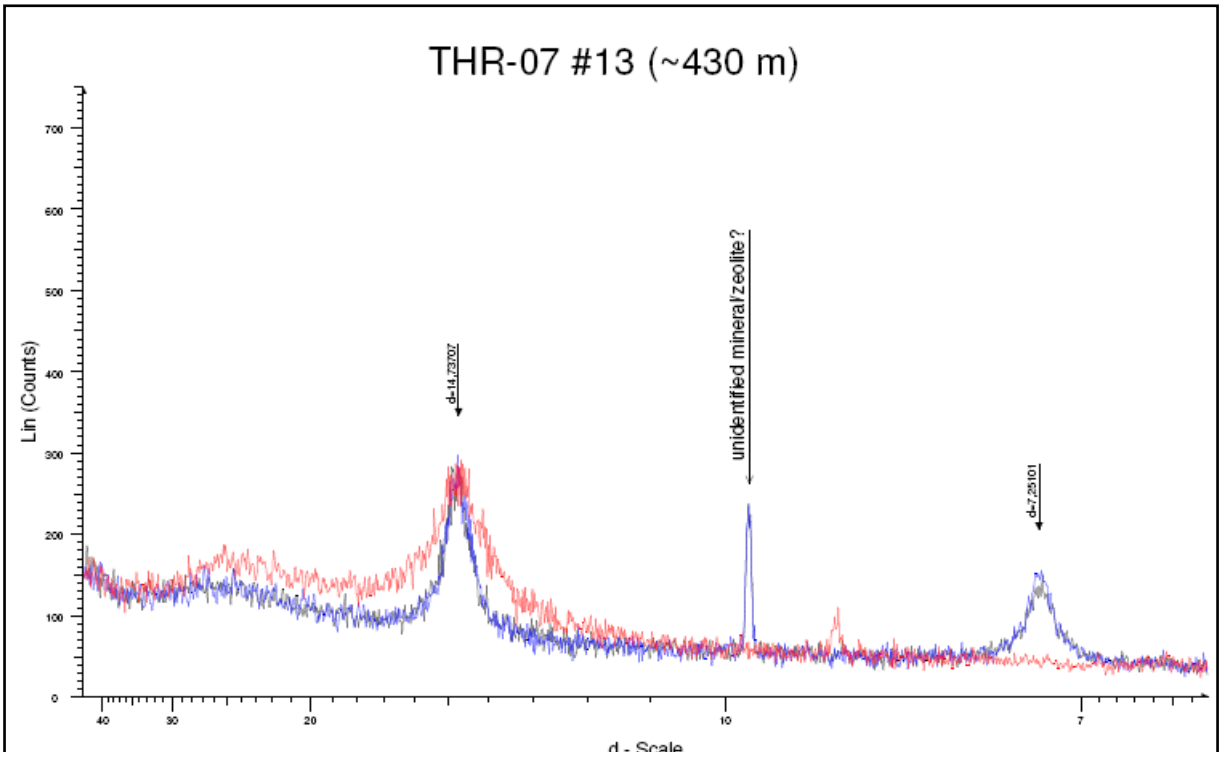

Figure 33: XRD pattern of chlorite (sample #13)

Figure 34 is a mixed-layer sample. It is visible that after heating, the peak broke down to 12,5 and 13,5 Å and not to 10 Å like smectite.

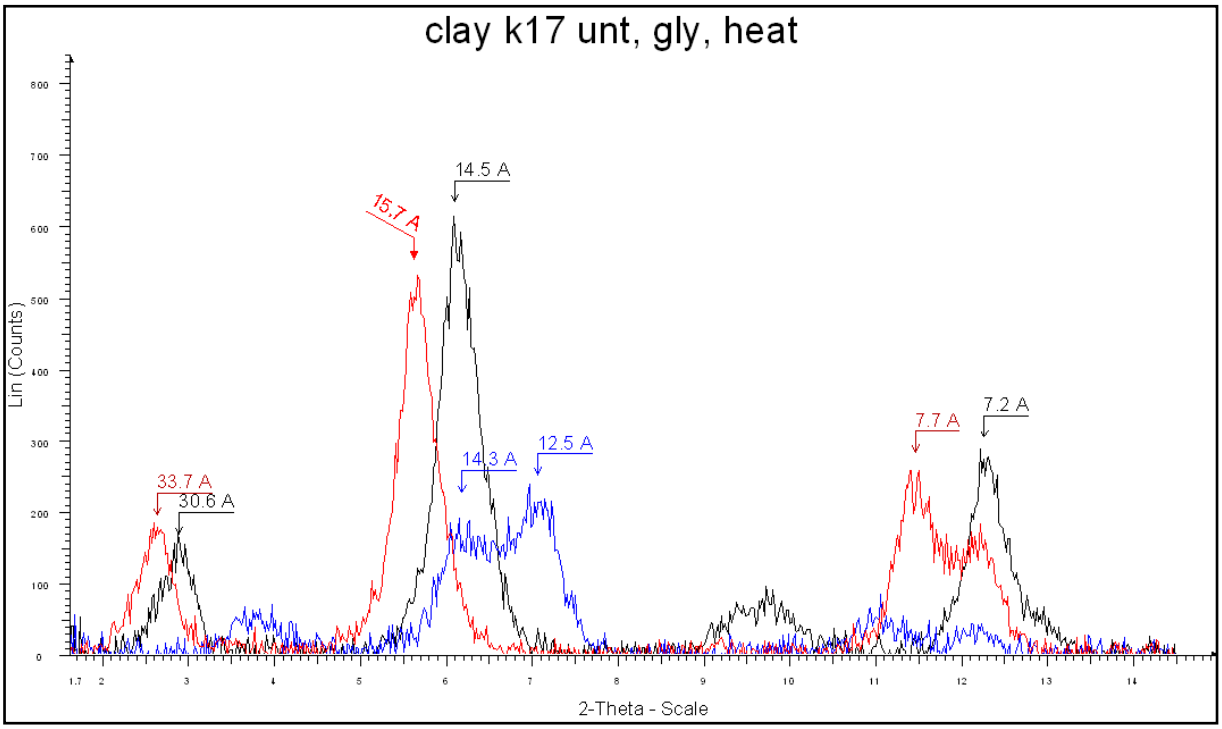

Figure 34: XRD pattern of mixed-layer

Sample #06 on the XRD pattern is identified as a mixed-layer mineral. In the Ísor report (Jónsson, 2008) this sample was identified as smectite. The untreated peak has a shoulder at 14 Å and the glycolated peak does not swell to 17 Å, which means it is not a regular smectite even though a low peak occurs at 10 Å after heating. Part of the substance (e.g. chlorite) does not swell after glycol saturation. So this is interpreted as a mixed-layer mineral of smectite-illite and poorly heat resistant chlorite.

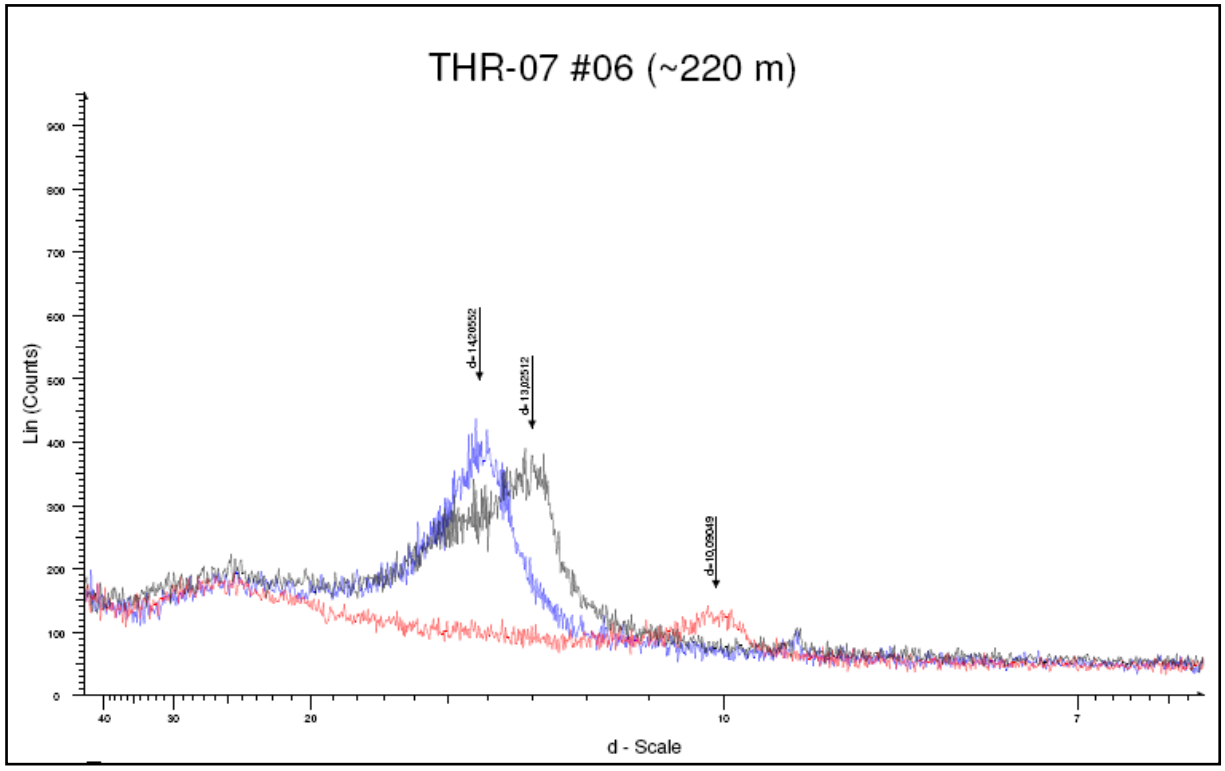

Figure 35: XRD pattern of mixed-layer (sample #06)

8 DISCUSSION

Well ÞR-07 is a shallow exploration drill hole with total depth of 458.1 m. The drill core primarily consists of breccia, altered basaltic rocks and tuffs with intercalated altered basaltic lava flows.

Low-temperature zeolites occur throughout the stratigraphic section, but no high-temperature minerals were detected except wairakite (see chapter 8.1). Analysis of the core showed that above and below the wairakite the dominant zeolite is the laumontite which is a typical low-temperature index zeolite. Yugawaralite and mordenite were found as well among the low-temperature index minerals.

Clay alteration in well ÞR-7 shows no progressive zonation. In the first 200 m there are no clays. Below that there are fund interbedded mostly mixed layers of minerals and smectite. The XRD diffraction patterns (chapter 8.1 and APPENDIX B, C) show the complexity of the material and the often poorly crystalline habit of the minerals. The mineralization, especially of low-temperature minerals like zeolites, laumontite, yugawaralite and mixed-layer clays (and sheet silicates), characterize the lithology in well ÞR-7 at Theistareykir.

The mineral assemblage shows that the temperature in the well has not been constant. The clay minerals were formed at higher temperature and later modified during retrograde alteration. The sequence of the other secondary minerals also points to an overprint of low temperature over higher-temperature minerals, but this is not always clearly demonstrated. Calcite is, by petrographic study, found to crystallize later than quartz and the high-temperature zeolite wairakite is found in the middle of the zone dominated by low-temperature zeolites. Any age relation between wairakite and the lower-temperature zeolites could not be established as wairakite was the only zeolite identified in the actual sample.

The study of the core samples therefore strongly indicates a drop in temperature in this area. The described alterations show that the present temperature is lower than the temperature in the past. Dramatic changes in surface activity have been observed in the Theistareykir area during the time of exploration (Ármannsson, et al., 2000). My study indicates that there have been considerable changes in the activity at depth as well. These results prove that this border zone marks the end of the active high-temperature area. No drilling should be performed beyond the border zone.

9 SUMMARY

The following conclusions can be made from the geological study of well ÞR-7.

1. The stratigraphy of well ÞR-7 (458 m depth) consists primarily of hyaloclastite rocks like breccia and tuff intercalated with altered basalt.
2. By hydrothermal alteration of basalt in Icelandic high-temperature geothermal fields three clay mineral zones are normally distinguished. They are characterized by a gradual transformation of trioctahedric smectite (Fe-Mg rich saponite) to chlorite through the mixed-layer stage where corrensite (smectite-chlorite mixed layer) is dominant.
3. In the core studied no distinct zoning of this kind is observed. Retrograde alteration is indicated by the irregular mixed-layer structures and thermally unstable chlorites and chlorite.
4. Zeolites are found from ~200-458 m depth. Laumontite is the most common (110-230 °C), but yugawaralite (100-120 °C), mesolite-scolecite (80-120 °C) and wairakite (>180 °C) are also found.
5. The zeolite yugawaralite has previously been encountered in only three localities in Iceland.
6. The occurrence of a high-temperature zeolite in the middle of low-temperature zeolite zones could also point to a later overprint of low temperature alteration.

ACKNOWLEDGEMENTS

Special thanks go to my helpful supervisor, **Hrefna Kristmannsdóttir**. The supervision and support that she gave me truly helped the progression of this project.

My grateful thanks also go to both **Christian Lacasse** and **Axel Björnsson**, my advisors.

Not to forget, great appreciation goes to my professor **Csaba Szabó** in Hungary who helped me to get this scholarship.

The whole program at RES brought us together and allowed us to really appreciate the true value of friendship and respect to each other.

Last but not least, I would like to thank my friends, especially those who I worked with at RES.

REFERENCES

Ármannsson, H., Gíslason, G. and Torfason, H. (1986) *Surface exploration of the Theistareykir high-temperature geothermal area, Iceland, with special reference to the application of geochemical methods*: Applied Geochemistry, Vol. 1, pp 47-64.

Ármannsson, H., Kristmannsdóttir, H., Torfason, H. and Ólafsson , M. (2000) *Natural changes in unexploited high – temperature geothermal areas in Iceland*: Proceedings World Geothermal Congress, Japan, p. 521-526.

Armbruster T. and Gunter M.E. (2001) *Crystal structures of natural zeolites*. In: Bish DL, Ming DW, (eds) Natural zeolites: occurrence, properties, application, vol 45, Mineralogical Society of America, Washington, DC, pp 1–57.

Arnórsson, S. (1974) *The composition of thermal fluids in Iceland and geological features related to the thermal activity: In Kristmannsdóttir, H. and Tómasson, J. (1978) Zeolite* zones in geothermal areas in Iceland.

Baerlocher C., Meier W. M.and Olson D. H. (2001) *Atlas of zeolite framework types.* Fifth Revised Edition, Elsevier, p.308.

Bailey, S.W. (1980) *Structure of layer silicates*: *In* Brindley, G.W., and Brown, G., Crystal structures of clay minerals and their x-ray identification: Mineralogical Society, London, p. 1-123.

Barnhisel, R. I. and Bertsch, P. M. (1989) *Chlorites and hydroxy-interlayered vermiculite and smectite: In* Dixon, J.B., Weed, S.B. (eds.) Minerals in soil environments, Soil Science Society of America Book Series, Soil Sci. Soc. Am., Madison, WI, 2nd Edition, p. 729-788.

Barrer, R. M. and Marshall, D. J. (1965) *Synthetic zeolites related to ferrierite and yugawaralite*. Amer. Mineral. 50, p. 484-489.

Björnsson, A. (1990) *Geothermal research*. A review of the nature of geothermal fields, exploration and production (In Icelandic). OS-90020/JHD-04, 50p.

Björnsson, A., Axelsson, G. and Flovenz, O. G. (1990) "*The origin of hot springs in Iceland"(In Icelandic)*. Natturufraedingurinn, 60, p. 15-38.

Björnsson, A., Sæmundsson, K., Sigmundsson, F., Halldórsson, P., Sigbjörnsson, P. and Snæbjörnsson, J. T. (2007): *Geothermal Projects in NE Iceland at Krafla, Bjarnarflag, jástykki and Theistareykir;* Assessment of geo-hazards affecting energy production and ransmission systems emphasizing structural design criteria and mitigation of risk: Landsvirkjun report LV-2007/075.

Borchardt, G.A. (1977) *Montmorillonite and other smectite minerals*. *In*: J.B. Dixon and S.B. Weed, Editors, Minerals in Soil Environments, Soil Science Society of America, Madison, Wisconsin USA, p. 293–330.

Böðvarsson (1961) *Physical characteristics of natural heat resources in Iceland*. Jökull, 11, p. 29-38

Brindley G. W. and Brown, G. (1980) *Crystal structures of clay minerals and their X-ray identification*; Mineralogical society

Browne, P. R. L. (1978) *Hydrothermal alteration in active geothermal systems.* Annu. Rev. Earth Planet. Sci., 6, p. 229-250. *In* Pendon, R. R. (2006) Borehole geology and hydrothermal mineralization of well HE-22, Ölkelduháls field, Hengill area, SW-Iceland. Geothermal Training in Iceland 2006, p. 357-390.

Deer, W. A., Howie, R. A., Zussman, J. and Wise, W. S. (2003) *Rock-forming Minerals*. Second Edition.

Einarsson, P. (1991) *Earthquakes and present-day tectonism in Iceland*, Tectonophys. 189, 261-279: *In* Trønnes, R.G. (2002) *Geology and geodynamics of Iceland: Reykjavik*. Nordic Volcanological Institute, University of Iceland, p.1-19.

Fanning, D. S., Keramidas, V. Z., and El-Desoky, M. A. (1989) *Micas*: *In* Dixon, J.B., and Weed, S.B., Minerals in soil environments, Soil Science of America, Madison, WI, p. 551-634.

Franzson, H. (2006) *Borehole geology*. UNU-GTP, Iceland, lecture notes, unpublished. *In* Pendon, R. R. (2006) Borehole geology and hydrothermal mineralization of well HE-22, Ölkelduháls field, Hengill area, SW-Iceland. Geothermal Training in Iceland 2006, p. 357-390.

Franzson, H.(2008) *Chemical transport in geothermal systems in Iceland: Evidence from hydrothermal alteration*. Journal of Volcanology and Geothermal Research, 173, p. 217–229.

Gíslason, G., Johnsen, G. V., Ármannsson, H., Torfason, H. and Árnason, K. (1984) *Þeistareykir – yfirborðsrannsóknir á háhitasvæðinu.* Skýrsla Orkustofnunar, OS-84089/JHD-16, Reykjavík

Grim, R. E. (1962). *Applied clay mineralogy*. McGraw Hill Book Co. Hong, Z. (1998). Effect of initial water content on compressibility of remoulded Ariake clays. Proc. Int. Symposium on Lowland Technology, Saga University.69- 74.

Halldórsson, P. (2005) *Earthquake activity in North Iceland (Jardskjálftavirkni á Nordurlandi),* Icelandic Meteorological Office (Vedurstofa Íslands), Report, 05021, VÍ-ES-10, 39 p.

Henley, R. W. and Ellis, A. J. (1983) *Geothermal systems ancient and modern. geochemical review*: Earth science and Reviews, 19, 1-50: *In* Pendon, R. R. (2006) Borehole geology and hydrothermal mineralization of well HE-22, Ölkelduháls field, Hengill area, SW-Iceland. Geothermal Training in Iceland 2006, p. 357-390.

Henley, R. W. and Ellis, A.J. (1983) *Geothermal systems ancient and modern: a geochemical review*. Earth Science and Reviews, 19, 1-50.

Jakobsson, S. P. (1988) *Ilvaít.* Steinn, Blad Félags áhugamanna um steinafraedi 1, p. 16-17.

Jóhannesson, H. and Sæmundsson, K. (1998) *Geological map of Iceland. 1:500 000*. Tectonics, Icelandic Inst. of Nat. Hist., Reukjavík: *In* Trønnes, R.G. (2002) *Geology and geodynamics of Iceland: Reykjavik*. Nordic Volcanological Institute, University of Iceland, p.1-19.

Jónsson, S.S. (2008) XRD-*greining á leirsteindum úr kjarnaholu ÞR-07 á Þeistareykjum.* ÍSOR-08034, Mars 2008.

Kristmannsdóttir, H. (1975) *Hydrothermal alteration of basaltic rocks in Icelandic geothermal areas*. Proceeding of the Second U.N. Symposium on Development and use of Geothermal Resources, p. 441-445.

Kristmannsdóttir, H. (1975) *Clay minerals formed by hydrothermal alteration of basaltic rocks in Icelandic geothermal fields*. GFF, Geological Society Sweden Trans.

Kristmannsdóttir, H. (1976) *Type of clay minerals in hydrothermally altered basaltic rocks*. Jökull. 26, p. 30-39.

Kristmannsdóttir, H. (1984) *Chemical evidence from Icelandic geothermal system as compared to submarine geothermal systems*. Hydrothermal Processes at seafloor spreading centers.

Kristmannsdóttir, H. (1985) *The role of clay minerals in geothermal energy research.* Uppsala Symposium Clay Minerals-Modern Society.

Kristmannsdóttir, H. and Tómasson, J. (1974) *Nesjavellir; Hydrothermal alteration in high temperature area*: International Symposium on Water Rock Interaction.

Kristmannsdóttir, H. and Tómasson, J. (1976) *Zeolite zones in geothermal areas in Iceland*. Pergamon press oxford,

Kristmannsdóttir, H. and Tómasson, J. (1978) *Zeolite zones in geothermal areas in Iceland. In* Sand., L. B., and Mumpton, F. A., editors, Natural Zeolites: Occurance, Properties, Use: Elmsford, New York, Pergamon Press, p. 277-284

Lacasse, C., Guðmundsson, G., Þrastarson, R.H., and Elefsen, S.Ó. (2007) *Boreholes ÞR-07, GR-03 in northeast Iceland*. VGK-Hönnun, VH 2007-125, December 2007.

Lawver, L. A. and Müller, R. D. (1994) Iceland *hotspot track*, Geology 22, 311-314: *In* Trønnes, R.G. (2002) *Geology and geodynamics of Iceland: Reykjavik*. Nordic Volcanological Institute, University of Iceland, p.1-19.

Leimer, H. W. and Slaughter, M. (1968) *The determination and refinement of the crystal structure of Yugawaralite*, Zeitschrift für Kristallographie, Bd, S. 88-111 (1969).

Liou J. G.(1970) *Synthesis and Stability Relations of Wairakite, CaAl2Si4O12•2H2O.* Contr. Mineral. And Partol. 27, p. 259-282.

Moore, D. M. and Reynolds, R. C. (1997) *X-ray diffraction and the identification and analysis of clay minerals*. Second Edition, Oxford University Press, New York, p. 378.

Pendon, R. R. (2006) *Borehole geology and hydrothermal mineralization of well HE-22, Ölkelduháls field, Hengill area, SW-Iceland*. Geothermal Training in Iceland 2006, p. 357-390.

Reyes, A. G. (2000) *Petrology and mineral alteration in hydrothermal systems: from diagenesis to volcanic catastrophes*. UNU-GTP, Iceland, report 18-1998, p. 77. *In* Pendon, R. R. (2006) Borehole geology and hydrothermal mineralization of well HE-22, Ölkelduháls field, Hengill area, SW-Iceland. Geothermal Training in Iceland 2006, p. 357-390.

Sigurdsson, H. (1970) *The petrology and chemistry of the Setberg volcanic region and of the intermediate and acid rocks of Iceland*. Univ. of Durham, Ph.D. diss. (unpubl.), p. 321

Sæmundsson, K. (1978) *Fissure swarms and central volcanoes of the neovolcanic zones of Iceland*. In: D.R. Bowes and B.E. Leake (editors), Crustal evolution of northwestern Britain and adjacent regions. Geol. J. Spec. Issue, No 10, 415–432.

Sæmundsson, K. (1979) *Outline of the geology of Iceland*. Jökull 29, 11-28: *In* Trønnes, R.G. (2002) *Geology and geodynamics of Iceland: Reykjavik*. Nordic Volcanological Institute, University of Iceland, p.1-19.

Sæmundsson, K. (2007) *Jarðfræðin á þeistareykjum*. Greinargerð ISOR.

Stefánsson, A., Gíslason S. R. and Arnórsson S. (2001) *Dissolution of primary minerals of basalt in natural waters. II. Mineral saturation state*. Chem. Geol. 172, p. 479-500.

Trønnes, R.G. (2002) *Geology and geodynamics of Iceland: Reykjavik*. Nordic Volcanological Institute, University of Iceland, p.1-19.

Veichow, C. J. And Huann-Jih L. (1971) *The stability fields of natural laumontite and Wairakite and their bearing on the zeolite facies:* Proceedings of the Geological Society of China, 14, p. 34-44.

Weisenberger, T. and Selbekk, R. S (2008) *Multi-stage zeolite facies mineralization in the Hvalfjördur area, Iceland*. International Journal of Earth Sciences, DOI 10.1007/s00531-007-0296-6.

Wilson, M. J. (1987) *X-ray powder diffraction*: *In* A Handbook of Determinative Methods in Clay Mineralogy, M. J. Wilson, ed., Blackie, Glasgow and London, p. 26.

Wolfe, C. J.; Bjarnason, I. T.; VanDecar, J. C. and Solomon, S. C. (1997) *Seismic structure of the Iceland plume*. Nature 385, 245-247: *In* Trønnes, R.G. (2002) *Geology and geodynamics of Iceland: Reykjavik*. Nordic Volcanological Institute, University of Iceland, p.1-19.

X-ray fluorescence spectroscopy (XRF) (2009 February 3). In Amptec Inc., from http://www.amptek.com/xrf.html

http://www.iza-structure.org/databases/pdf.htm -pdf

Clay mineral (2009 February 2). In Sci-Tech Encyclopedia, Answers.com, from http://www.answers.com/topic/clay-minerals

Zeolite (2009, January 30). In Wikipedia, The Free Encyclopedia. Retrieved 23:30, February 6, 2009, from http://en.wikipedia.org/w/index.php?title=Zeolite&oldid=267453893

The Zeolite Group of Minerals (2009, February 1). In Amethyst Galleries, from http://www.galleries.com//minerals/Silicate/ZEOLITES.htm

The Clay Mineral Group (2009 February 1). In Amethyst Galleries, from http://www.galleries.com/minerals/silicate/clays.htm

Smectite Group (2009 February 2). In U. S. Geological Survey Open-file report 01-041, from http://pubs.usgs.gov/of/2001/of01-041/htmldocs/clays/smc.htm

Chlorite Group (2009 February 2). In U. S. Geological Survey Open-file report 01-041, from http://pubs.usgs.gov/of/2001/of01-041/htmldocs/clays/chlor.htm

Illite Group (2009 February 2). In U. S. Geological Survey Open-file report 01-041, from http://pubs.usgs.gov/of/2001/of01-041/htmldocs/clays/illite.htm

Chapter 7: Basics of X-ray Diffraction, (1999) Scintag Inc., from http://epswww.unm.edu/xrd/xrdbasics.pdf

APPENDIX A

XRD patterns of zeolites

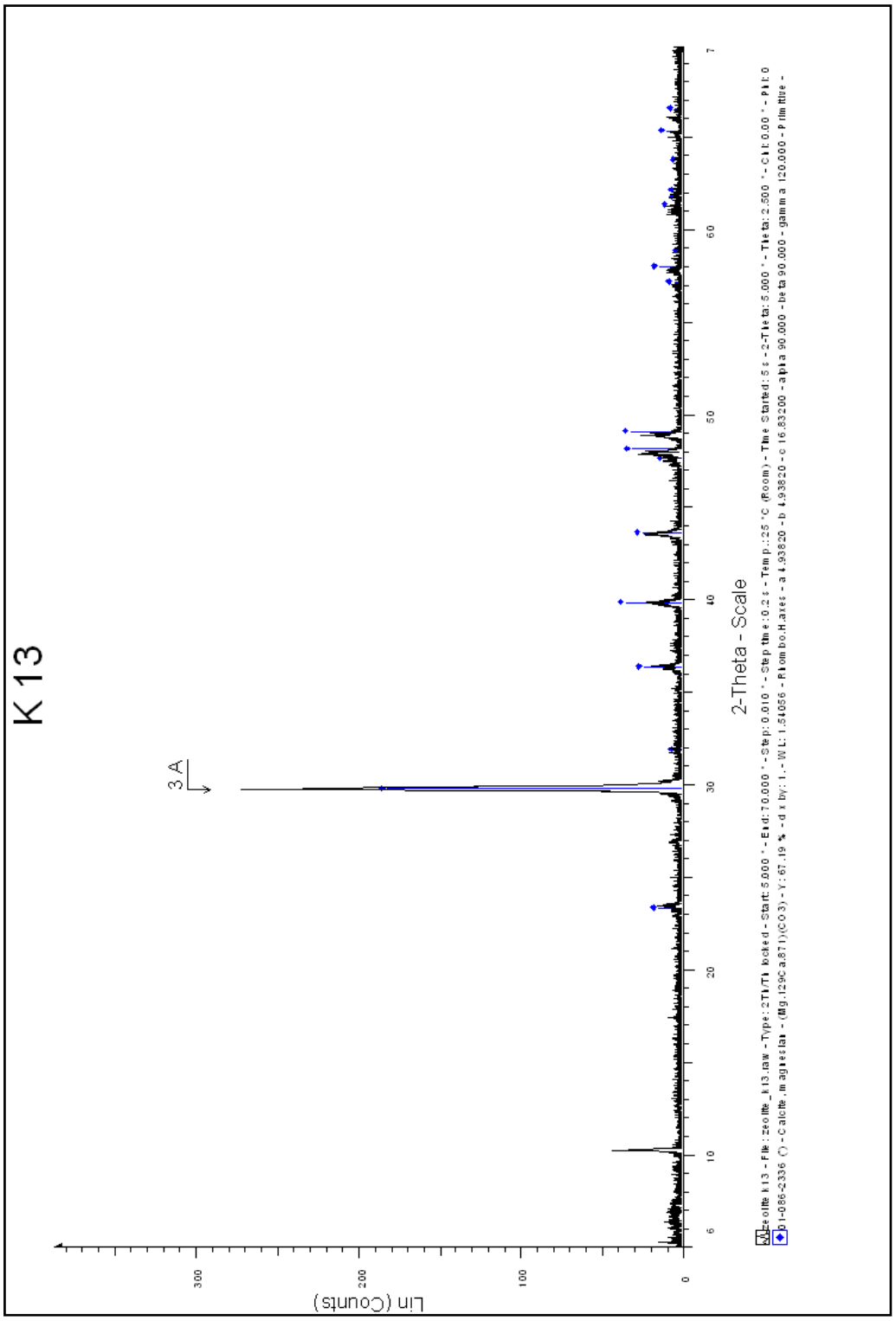

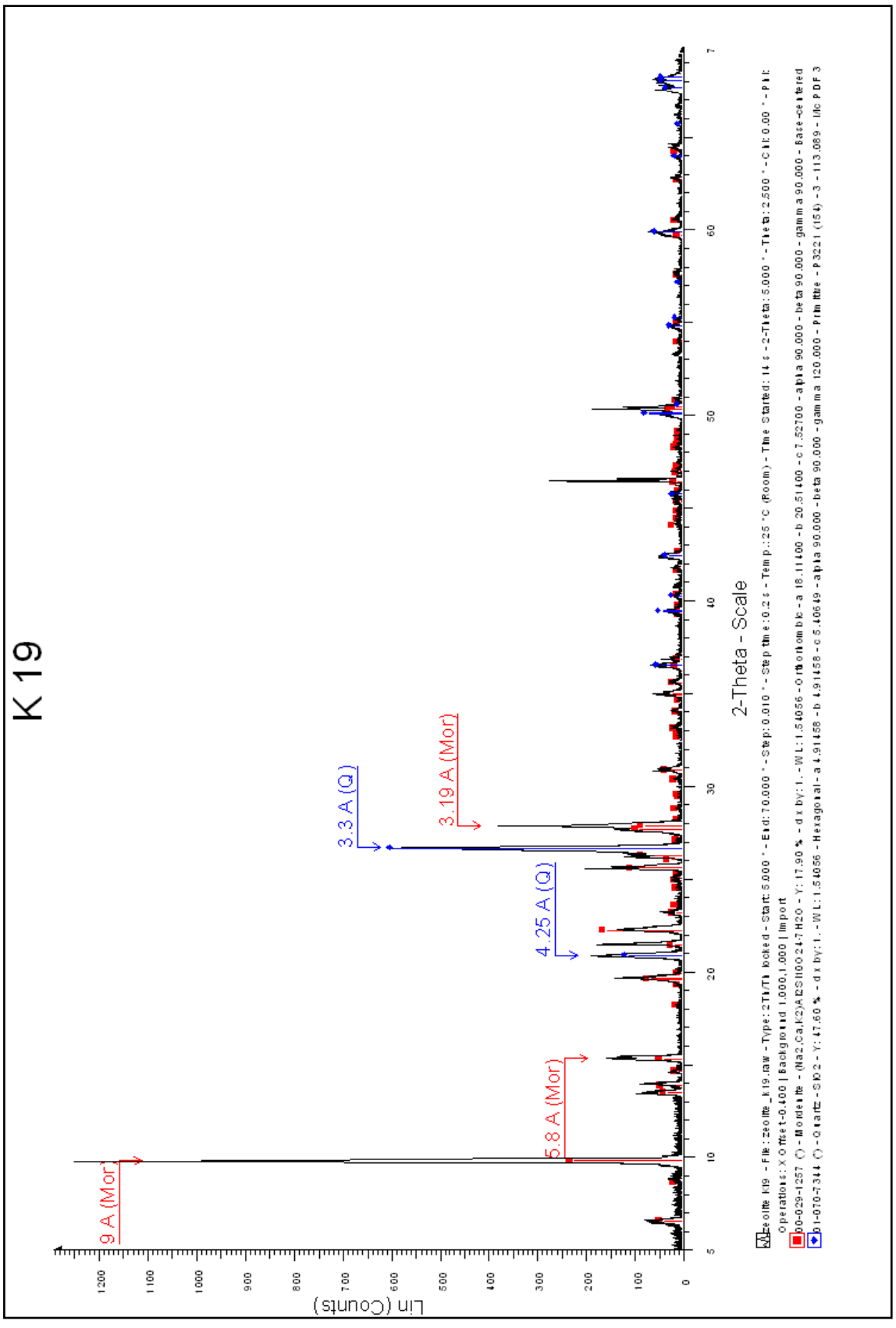
K 19
9 A (Mor)
5.8 A (Mor)
4.25 A (Q)
3.3 A (Q)
3.19 A (Mor)
Lin (Counts)
2-Theta - Scale

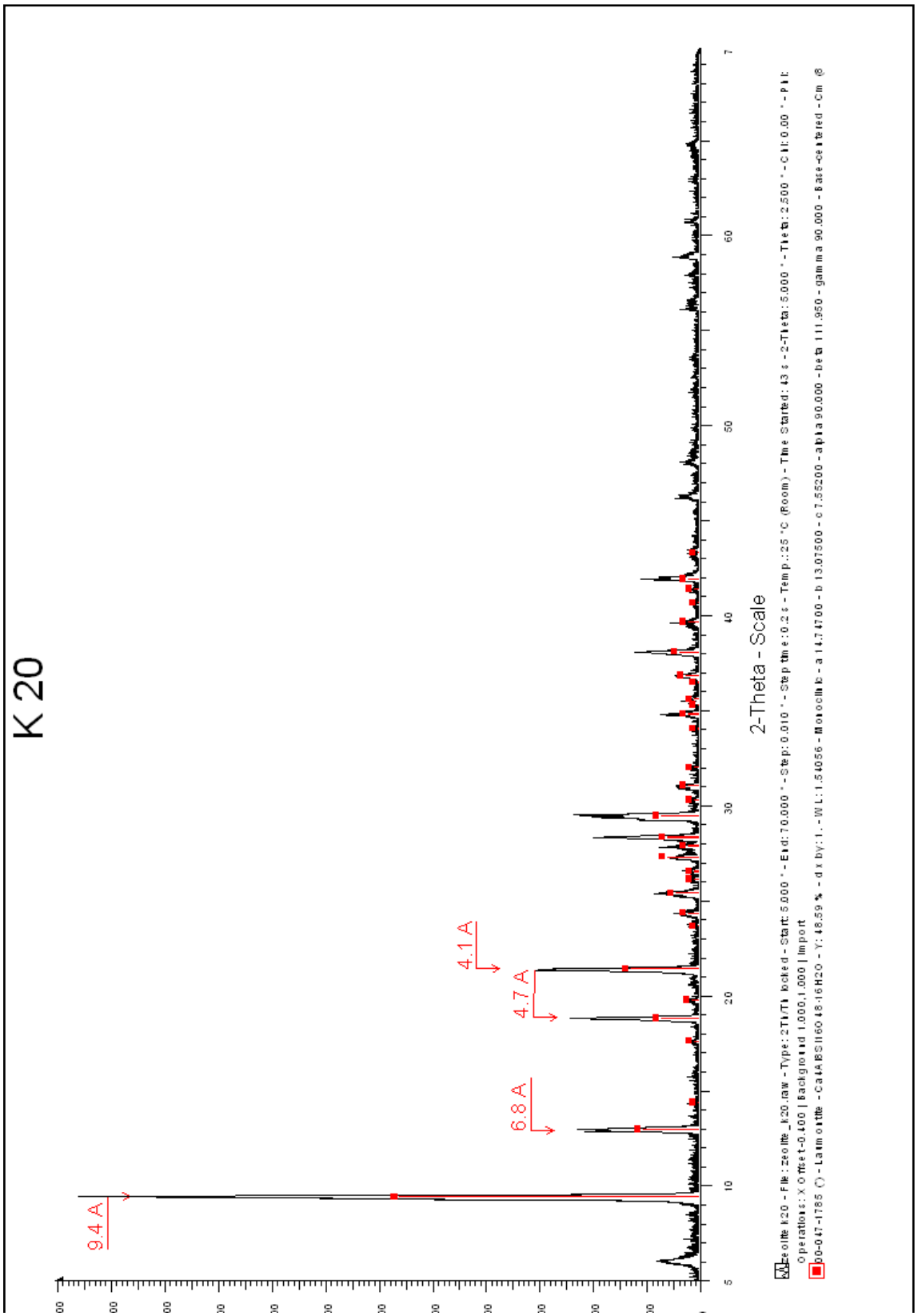
K 20
9.4 A
6.8 A
4.7 A
4.1 A
2-Theta - Scale

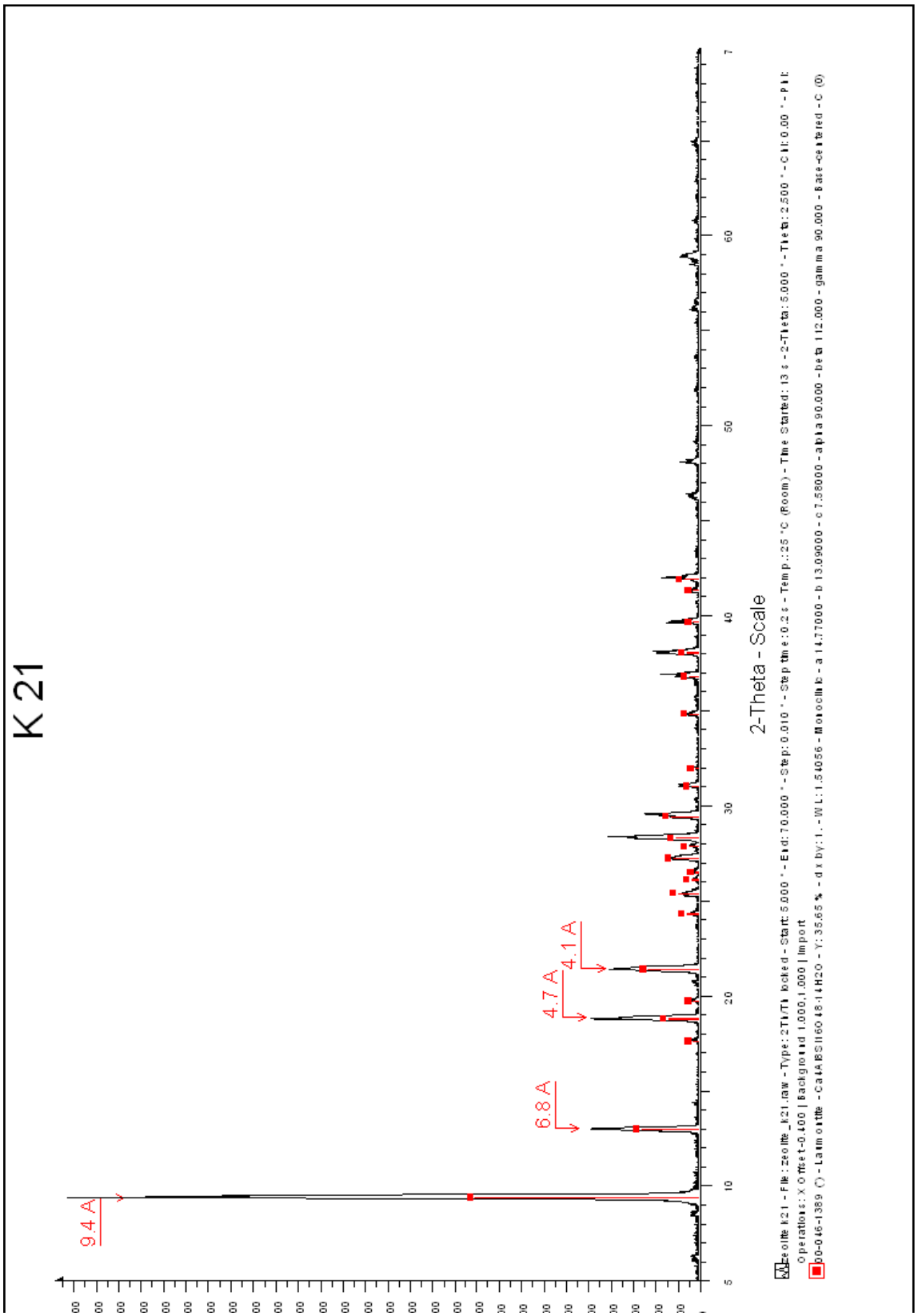
K 21
9.4 A
6.8 A
4.7 A
4.1 A
2-Theta - Scale

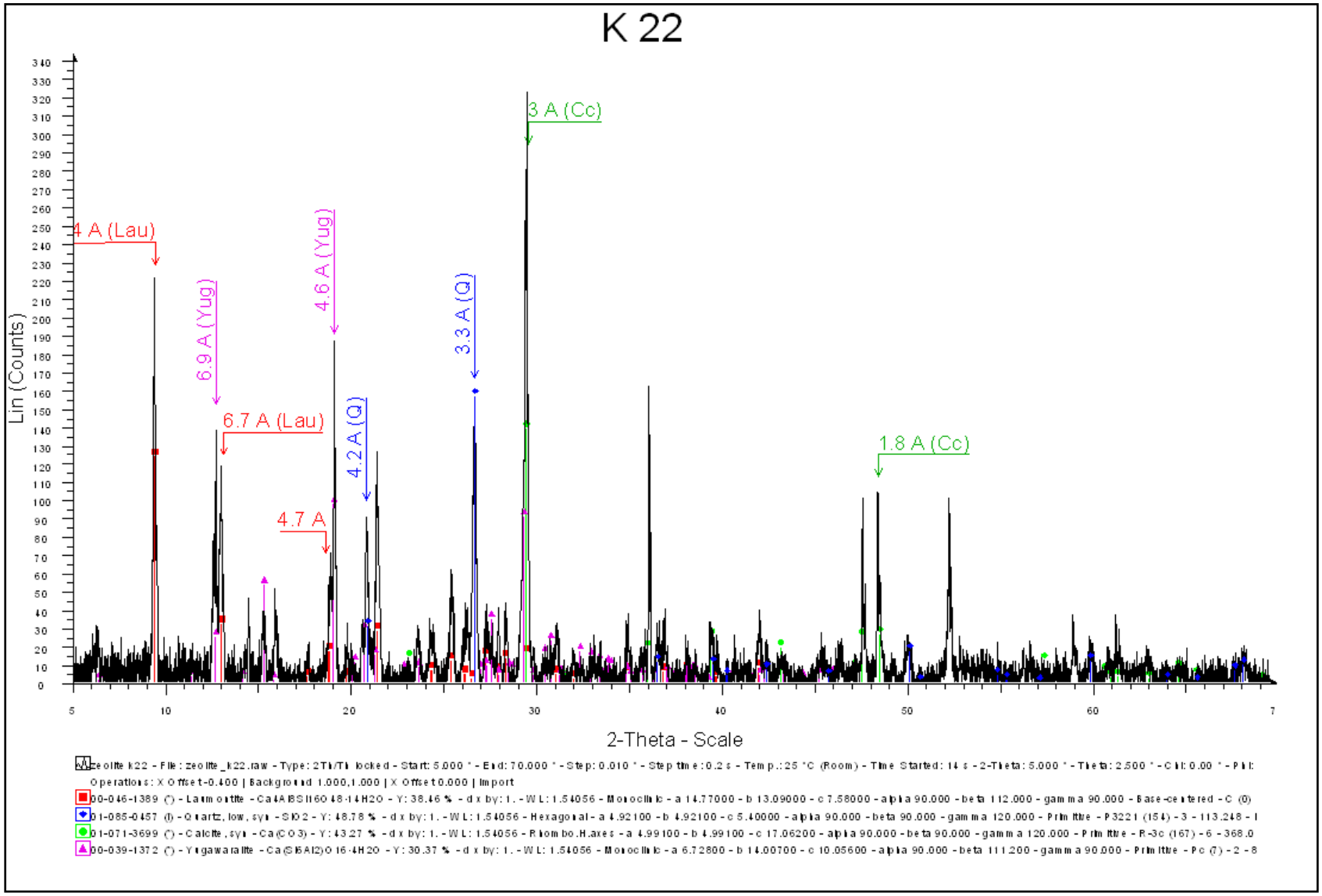
K 22
Lin (Counts)
2-Theta - Scale
4 A (Lau)
6.9 A (Yug)
6.7 A (Lau)
4.7 A
4.6 A (Yug)
4.2 A (Q)
3.3 A (Q)
3 A (Cc)
1.8 A (Cc)
Zeolite k22 - File: zeolite_k22.raw - Type: 2Th/Th locked - Start: 5.000 ° - End: 70.000 ° - Step: 0.010 ° - Step time: 0.2 s - Temp.: 25 °C (Room) - Time Started: 14 s - 2-Theta: 5.000 ° - Theta: 2.500 ° - Chi: 0.00 ° - Phi: 0.00 °
Operations: X Offset -0.400 | Background 1.000,1.000 | X Offset 0.000 | Import
00-046-1389 (*) - Laumontite - Ca4Al8Si16O48·14H2O - Y: 38.46 % - d x by: 1. - WL: 1.54056 - Monoclinic - a 14.77000 - b 13.09000 - c 7.58000 - alpha 90.000 - beta 112.000 - gamma 90.000 - Base-centered - C (0)
01-085-0457 (I) - Quartz, low, syn - SiO2 - Y: 48.78 % - d x by: 1. - WL: 1.54056 - Hexagonal - a 4.92100 - b 4.92100 - c 5.40000 - alpha 90.000 - beta 90.000 - gamma 120.000 - Primitive - P3221 (154) - 3 - 113.248 - I
01-071-3699 (*) - Calcite, syn - Ca(CO3) - Y: 43.27 % - d x by: 1. - WL: 1.54056 - Rhombo.H.axes - a 4.99100 - b 4.99100 - c 17.06200 - alpha 90.000 - beta 90.000 - gamma 120.000 - Primitive - R-3c (167) - 6 - 368.0
00-039-1372 (*) - Yugawaralite - Ca(Si6Al2)O16·4H2O - Y: 30.37 % - d x by: 1. - WL: 1.54056 - Monoclinic - a 6.72800 - b 14.00700 - c 10.05600 - alpha 90.000 - beta 111.200 - gamma 90.000 - Primitive - Pc (7) - 2 - 8

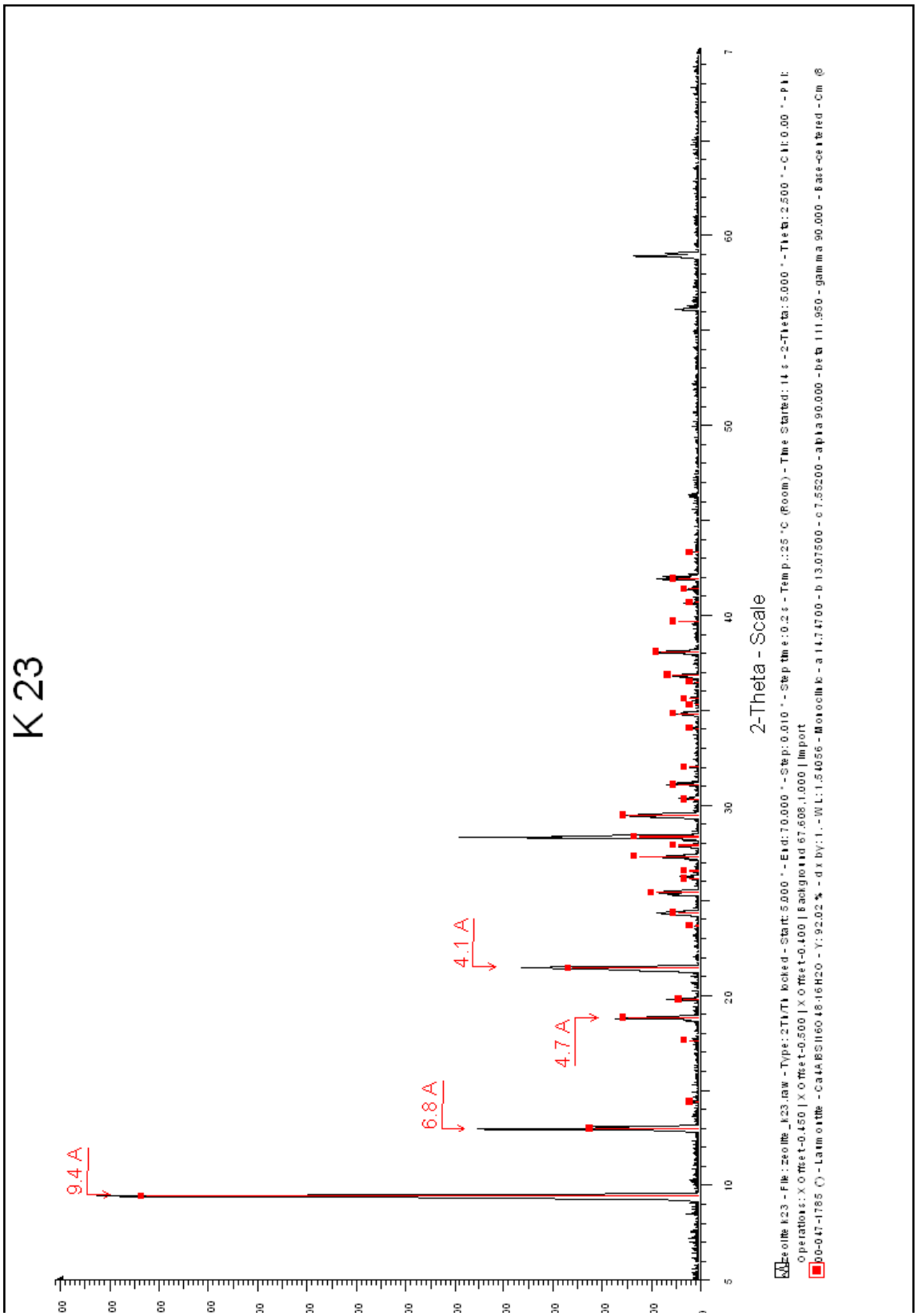
K 23
9.4 A
6.8 A
4.7 A
4.1 A
2-Theta - Scale

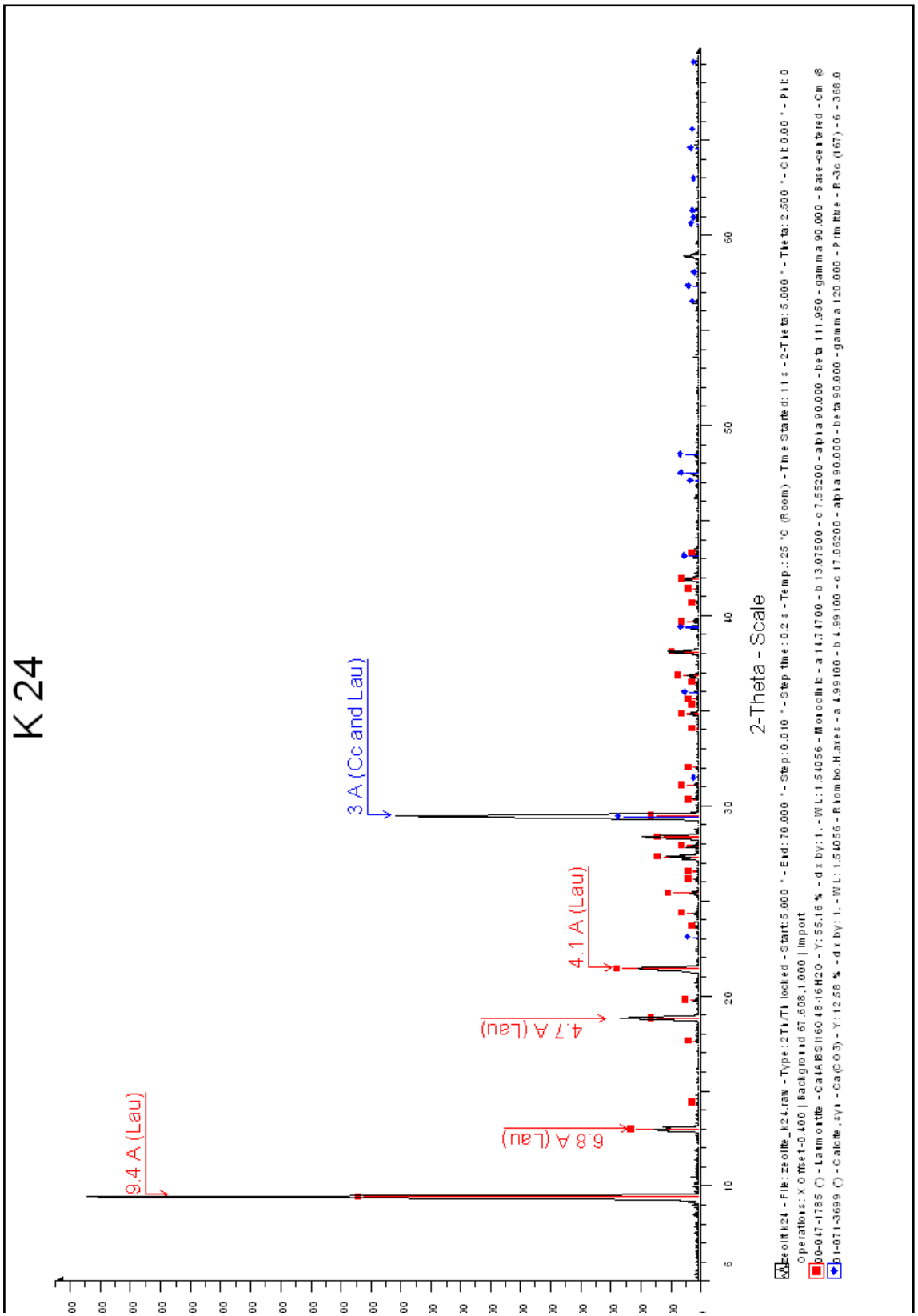
K 24
9.4 A (Lau)
6.8 A (Lau)
4.7 A (Lau)
4.1 A (Lau)
3 A (Cc and Lau)
2-Theta - Scale

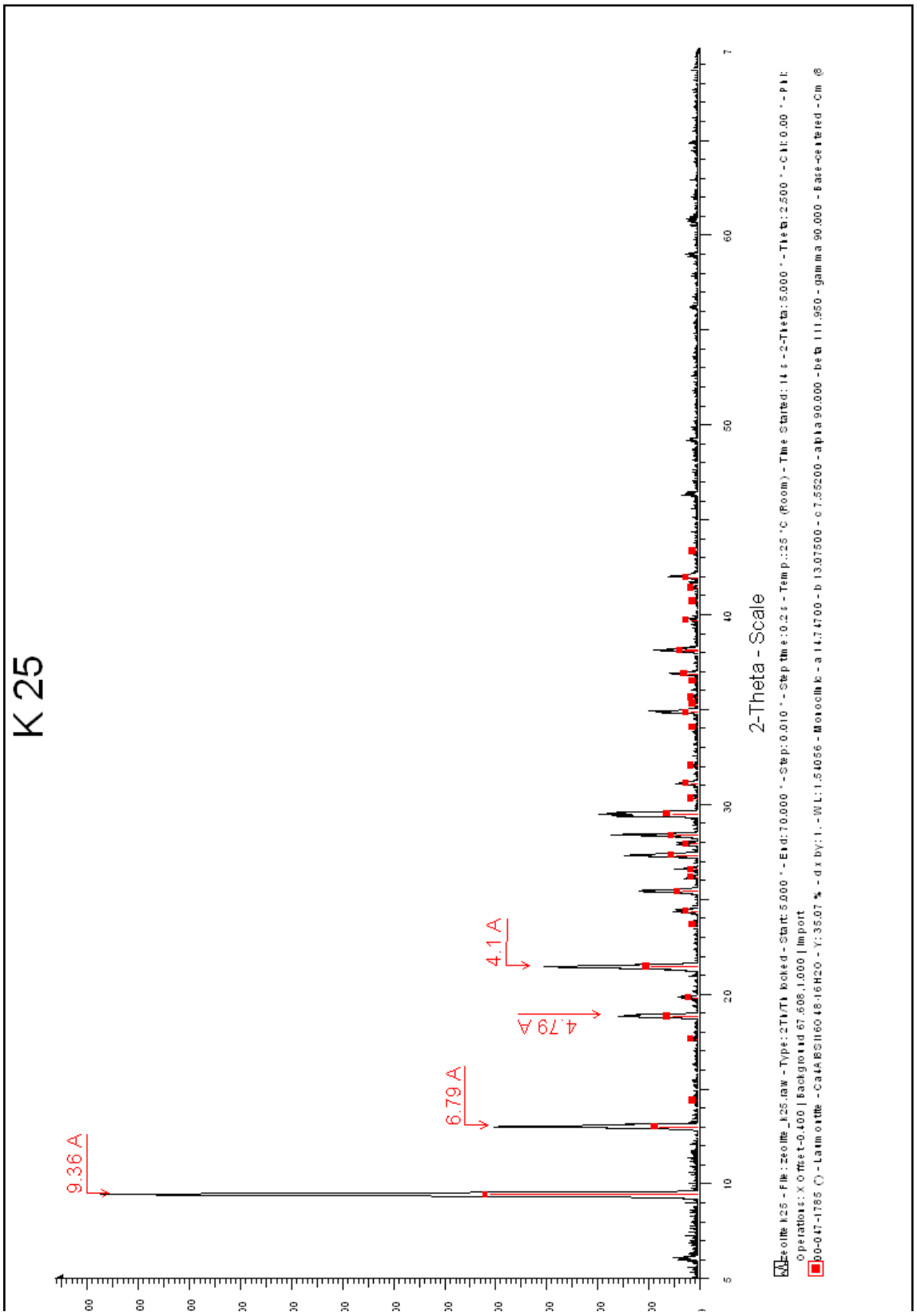
K 25
9.36 A
6.79 A
4.79 A
4.1 A
2-Theta - Scale

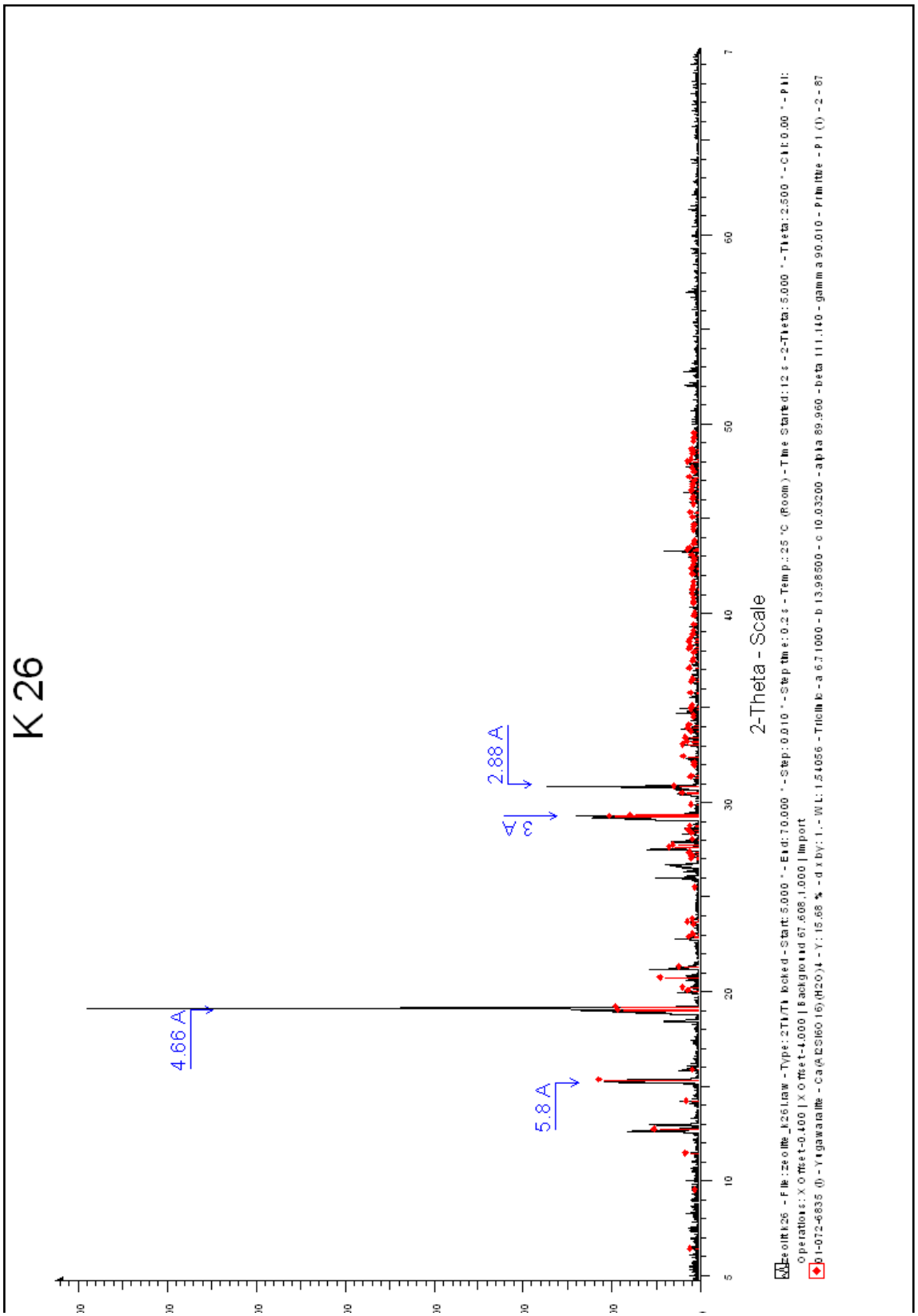
K 26
4.66 A
5.8 A
3.34 A
2.88 A
2-Theta - Scale

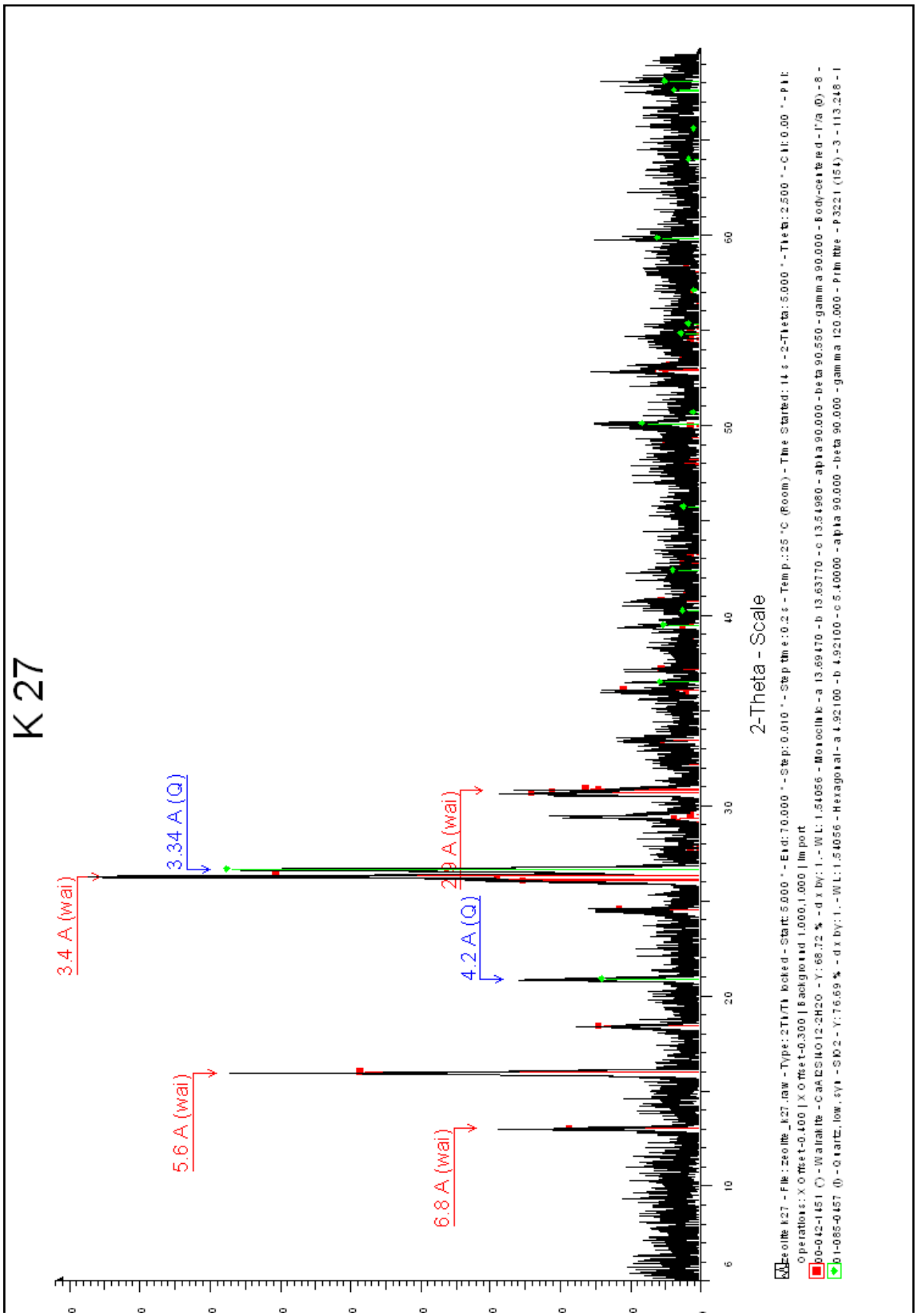
K 27
3.4 A (wai)
3.34 A (Q)
5.6 A (wai)
6.8 A (wai)
2.9 A (wai)
4.2 A (Q)
2-Theta - Scale

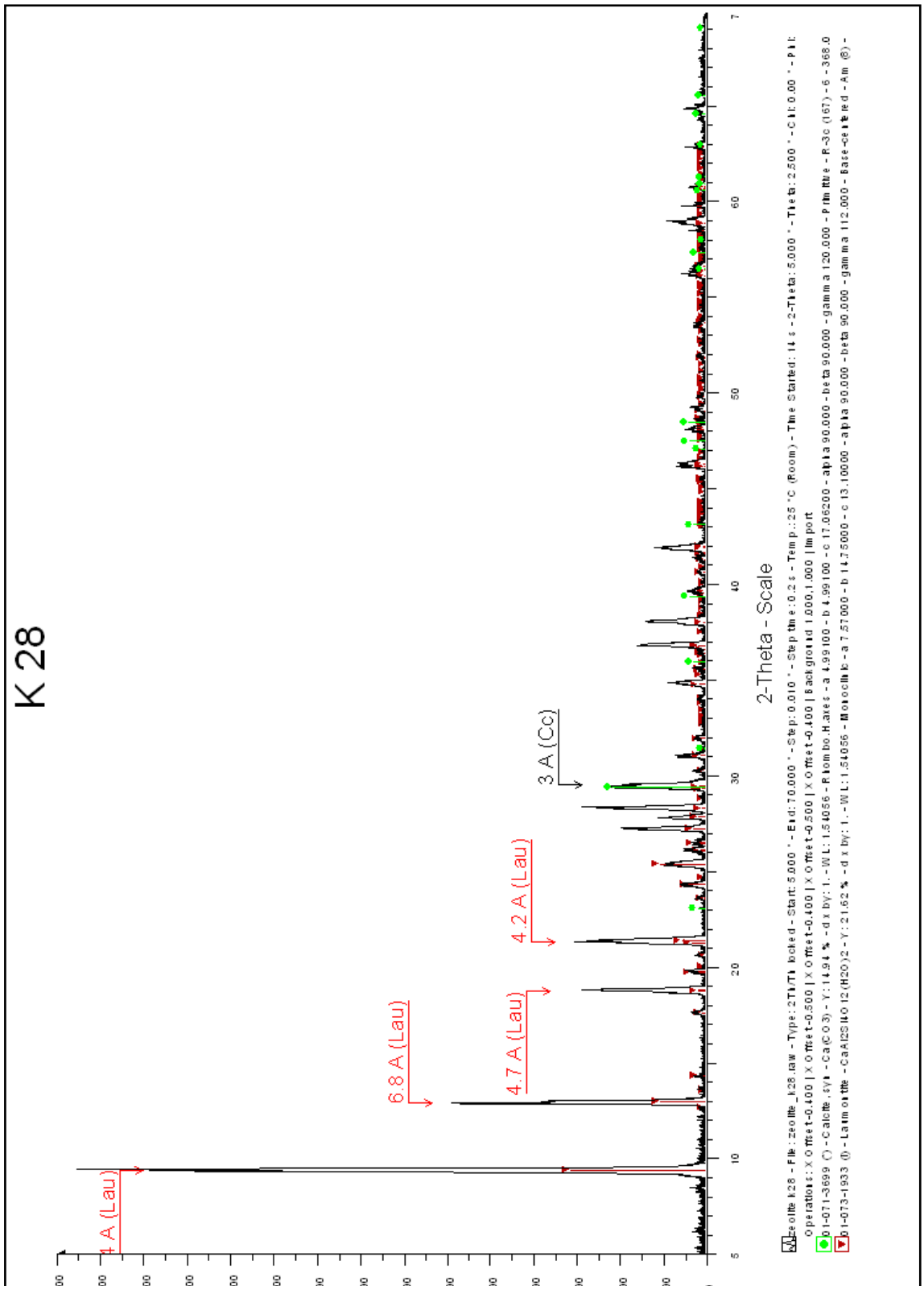
K 28
11 A (Lau)
6.8 A (Lau)
4.7 A (Lau)
4.2 A (Lau)
3 A (Cc)
2-Theta - Scale

APPENDIX B

XRD patterns of clay samples

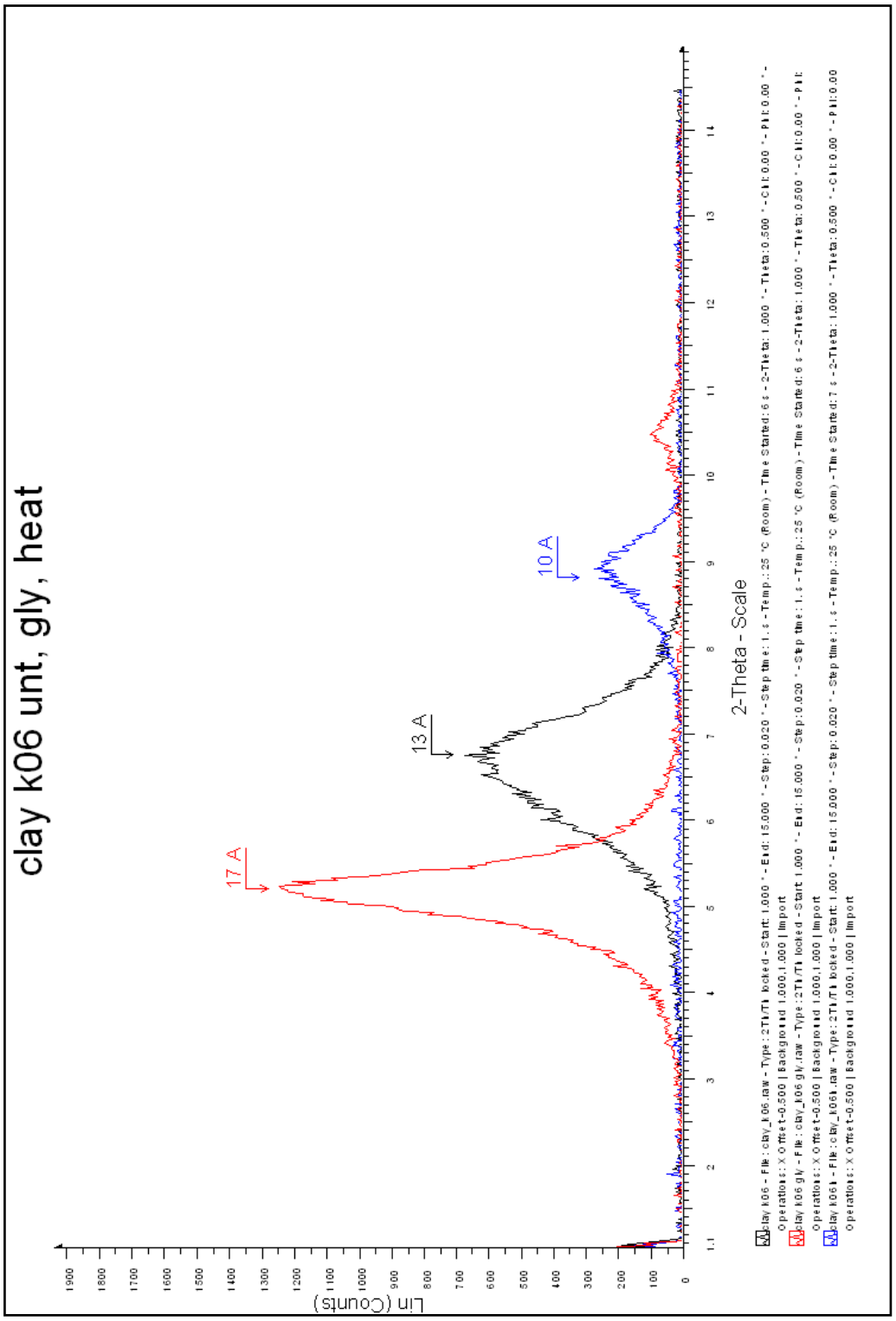

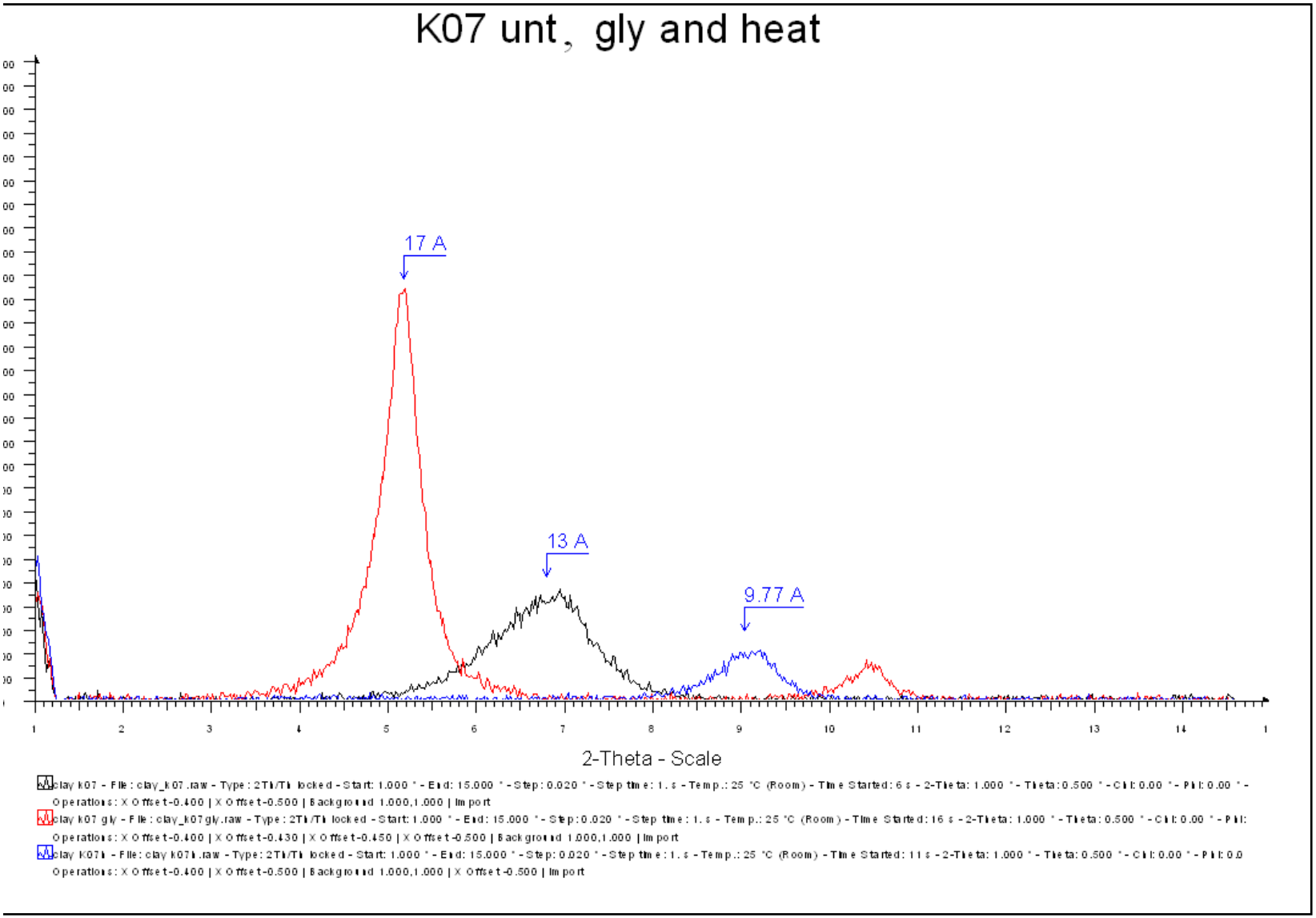
K07 unt, gly and heat
17 A
13 A
9.77 A
2-Theta - Scale
clay k07 - File: clay_k07.raw - Type: 2Th/Th locked - Start: 1.000 ° - End: 15.000 ° - Step: 0.020 ° - Step time: 1. s - Temp.: 25 °C (Room) - Time Started: 6 s - 2-Theta: 1.000 ° - Theta: 0.500 ° - Chi: 0.00 ° - Phi: 0.00 ° -
Operations: X Offset -0.400 | X Offset -0.500 | Background 1.000,1.000 | Import
clay k07 gly - File: clay_k07 gly.raw - Type: 2Th/Th locked - Start: 1.000 ° - End: 15.000 ° - Step: 0.020 ° - Step time: 1. s - Temp.: 25 °C (Room) - Time Started: 16 s - 2-Theta: 1.000 ° - Theta: 0.500 ° - Chi: 0.00 ° - Phi:
Operations: X Offset -0.400 | X Offset -0.430 | X Offset -0.450 | X Offset -0.500 | Background 1.000,1.000 | Import
clay K07h - File: clay k07h.raw - Type: 2Th/Th locked - Start: 1.000 ° - End: 15.000 ° - Step: 0.020 ° - Step time: 1. s - Temp.: 25 °C (Room) - Time Started: 11 s - 2-Theta: 1.000 ° - Theta: 0.500 ° - Chi: 0.00 ° - Phi: 0.0
Operations: X Offset -0.400 | X Offset -0.500 | Background 1.000,1.000 | X Offset -0.500 | Import

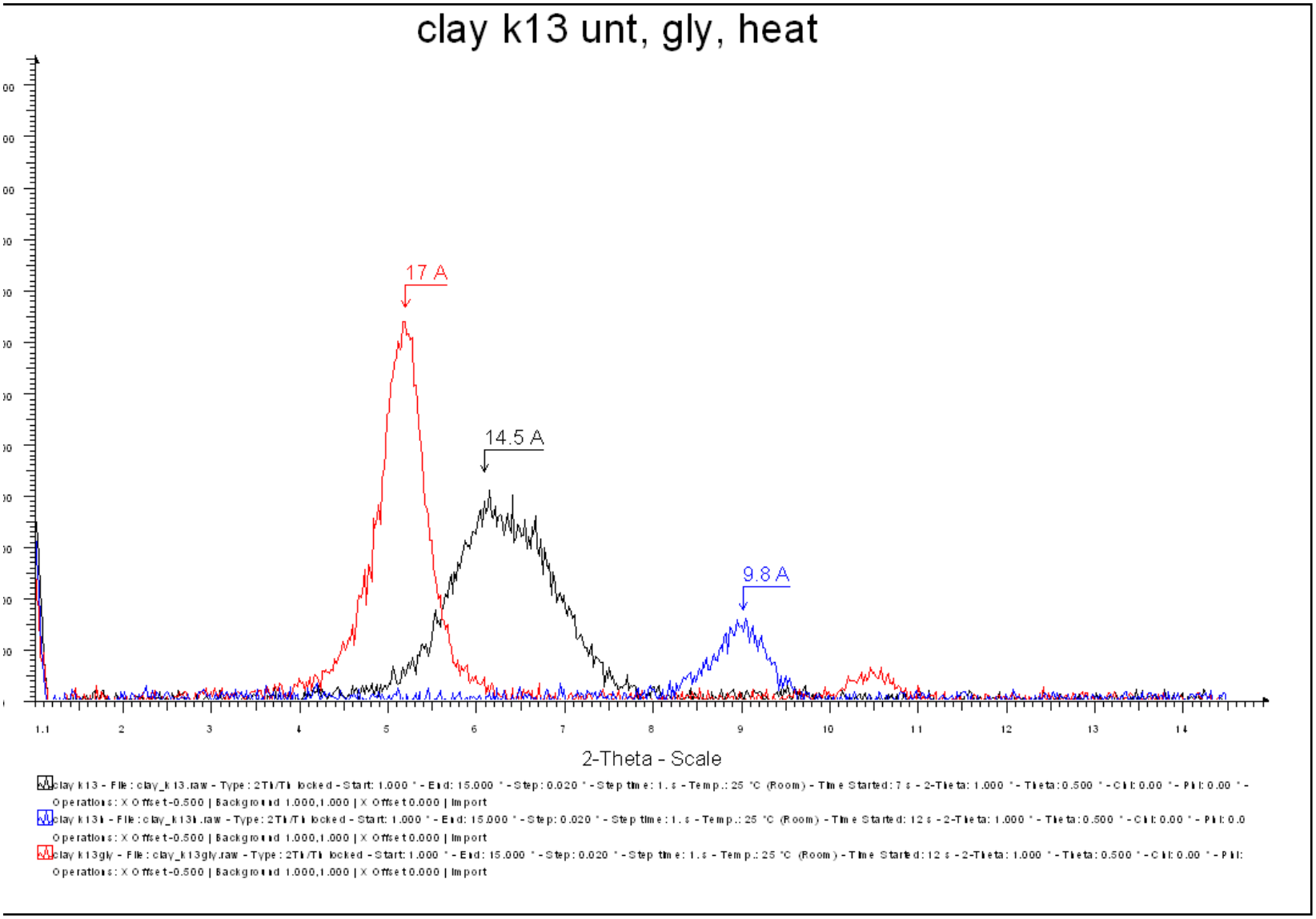
clay k13 unt, gly, heat
17 A
14.5 A
9.8 A
2-Theta - Scale
clay k13 - File: clay_k13.raw - Type: 2Th/Th locked - Start: 1.000 ° - End: 15.000 ° - Step: 0.020 ° - Step time: 1. s - Temp.: 25 °C (Room) - Time Started: 7 s - 2-Theta: 1.000 ° - Theta: 0.500 ° - Chi: 0.00 ° - Phi: 0.00 ° -
Operations: X Offset -0.500 | Background 1.000,1.000 | X Offset 0.000 | Import
clay k13i - File: clay_k13i.raw - Type: 2Th/Th locked - Start: 1.000 ° - End: 15.000 ° - Step: 0.020 ° - Step time: 1. s - Temp.: 25 °C (Room) - Time Started: 12 s - 2-Theta: 1.000 ° - Theta: 0.500 ° - Chi: 0.00 ° - Phi: 0.0
Operations: X Offset -0.500 | Background 1.000,1.000 | X Offset 0.000 | Import
clay k13gly - File: clay_k13gly.raw - Type: 2Th/Th locked - Start: 1.000 ° - End: 15.000 ° - Step: 0.020 ° - Step time: 1. s - Temp.: 25 °C (Room) - Time Started: 12 s - 2-Theta: 1.000 ° - Theta: 0.500 ° - Chi: 0.00 ° - Phi:
Operations: X Offset -0.500 | Background 1.000,1.000 | X Offset 0.000 | Import

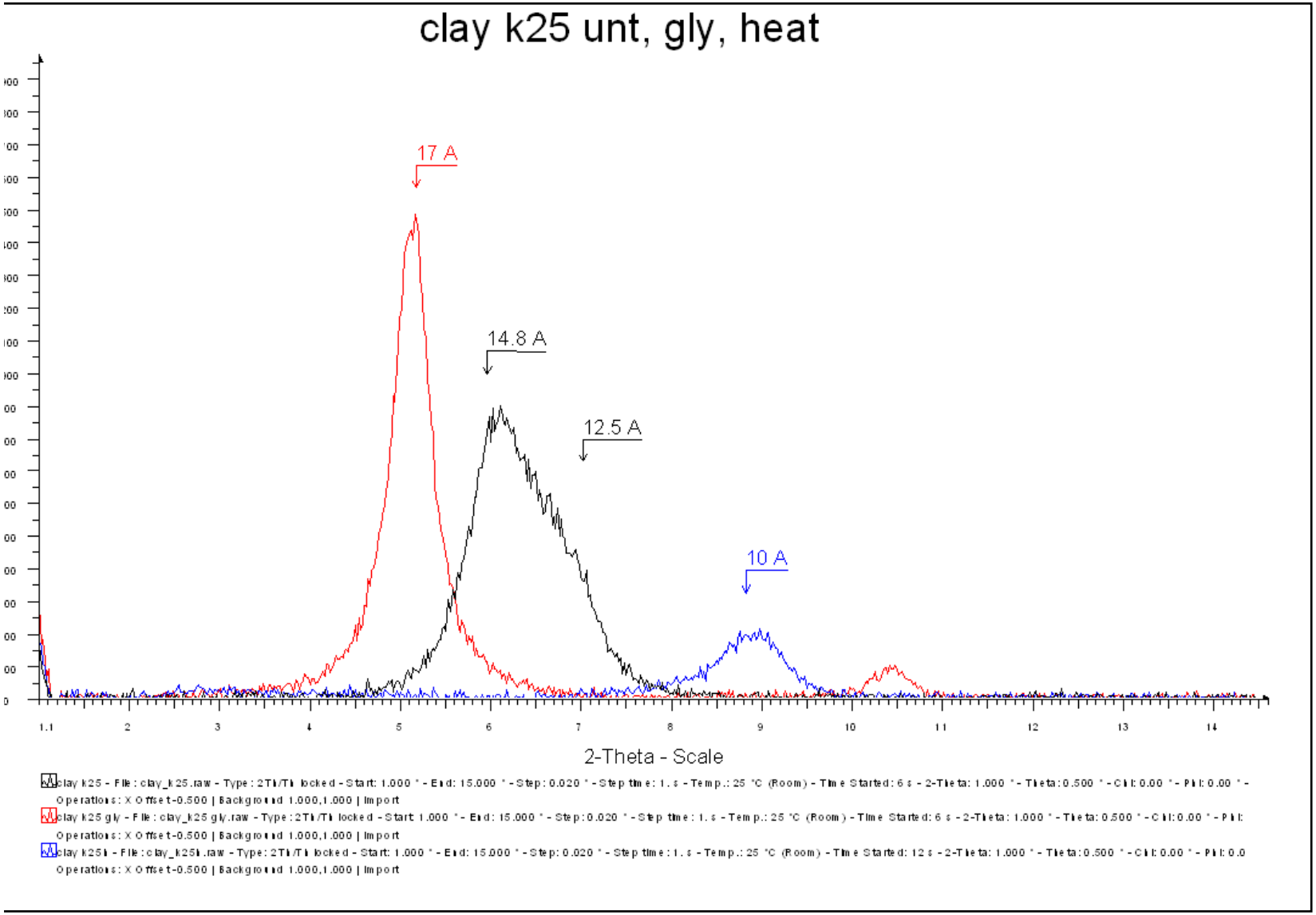
clay k25 unt, gly, heat
17 A
14.8 A
12.5 A
10 A
2-Theta - Scale
clay k25 - File: clay_k25.raw - Type: 2Th/Th locked - Start: 1.000 ° - End: 15.000 ° - Step: 0.020 ° - Step time: 1. s - Temp.: 25 °C (Room) - Time Started: 6 s - 2-Theta: 1.000 ° - Theta: 0.500 ° - Chi: 0.00 ° - Phi: 0.00 ° -
Operations: X Offset -0.500 | Background 1.000,1.000 | Import
clay k25 gly - File: clay_k25 gly.raw - Type: 2Th/Th locked - Start: 1.000 ° - End: 15.000 ° - Step: 0.020 ° - Step time: 1. s - Temp.: 25 °C (Room) - Time Started: 6 s - 2-Theta: 1.000 ° - Theta: 0.500 ° - Chi: 0.00 ° - Phi:
Operations: X Offset -0.500 | Background 1.000,1.000 | Import
clay k25i - File: clay_k25i.raw - Type: 2Th/Th locked - Start: 1.000 ° - End: 15.000 ° - Step: 0.020 ° - Step time: 1. s - Temp.: 25 °C (Room) - Time Started: 12 s - 2-Theta: 1.000 ° - Theta: 0.500 ° - Chi: 0.00 ° - Phi: 0.0
Operations: X Offset -0.500 | Background 1.000,1.000 | Import

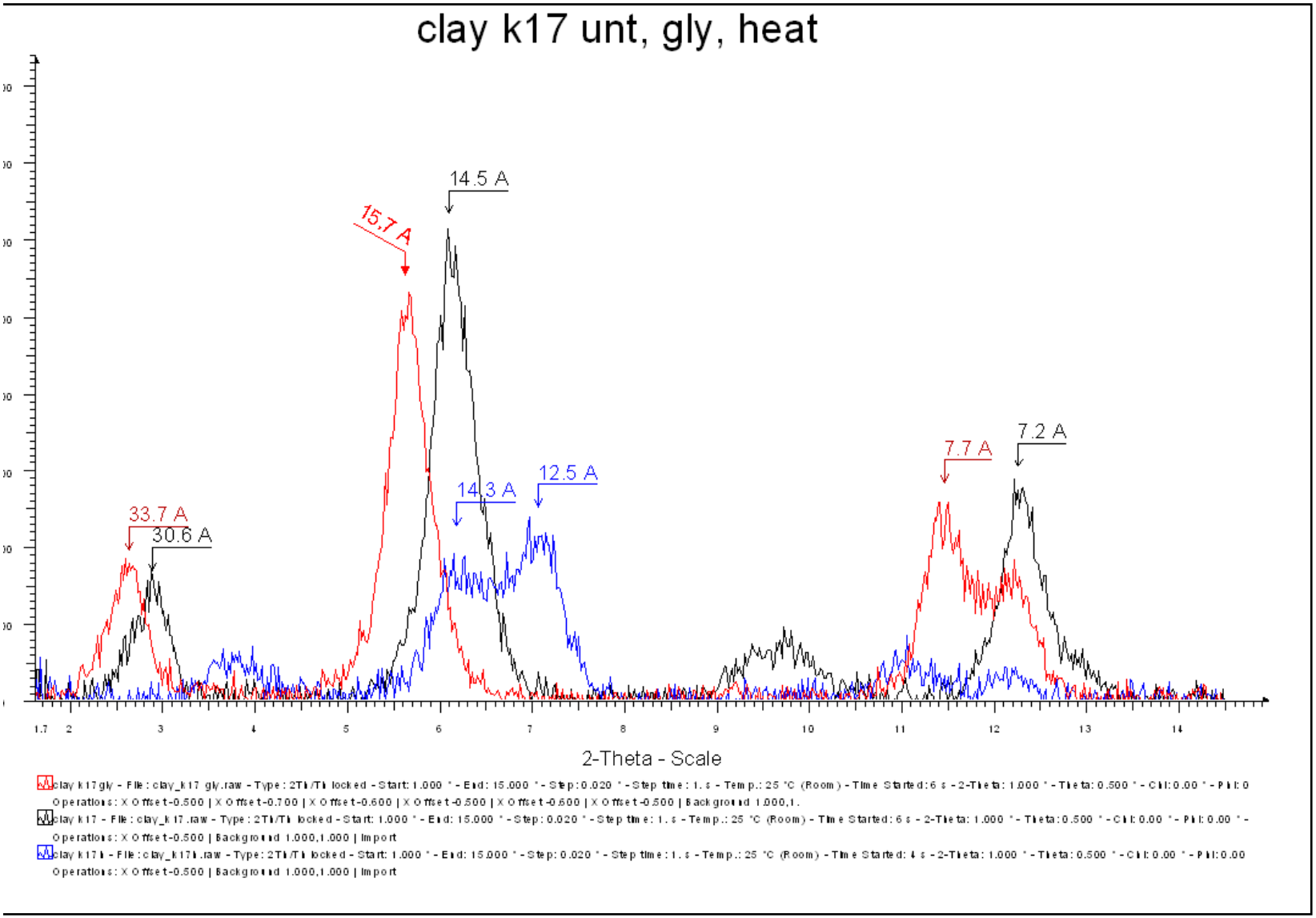
clay k17 unt, gly, heat
14.5 A
15.7 A
33.7 A
30.6 A
14.3 A
12.5 A
7.7 A
7.2 A
2-Theta - Scale
clay k17 gly - File: clay_k17 gly.raw - Type: 2Th/Th locked - Start: 1.000 ° - End: 15.000 ° - Step: 0.020 ° - Step time: 1. s - Temp.: 25 °C (Room) - Time Started: 6 s - 2-Theta: 1.000 ° - Theta: 0.500 ° - Chi: 0.00 ° - Phi: 0
Operations: X Offset -0.500 | X Offset -0.700 | X Offset -0.600 | X Offset -0.500 | X Offset -0.600 | X Offset -0.500 | Background 1.000,1.
clay k17 - File: clay_k17.raw - Type: 2Th/Th locked - Start: 1.000 ° - End: 15.000 ° - Step: 0.020 ° - Step time: 1. s - Temp.: 25 °C (Room) - Time Started: 6 s - 2-Theta: 1.000 ° - Theta: 0.500 ° - Chi: 0.00 ° - Phi: 0.00 ° -
Operations: X Offset -0.500 | Background 1.000,1.000 | Import
clay k17 h - File: clay_k17h.raw - Type: 2Th/Th locked - Start: 1.000 ° - End: 15.000 ° - Step: 0.020 ° - Step time: 1. s - Temp.: 25 °C (Room) - Time Started: 4 s - 2-Theta: 1.000 ° - Theta: 0.500 ° - Chi: 0.00 ° - Phi: 0.00
Operations: X Offset -0.500 | Background 1.000,1.000 | Import

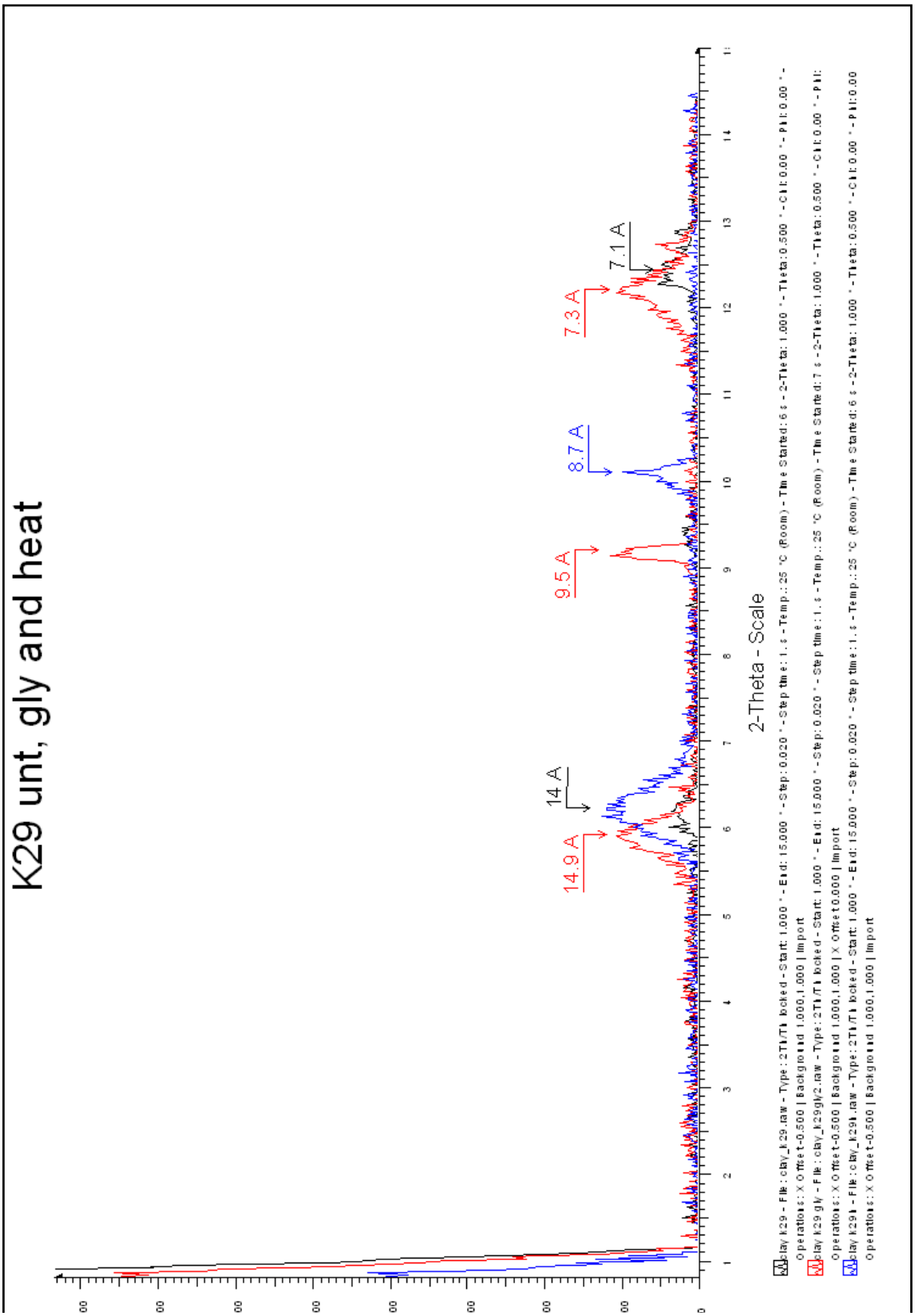
K29 unt, gly and heat
14.9 A
14 A
9.5 A
8.7 A
7.3 A
7.1 A
2-Theta - Scale

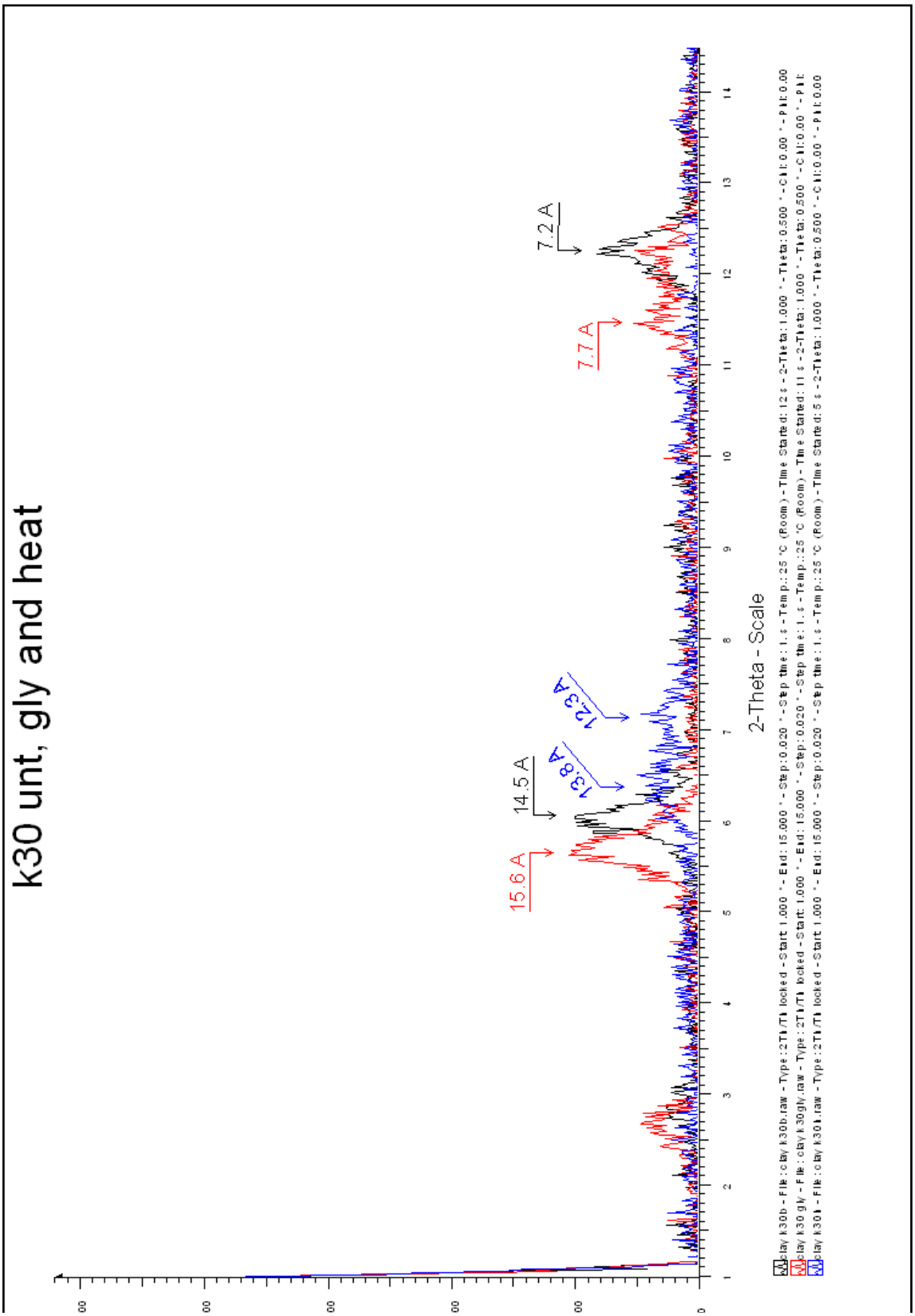
k30 unt, gly and heat
15.6 A
14.5 A
13 A
12.3 A
7.7 A
7.2 A
2-Theta - Scale
clay k30b - File: clay k30b.raw - Type: 2Th/Th locked - Start: 1.000 ° - End: 15.000 ° - Step: 0.020 ° - Step time: 1 s - Temp.: 25 °C (Room) - Time Started: 12 s - 2-Theta: 1.000 ° - Theta: 0.500 ° - Chi: 0.00 ° - Phi: 0.00
clay k30 gly - File: clay k30gly.raw - Type: 2Th/Th locked - Start: 1.000 ° - End: 15.000 ° - Step: 0.020 ° - Step time: 1 s - Temp.: 25 °C (Room) - Time Started: 11 s - 2-Theta: 1.000 ° - Theta: 0.500 ° - Chi: 0.00 ° - Phi:
clay k30t - File: clay k30t.raw - Type: 2Th/Th locked - Start: 1.000 ° - End: 15.000 ° - Step: 0.020 ° - Step time: 1 s - Temp.: 25 °C (Room) - Time Started: 5 s - 2-Theta: 1.000 ° - Theta: 0.500 ° - Chi: 0.00 ° - Phi: 0.00

APPENDIX C

XRD patterns from the Ísor report (Jónsson, 2008)

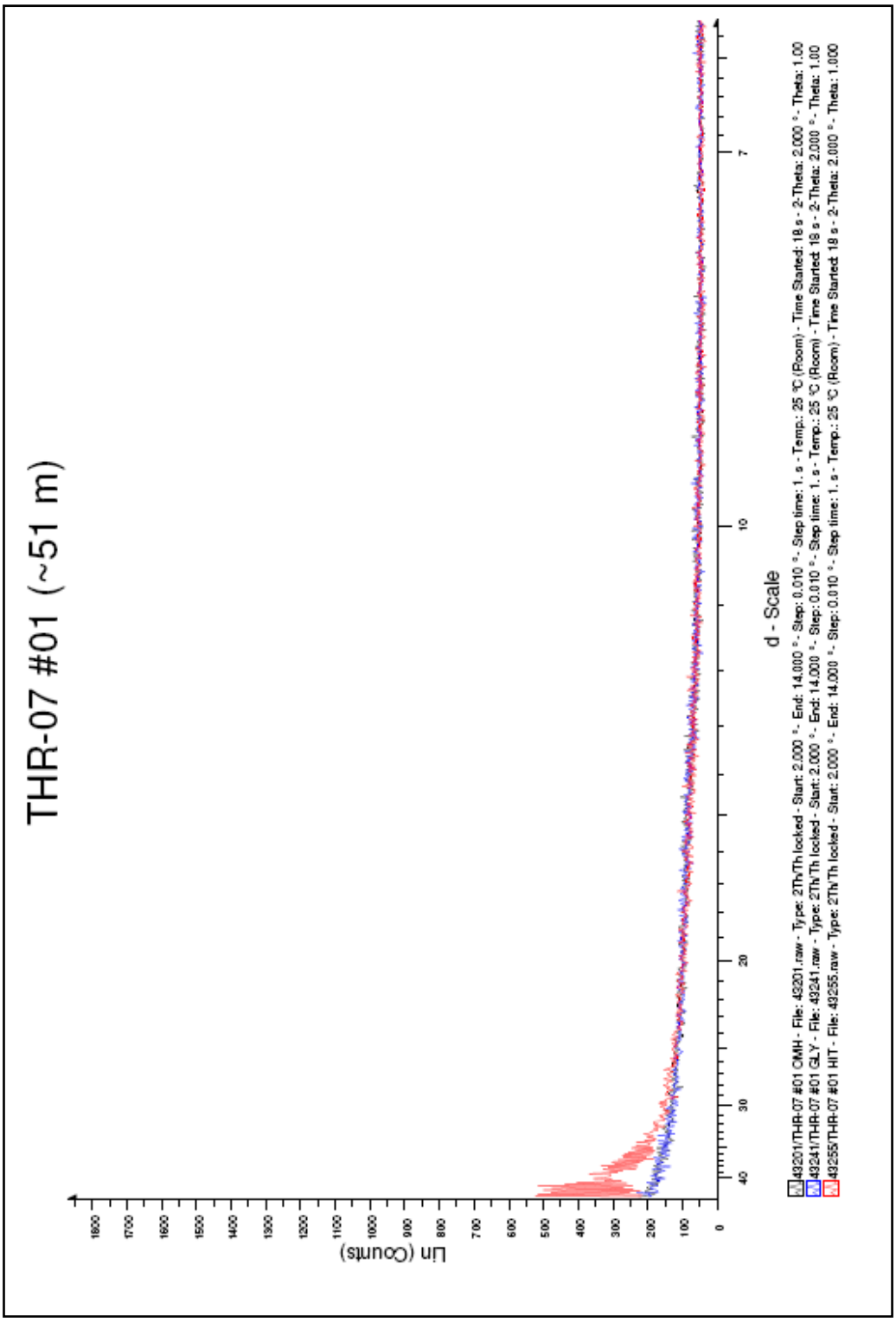

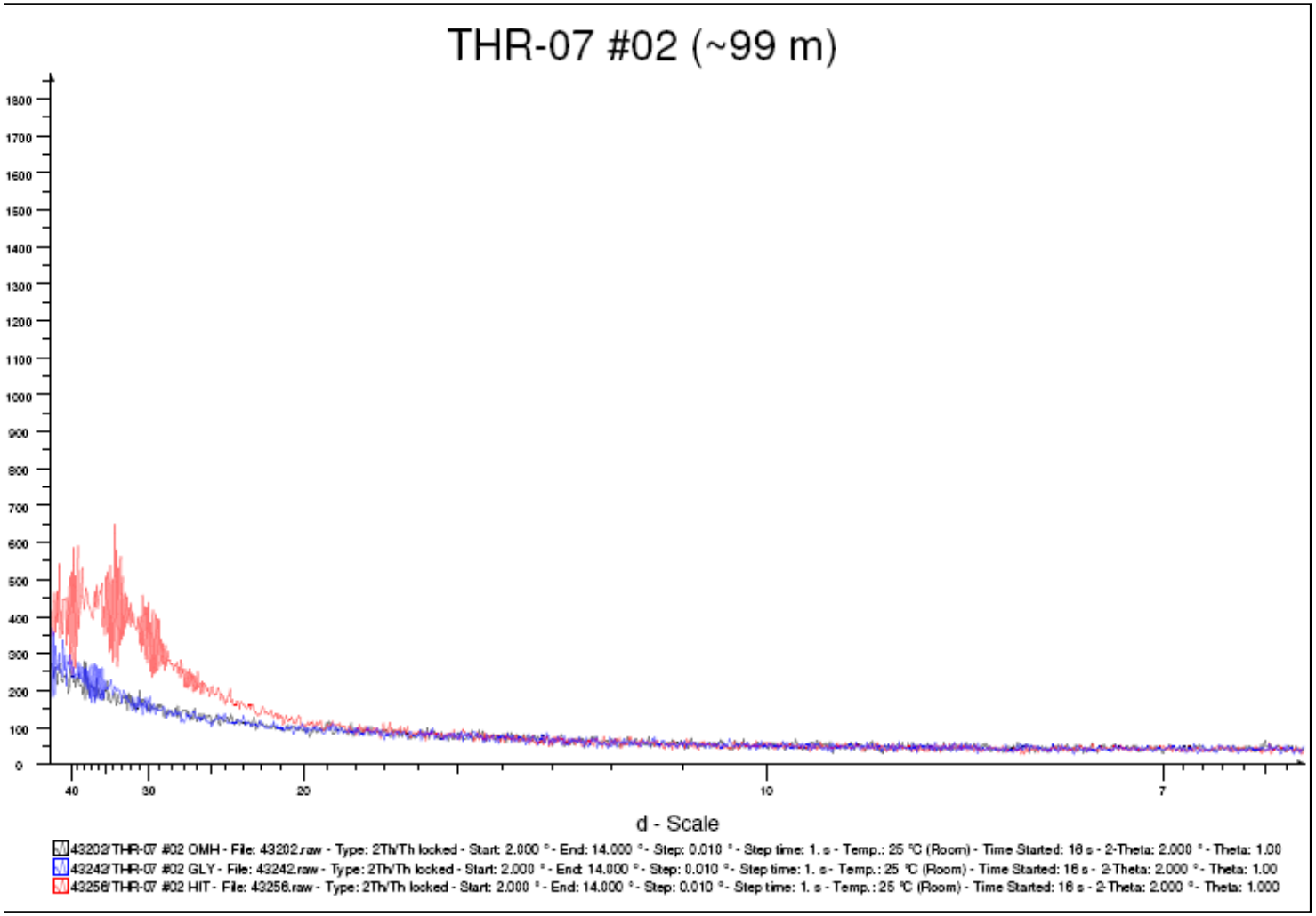
THR-07 #02 (~99 m)
1800
1700
1600
1500
1400
1300
1200
1100
1000
900
800
700
600
500
400
300
200
100
0
40
30
20
10
7
d - Scale
43202/THR-07 #02 OMH - File: 43202.raw - Type: 2Th/Th locked - Start: 2.000 ° - End: 14.000 ° - Step: 0.010 ° - Step time: 1. s - Temp.: 25 °C (Room) - Time Started: 16 s - 2-Theta: 2.000 ° - Theta: 1.00
43242/THR-07 #02 GLY - File: 43242.raw - Type: 2Th/Th locked - Start: 2.000 ° - End: 14.000 ° - Step: 0.010 ° - Step time: 1. s - Temp.: 25 °C (Room) - Time Started: 16 s - 2-Theta: 2.000 ° - Theta: 1.00
43256/THR-07 #02 HIT - File: 43256.raw - Type: 2Th/Th locked - Start: 2.000 ° - End: 14.000 ° - Step: 0.010 ° - Step time: 1. s - Temp.: 25 °C (Room) - Time Started: 16 s - 2-Theta: 2.000 ° - Theta: 1.000

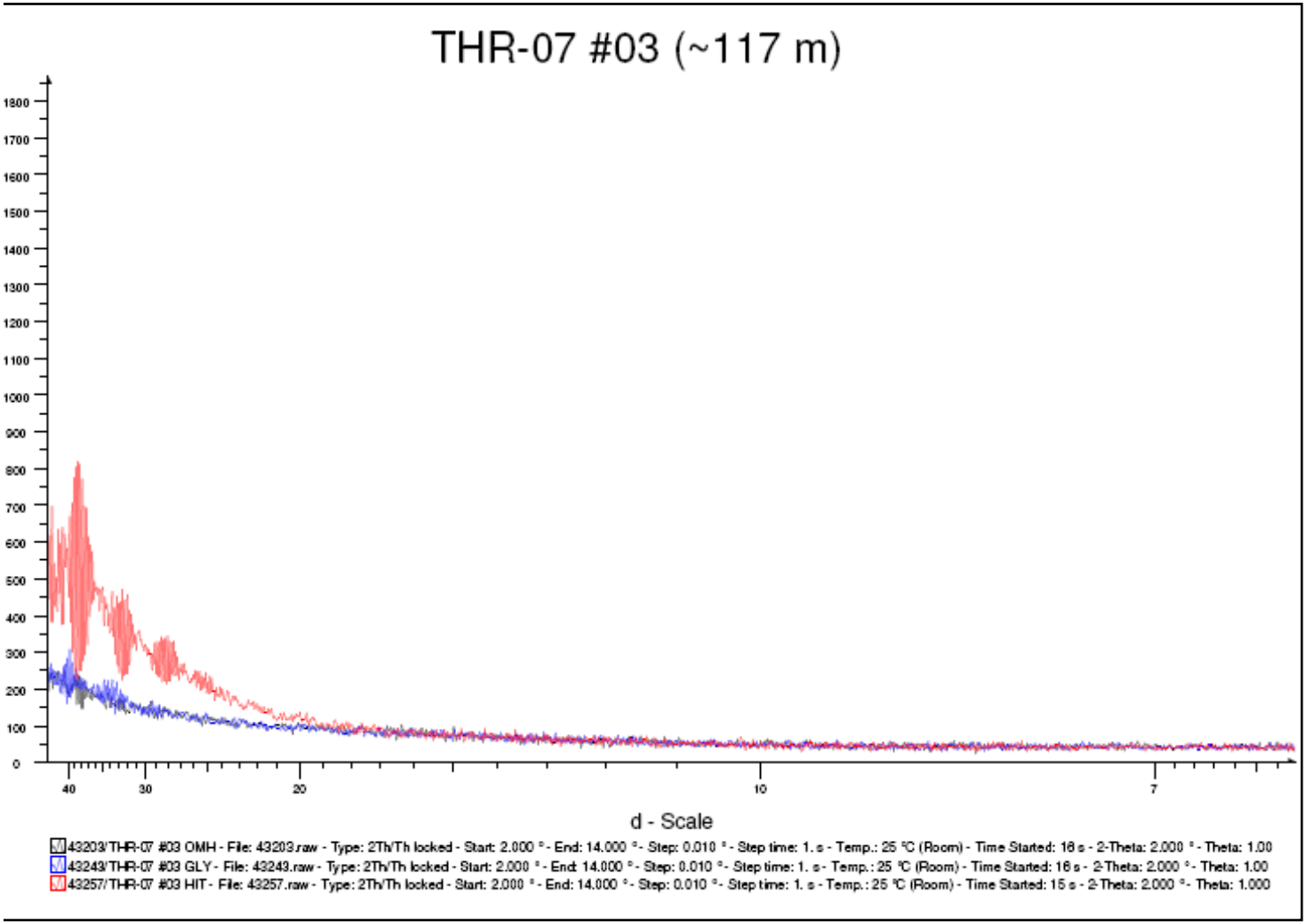
THR-07 #03 (~117 m)
1800
1700
1600
1500
1400
1300
1200
1100
1000
900
800
700
600
500
400
300
200
100
0
40
30
20
10
7
d - Scale
43203/THR-07 #03 OMH - File: 43203.raw - Type: 2Th/Th locked - Start: 2.000 ° - End: 14.000 ° - Step: 0.010 ° - Step time: 1. s - Temp.: 25 °C (Room) - Time Started: 16 s - 2-Theta: 2.000 ° - Theta: 1.00
43243/THR-07 #03 GLY - File: 43243.raw - Type: 2Th/Th locked - Start: 2.000 ° - End: 14.000 ° - Step: 0.010 ° - Step time: 1. s - Temp.: 25 °C (Room) - Time Started: 16 s - 2-Theta: 2.000 ° - Theta: 1.00
43257/THR-07 #03 HIT - File: 43257.raw - Type: 2Th/Th locked - Start: 2.000 ° - End: 14.000 ° - Step: 0.010 ° - Step time: 1. s - Temp.: 25 °C (Room) - Time Started: 15 s - 2-Theta: 2.000 ° - Theta: 1.000

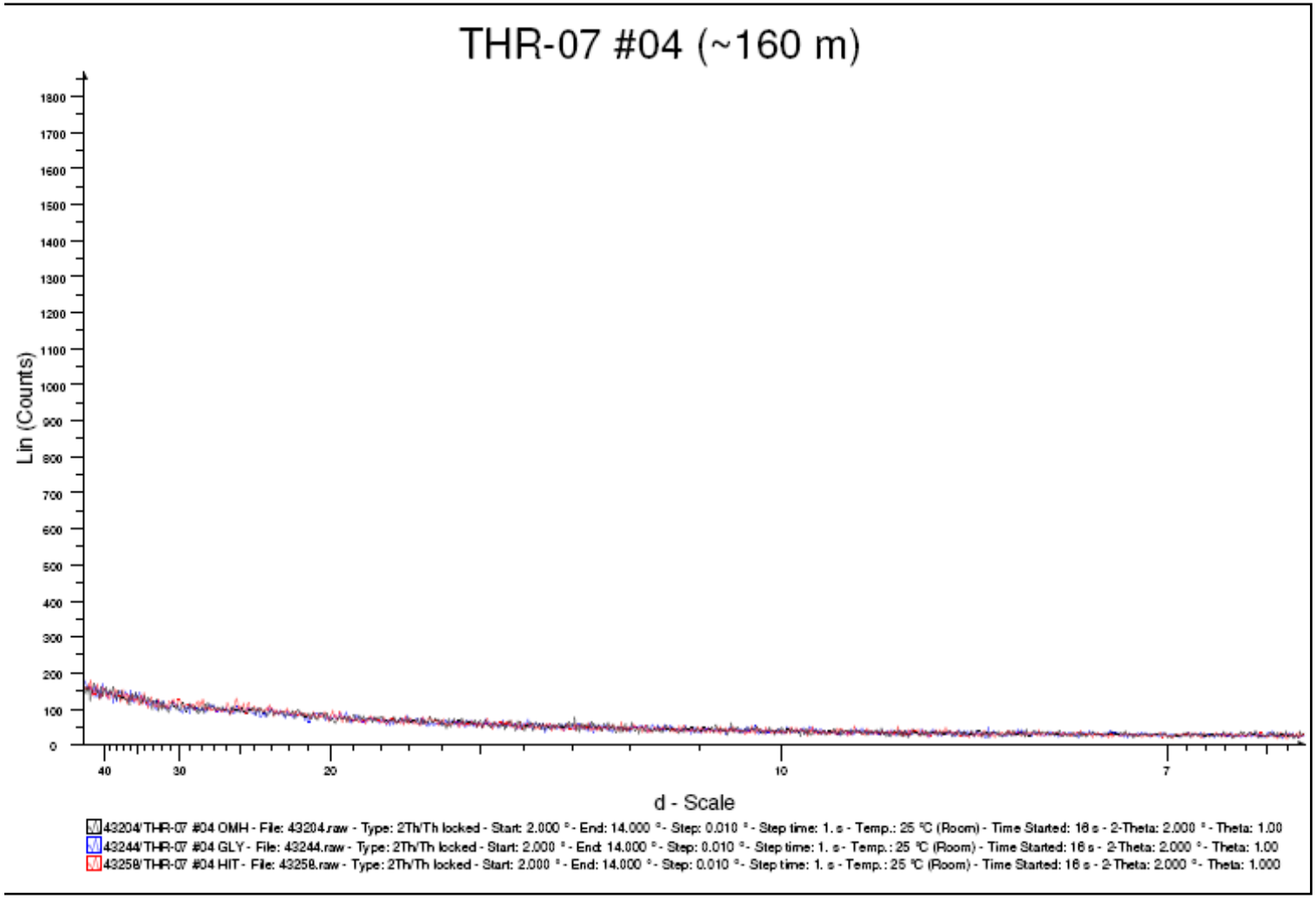
THR-07 #04 (~160 m)
Lin (Counts)
1800
1700
1600
1500
1400
1300
1200
1100
1000
900
800
700
600
500
400
300
200
100
0
40
30
20
10
7
d - Scale
43204/THR-07 #04 OMH - File: 43204.raw - Type: 2Th/Th locked - Start: 2.000 ° - End: 14.000 ° - Step: 0.010 ° - Step time: 1. s - Temp.: 25 °C (Room) - Time Started: 16 s - 2-Theta: 2.000 ° - Theta: 1.00
43244/THR-07 #04 GLY - File: 43244.raw - Type: 2Th/Th locked - Start: 2.000 ° - End: 14.000 ° - Step: 0.010 ° - Step time: 1. s - Temp.: 25 °C (Room) - Time Started: 16 s - 2-Theta: 2.000 ° - Theta: 1.00
43258/THR-07 #04 HIT - File: 43258.raw - Type: 2Th/Th locked - Start: 2.000 ° - End: 14.000 ° - Step: 0.010 ° - Step time: 1. s - Temp.: 25 °C (Room) - Time Started: 16 s - 2-Theta: 2.000 ° - Theta: 1.000

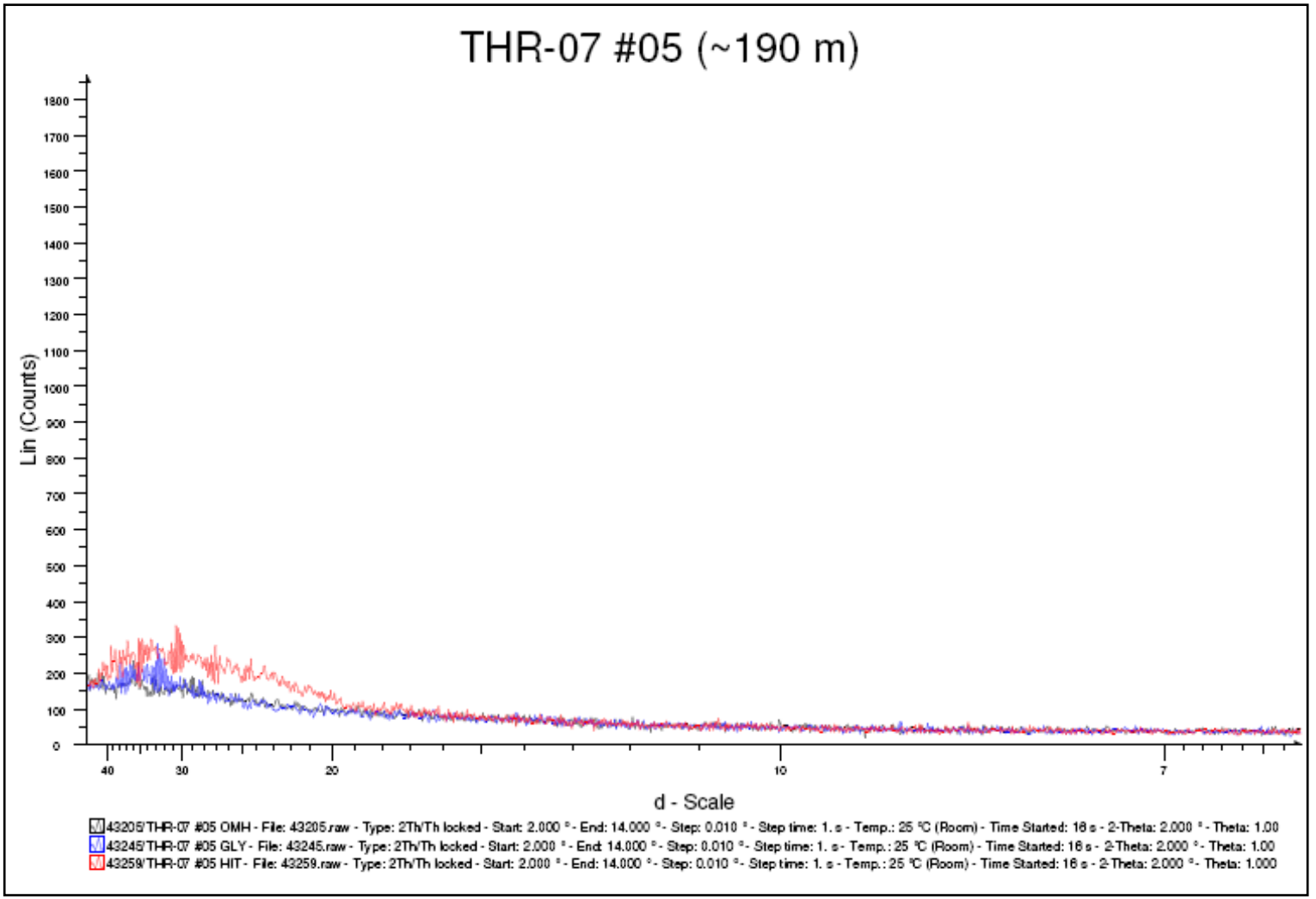
THR-07 #05 (~190 m)
Lin (Counts)
1800
1700
1600
1500
1400
1300
1200
1100
1000
900
800
700
600
500
400
300
200
100
0
40
30
20
10
7
d - Scale
43205/THR-07 #05 OMH - File: 43205.raw - Type: 2Th/Th locked - Start: 2.000 ° - End: 14.000 ° - Step: 0.010 ° - Step time: 1. s - Temp.: 25 °C (Room) - Time Started: 16 s - 2-Theta: 2.000 ° - Theta: 1.00
43245/THR-07 #05 GLY - File: 43245.raw - Type: 2Th/Th locked - Start: 2.000 ° - End: 14.000 ° - Step: 0.010 ° - Step time: 1. s - Temp.: 25 °C (Room) - Time Started: 16 s - 2-Theta: 2.000 ° - Theta: 1.00
43259/THR-07 #05 HIT - File: 43259.raw - Type: 2Th/Th locked - Start: 2.000 ° - End: 14.000 ° - Step: 0.010 ° - Step time: 1. s - Temp.: 25 °C (Room) - Time Started: 16 s - 2-Theta: 2.000 ° - Theta: 1.000

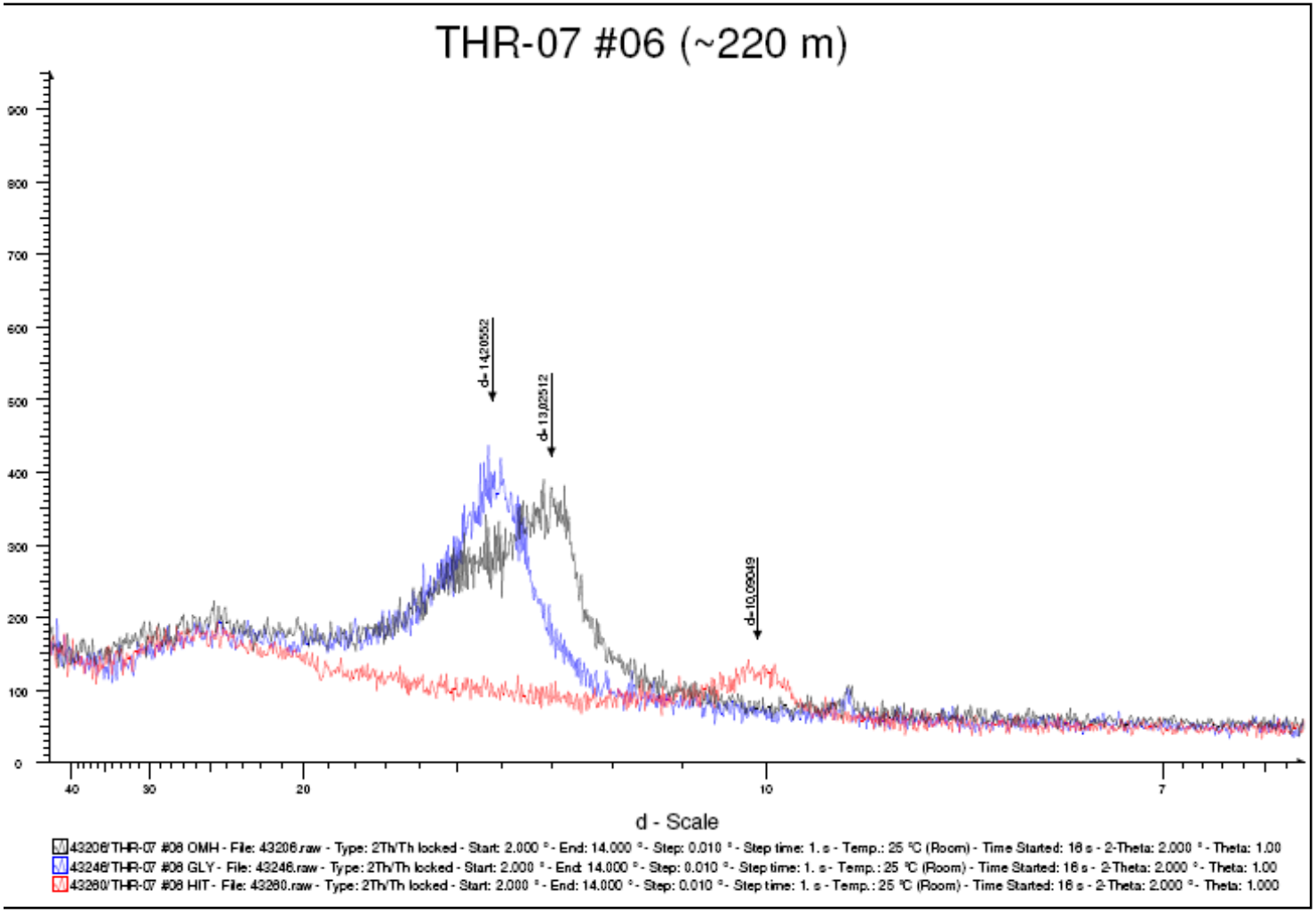
THR-07 #06 (~220 m)
900
800
700
600
500
400
300
200
100
0
d=14,20552
d=13,02512
d=10,09049
40
30
20
10
7
d - Scale
43206/THR-07 #06 OMH - File: 43206.raw - Type: 2Th/Th locked - Start: 2.000 ° - End: 14.000 ° - Step: 0.010 ° - Step time: 1. s - Temp.: 25 °C (Room) - Time Started: 16 s - 2-Theta: 2.000 ° - Theta: 1.00
43246/THR-07 #06 GLY - File: 43246.raw - Type: 2Th/Th locked - Start: 2.000 ° - End: 14.000 ° - Step: 0.010 ° - Step time: 1. s - Temp.: 25 °C (Room) - Time Started: 16 s - 2-Theta: 2.000 ° - Theta: 1.00
43260/THR-07 #06 HIT - File: 43260.raw - Type: 2Th/Th locked - Start: 2.000 ° - End: 14.000 ° - Step: 0.010 ° - Step time: 1. s - Temp.: 25 °C (Room) - Time Started: 16 s - 2-Theta: 2.000 ° - Theta: 1.000

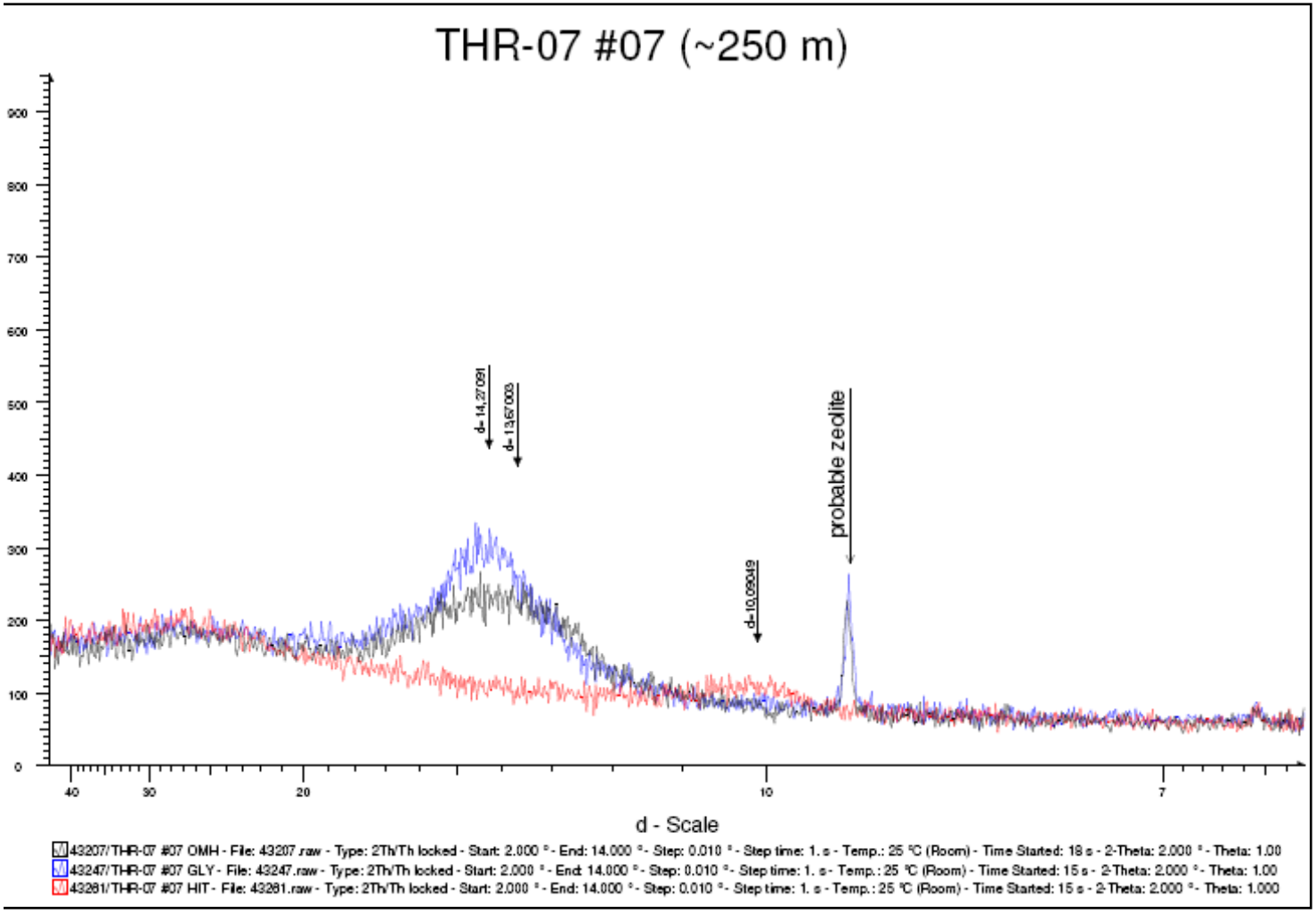
THR-07 #07 (~250 m)
900
800
700
600
500
400
300
200
100
0
d= 14,27091
d= 13,67003
d= 10,09049
probable zeolite
40
30
20
10
7
d - Scale
43207/THR-07 #07 OMH - File: 43207.raw - Type: 2Th/Th locked - Start: 2.000 ° - End: 14.000 ° - Step: 0.010 ° - Step time: 1. s - Temp.: 25 °C (Room) - Time Started: 18 s - 2-Theta: 2.000 ° - Theta: 1.00
43247/THR-07 #07 GLY - File: 43247.raw - Type: 2Th/Th locked - Start: 2.000 ° - End: 14.000 ° - Step: 0.010 ° - Step time: 1. s - Temp.: 25 °C (Room) - Time Started: 15 s - 2-Theta: 2.000 ° - Theta: 1.00
43281/THR-07 #07 HIT - File: 43281.raw - Type: 2Th/Th locked - Start: 2.000 ° - End: 14.000 ° - Step: 0.010 ° - Step time: 1. s - Temp.: 25 °C (Room) - Time Started: 15 s - 2-Theta: 2.000 ° - Theta: 1.000

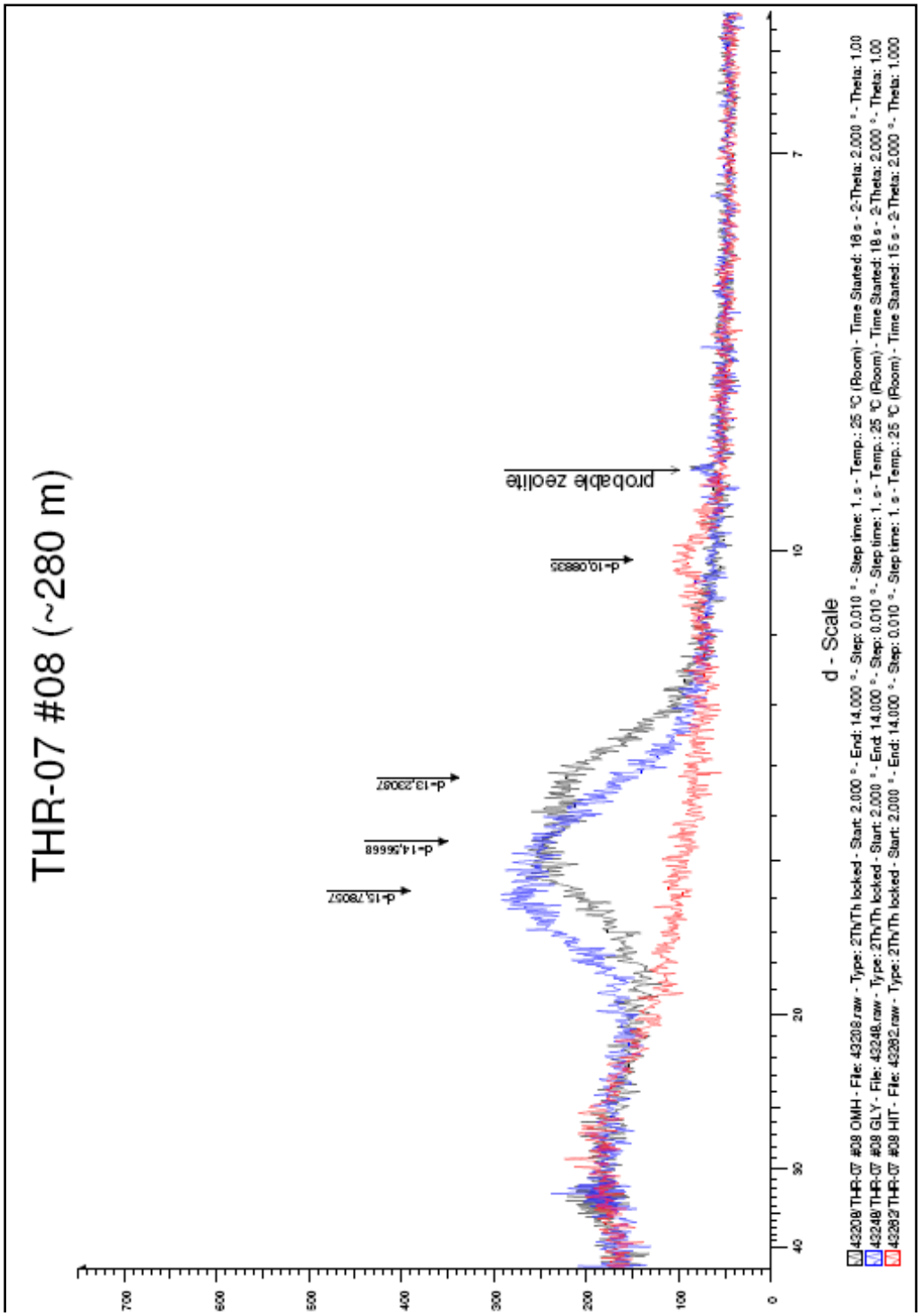
THR-07 #08 (~280 m)
probable zeolite
d-10,08835
d-13,23087
d-14,25668
d-15,78057
d - Scale
0
100
200
300
400
500
600
700
10
20
30
40
7
43208 THR-07 #08 OMH - File: 43208.raw - Type: 2Th/Th locked - Start: 2.000 ° - End: 14.000 ° - Step: 0.010 ° - Step time: 1. s - Temp.: 25 °C (Room) - Time Started: 18 s - 2-Theta: 2.000 ° - Theta: 1.00
43248 THR-07 #08 GLY - File: 43248.raw - Type: 2Th/Th locked - Start: 2.000 ° - End: 14.000 ° - Step: 0.010 ° - Step time: 1. s - Temp.: 25 °C (Room) - Time Started: 18 s - 2-Theta: 2.000 ° - Theta: 1.00
43282 THR-07 #08 HIT - File: 43282.raw - Type: 2Th/Th locked - Start: 2.000 ° - End: 14.000 ° - Step: 0.010 ° - Step time: 1. s - Temp.: 25 °C (Room) - Time Started: 15 s - 2-Theta: 2.000 ° - Theta: 1.000

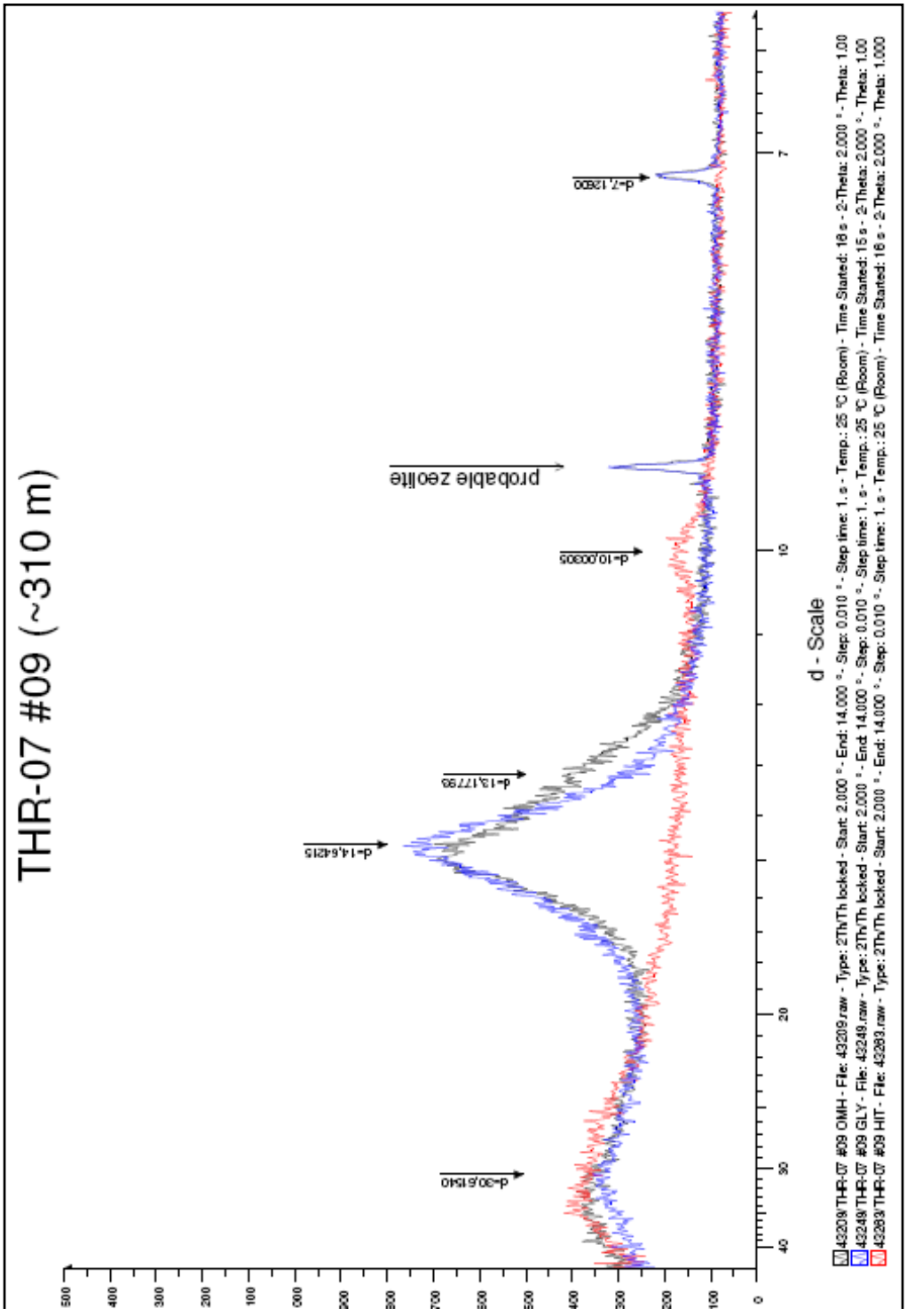
THR-07 #09 (~310 m)
d-30,61340
d-14,64215
d-13,17780
d-10,00305
probable zeolite
d-7,12800
d - Scale
43209 THR-07 #09 OMH - File: 43209.raw - Type: 2Th/Th locked - Start: 2.000 ° - End: 14.000 ° - Step: 0.010 ° - Step time: 1. s - Temp.: 25 °C (Room) - Time Started: 18 s - 2-Theta: 2.000 ° - Theta: 1.00
43249 THR-07 #09 GLY - File: 43249.raw - Type: 2Th/Th locked - Start: 2.000 ° - End: 14.000 ° - Step: 0.010 ° - Step time: 1. s - Temp.: 25 °C (Room) - Time Started: 15 s - 2-Theta: 2.000 ° - Theta: 1.00
43283 THR-07 #09 HIT - File: 43283.raw - Type: 2Th/Th locked - Start: 2.000 ° - End: 14.000 ° - Step: 0.010 ° - Step time: 1. s - Temp.: 25 °C (Room) - Time Started: 16 s - 2-Theta: 2.000 ° - Theta: 1.000

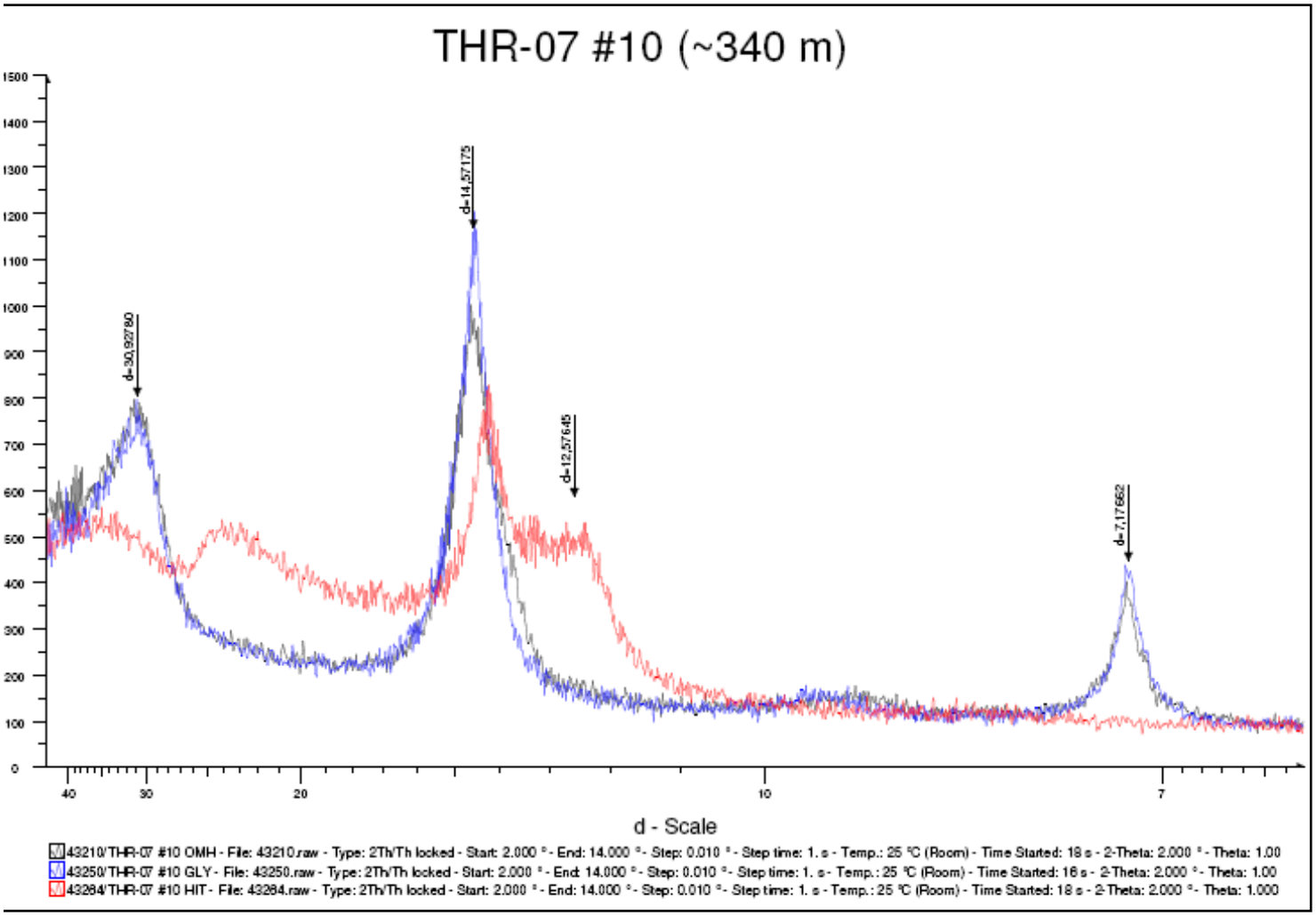
THR-07 #10 (~340 m)
d=30,92780
d=14,57175
d=12,57645
d=7,17662
d - Scale
43210/THR-07 #10 OMH - File: 43210.raw - Type: 2Th/Th locked - Start: 2.000 ° - End: 14.000 ° - Step: 0.010 ° - Step time: 1. s - Temp.: 25 °C (Room) - Time Started: 18 s - 2-Theta: 2.000 ° - Theta: 1.00
43250/THR-07 #10 GLY - File: 43250.raw - Type: 2Th/Th locked - Start: 2.000 ° - End: 14.000 ° - Step: 0.010 ° - Step time: 1. s - Temp.: 25 °C (Room) - Time Started: 18 s - 2-Theta: 2.000 ° - Theta: 1.00
43284/THR-07 #10 HIT - File: 43284.raw - Type: 2Th/Th locked - Start: 2.000 ° - End: 14.000 ° - Step: 0.010 ° - Step time: 1. s - Temp.: 25 °C (Room) - Time Started: 18 s - 2-Theta: 2.000 ° - Theta: 1.000

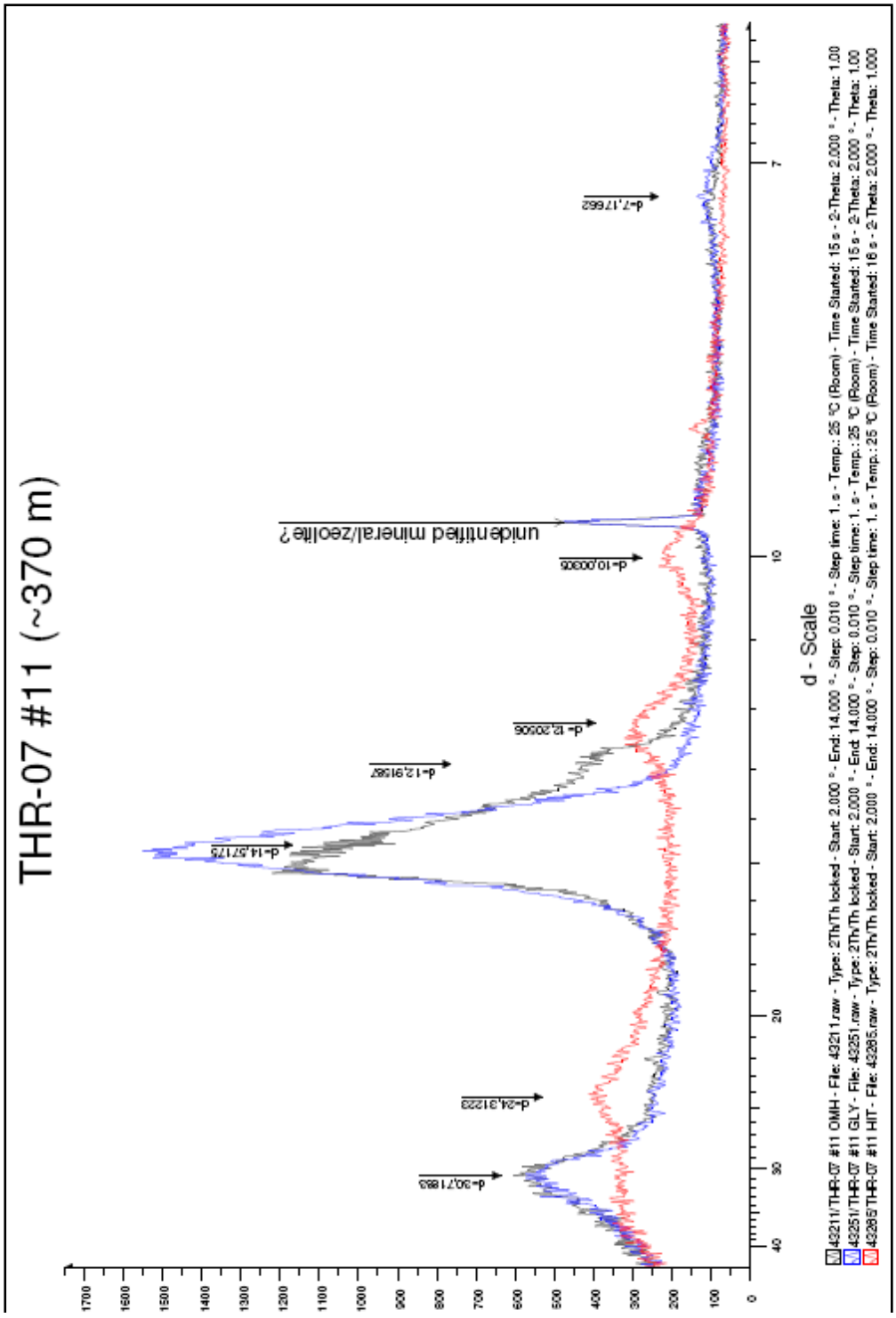
THR-07 #11 (~370 m)
d - Scale
d=14,57173
d=12,91587
d=12,20306
d=10,00326
unidentified mineral/zeolite?
d=7,17662
d=24,91223
d=30,71883
43211/THR-07 #11 OMH - File: 43211.raw - Type: 2Th/Th locked - Start: 2.000 ° - End: 14.000 ° - Step: 0.010 ° - Step time: 1. s - Temp.: 25 °C (Room) - Time Started: 15 s - 2-Theta: 2.000 ° - Theta: 1.00
43251/THR-07 #11 GLY - File: 43251.raw - Type: 2Th/Th locked - Start: 2.000 ° - End: 14.000 ° - Step: 0.010 ° - Step time: 1. s - Temp.: 25 °C (Room) - Time Started: 15 s - 2-Theta: 2.000 ° - Theta: 1.00
43285/THR-07 #11 HIT - File: 43285.raw - Type: 2Th/Th locked - Start: 2.000 ° - End: 14.000 ° - Step: 0.010 ° - Step time: 1. s - Temp.: 25 °C (Room) - Time Started: 16 s - 2-Theta: 2.000 ° - Theta: 1.000

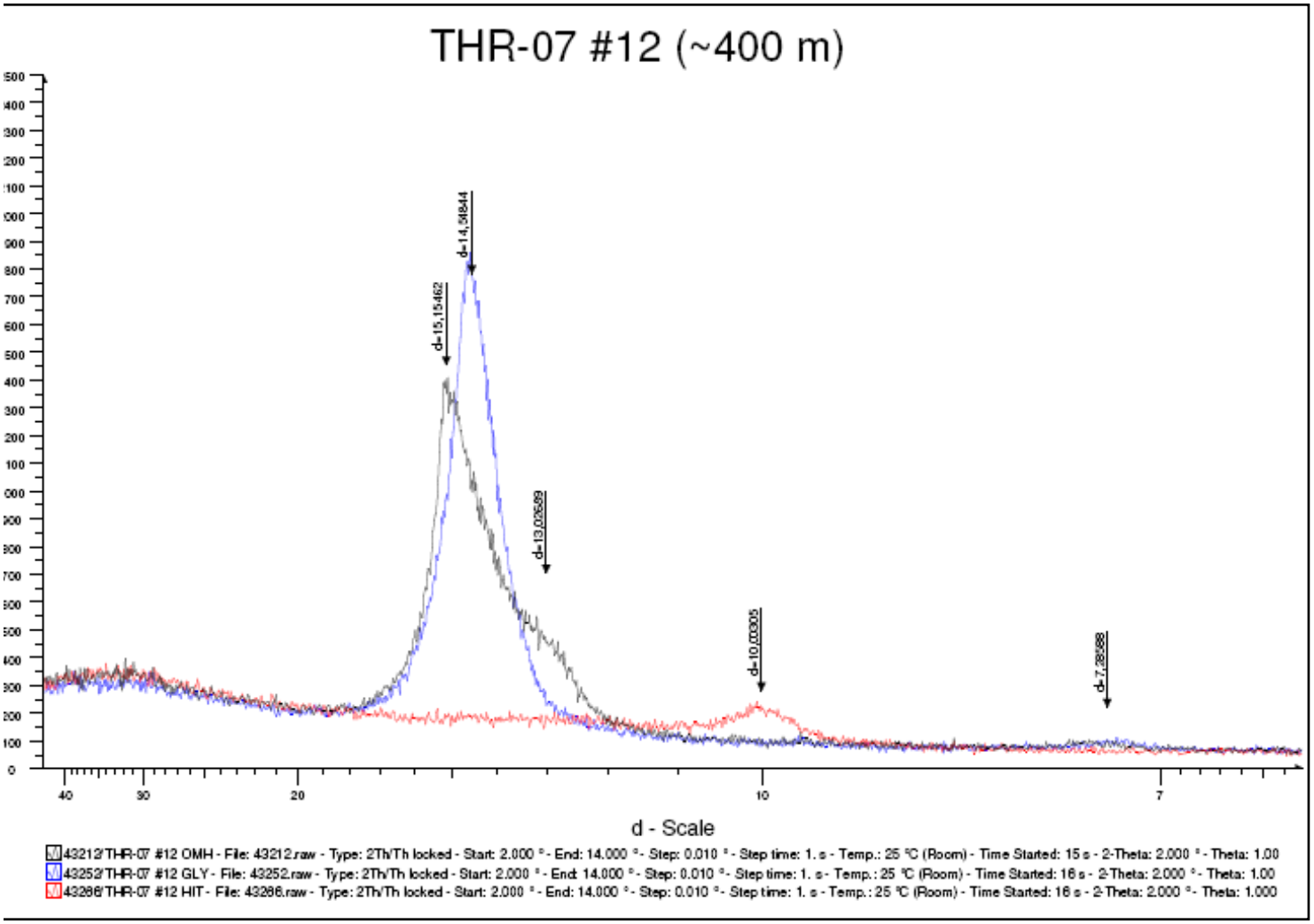
THR-07 #12 (~400 m)
d=14,5844
d=15,1562
d=13,0689
d=10,0005
d=7,2588
d - Scale
43212 THR-07 #12 OMH - File: 43212.raw - Type: 2Th/Th locked - Start: 2.000 ° - End: 14.000 ° - Step: 0.010 ° - Step time: 1. s - Temp.: 25 °C (Room) - Time Started: 15 s - 2-Theta: 2.000 ° - Theta: 1.00
43252 THR-07 #12 GLY - File: 43252.raw - Type: 2Th/Th locked - Start: 2.000 ° - End: 14.000 ° - Step: 0.010 ° - Step time: 1. s - Temp.: 25 °C (Room) - Time Started: 16 s - 2-Theta: 2.000 ° - Theta: 1.00
43286 THR-07 #12 HIT - File: 43286.raw - Type: 2Th/Th locked - Start: 2.000 ° - End: 14.000 ° - Step: 0.010 ° - Step time: 1. s - Temp.: 25 °C (Room) - Time Started: 16 s - 2-Theta: 2.000 ° - Theta: 1.000

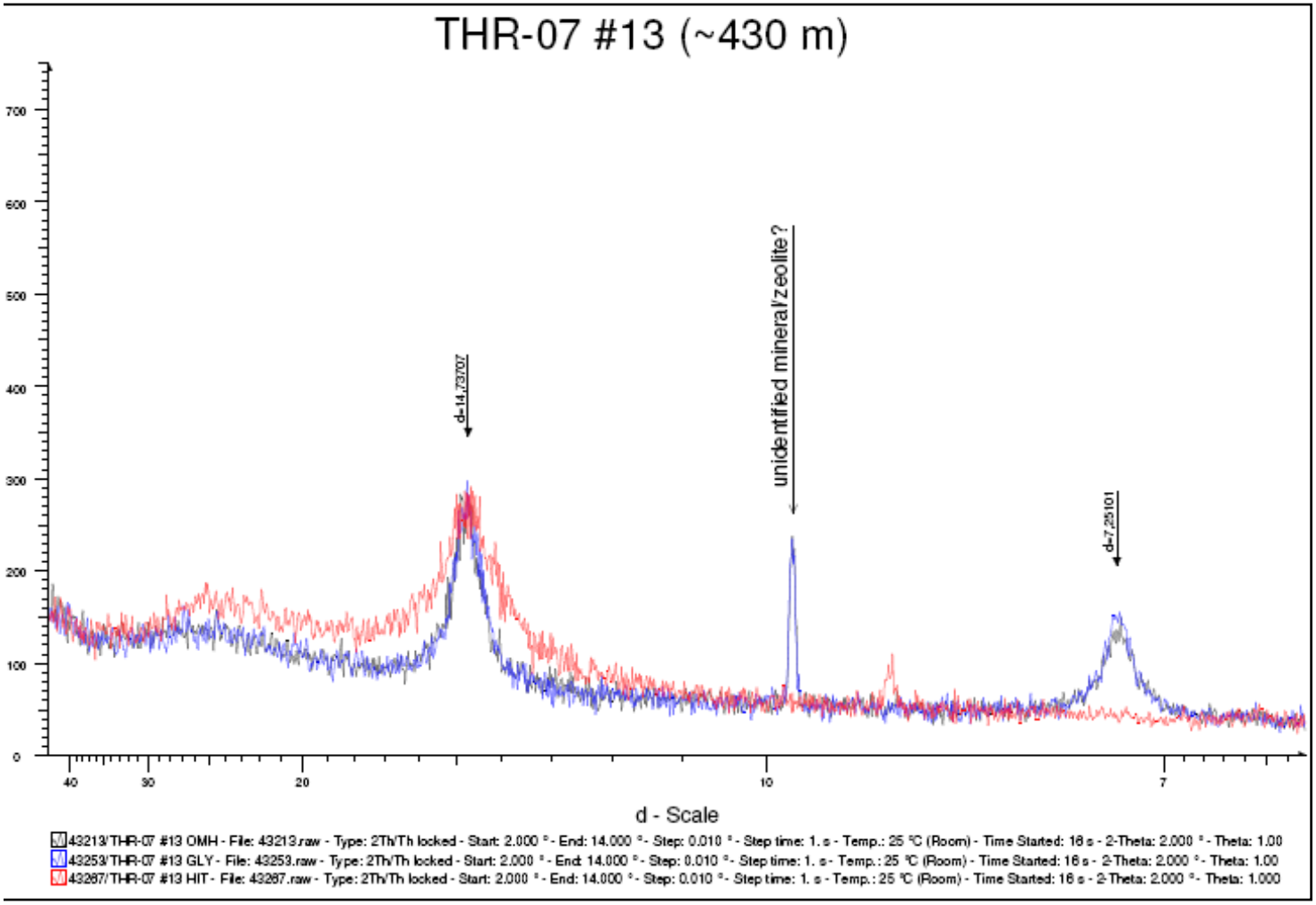
THR-07 #13 (~430 m)
d=14,73707
unidentified mineral/zeolite?
d=7,25101
700
600
500
400
300
200
100
0
40
30
20
10
7
d - Scale
43213/THR-07 #13 OMH - File: 43213.raw - Type: 2Th/Th locked - Start: 2.000 ° - End: 14.000 ° - Step: 0.010 ° - Step time: 1. s - Temp.: 25 °C (Room) - Time Started: 16 s - 2-Theta: 2.000 ° - Theta: 1.00
43253/THR-07 #13 GLY - File: 43253.raw - Type: 2Th/Th locked - Start: 2.000 ° - End: 14.000 ° - Step: 0.010 ° - Step time: 1. s - Temp.: 25 °C (Room) - Time Started: 16 s - 2-Theta: 2.000 ° - Theta: 1.00
43287/THR-07 #13 HIT - File: 43287.raw - Type: 2Th/Th locked - Start: 2.000 ° - End: 14.000 ° - Step: 0.010 ° - Step time: 1. s - Temp.: 25 °C (Room) - Time Started: 16 s - 2-Theta: 2.000 ° - Theta: 1.000

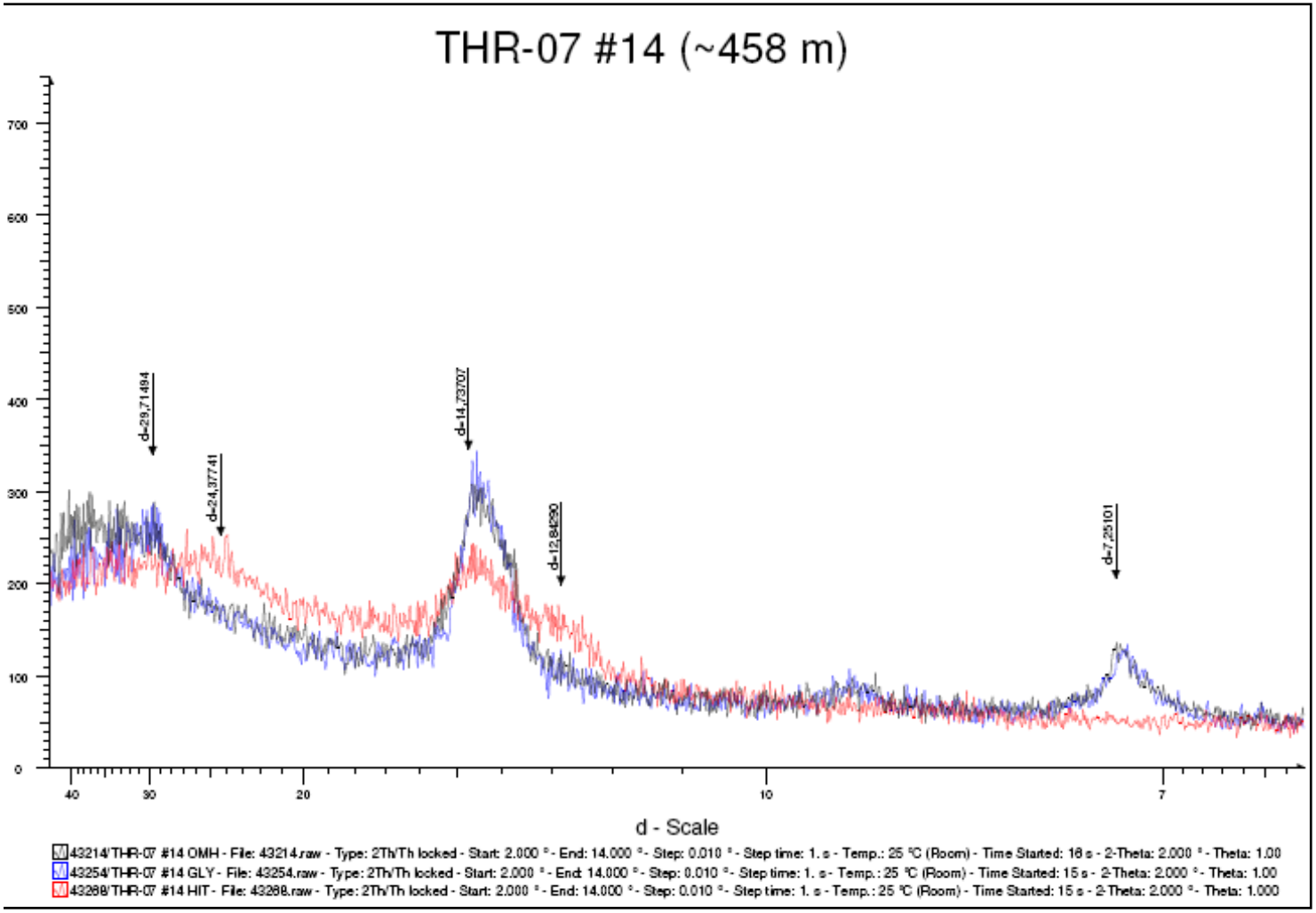
THR-07 #14 (~458 m)
700
600
500
400
300
200
100
0
d=29,71494
d=24,37741
d=14,73707
d=12,84290
d=7,25101
40
30
20
10
7
d - Scale
43214'THR-07 #14 OMH - File: 43214.raw - Type: 2Th/Th locked - Start: 2.000 ° - End: 14.000 ° - Step: 0.010 ° - Step time: 1. s - Temp.: 25 °C (Room) - Time Started: 18 s - 2-Theta: 2.000 ° - Theta: 1.00
43254'THR-07 #14 GLY - File: 43254.raw - Type: 2Th/Th locked - Start: 2.000 ° - End: 14.000 ° - Step: 0.010 ° - Step time: 1. s - Temp.: 25 °C (Room) - Time Started: 15 s - 2-Theta: 2.000 ° - Theta: 1.00
43288'THR-07 #14 HIT - File: 43288.raw - Type: 2Th/Th locked - Start: 2.000 ° - End: 14.000 ° - Step: 0.010 ° - Step time: 1. s - Temp.: 25 °C (Room) - Time Started: 15 s - 2-Theta: 2.000 ° - Theta: 1.000